ADHESIVE-BONDED DOUBLE-LAP JOINTS

TECHNICAL REPORT

by

L. J. HART-SMITH

January 1973

for

Langley Research Center
Hampton, Virginia 23366

NATIONAL AERONAUTICS AND SPACE ADMINISTRATION

ADHESIVE-BONDED DOUBLE-LAP JOINTS

TECHNICAL REPORT

by

L. J. HART-SMITH

JANUARY 1973

for

Langley Research Center
Hampton, Virginia 23366

NATIONAL AERONAUTICS AND SPACE ADMINISTRATION

ABSTRACT

Explicit analytical solutions are derived for the static load carrying capacity of double-lap adhesive-bonded joints. The analyses extend the elastic solution of Volkersen and cover adhesive plasticity, adherend stiffness imbalance and thermal mismatch between the adherends. Both elastic-plastic and bi-elastic adhesive representations lead to the explicit result that the influence of the adhesive on the maximum potential bond strength is defined uniquely by the strain energy in shear per unit area of bond. Failures induced by peel stresses at the ends of the joint are examined. This failure mode is particularly important for composite adherends. The explicit solutions are sufficiently simple to be used for design purposes.

KEYWORD DESCRIPTORS

Bonded Joints   Double-Lap Joints

Adhesive Stresses and Strains   Static Strength

Adherend Thermal Mismatch   Shear Strain Energy

Adherend Stiffness Imbalance   Elastic-Plastic Formulation

Peel Stresses   Bi-Elastic Formulation

Fatigue Loads   Advanced Composite Joints

iii

FOREWORD

This report was prepared by the Douglas Aircraft Company, McDonnell Douglas Corporation, Long Beach, California under the terms of Contract NAS1-11234. One summary report (NASA CR 2218) and four technical reports (NASA CR 112235, -6, -7, and -8) cover the work, which was performed between November 1971 and January 1973. The program was sponsored by the National Aeronautics and Space Administration's Langley Research Center, Hampton, Virginia. Dr. M. F. Card and Mr. H. G. Bush were the Contracting Agency's Technical Monitors.

The basic concept of bonded joint shear analysis by classical mechanics of continuous structures in terms of the elastic-plastic adhesive model was developed initially under Douglas IRAD funding between 1968 and 1970. This contract has permitted the work to be expanded greatly in both scope and detail. All of the peel-stress studies were performed under this contract.

CONTENTS

ILLUSTRATIONS

SYMBOLS

$\begin{matrix} A,B,C \\ F,H,J \end{matrix}$ = Integration constants

a,b,c = Extents of plastic stress state in adhesive at ends of bonded joint (in.)

CTHERM = Non-dimensionalized adherend thermal mismatch coefficient

D = Flexural rigidity of adherends (lb in.^{2})

d = Length of elastic zone in adhesive bond (in.)

E = Young's modulus (longitudinal) for adherend (psi)

E_c, E_c' = Adhesive peel (transverse tension) modulus (psi)

ETR = Adherend extensional stiffness ratio

G = Adhesive shear modulus for elastic-plastic representation (psi)

G_e, G_p = Initial and final, respectively, adhesive shear moduli for bi-elastic representation (psi)

G_i, G_o = Adherend in-plane shear moduli (psi)

k_1, k_2 = Factors [see Equation(68)]

ℓ = Overlap (length of bond) (in.)

M = Bending moment in adherend (lb in. / in.)

P = Applied direct load on entire joint (lb / in.)

Q = Applied running shear load on joint (lb / in.)

S = Shear stress resultant (in-plane) in adherend (lb / in.)

T = Temperature (°F)

ΔT = Temperature change $(T_{operating} - T_{cure})$ (°F)

T = Direct stress resultants in adherends (lb / in.)

t = Thickness of adherend (in.)

V = Transverse shear force on adherend (lb / in.)

w	=	Transverse displacement of adherend (in.)
x	=	Axial (longitudinal) co-ordinate parallel to direction of load
α	=	Coefficient of thermal expansion (/°F)
γ	=	Adhesive shear strain
γ_e	=	Elastic adhesive shear strain
γ_{max}	=	Maximum total adhesive shear strain
γ_p	=	Plastic adhesive shear strain
δ	=	Axial (longitudinal) displacement of adherend (in.)
ζ, ξ, χ	=	Axial co-ordinates (different origin and/or sense from x)
η	=	Thickness of adhesive layer (in.)
θ	=	$\lambda_p (\ell - d) / 2$ = Non-dimensionalized extent of plastic adhesive zone
λ	=	Exponent of elastic shear stress distribution (in^{-1})
λ_e, λ_p	=	Exponents of bi-elastic adhesive shear stress distribution (in^{-1})
ν	=	Poisson's ratio for adherend(s)
σ_c, σ_p	=	Peel stresses in adhesive (psi)
σ_y	=	Yield stress of adherend (psi)
τ, τ_a	=	Adhesive shear stress (psi)
τ_{av}	=	Average adhesive shear stress (psi)
τ_{max}	=	Maximum elastic adhesive shear stress induced ($\leq \tau_p$) (psi)
τ_p	=	Plastic adhesive shear stress (psi)
χ	=	Peel stress distribution exponent (in^{-1})

SUBSCRIPTS

a,c	=	Adhesive (cement)
i,o	=	Inner and outer adherends of double-lap bonded joint
n	=	Property normal to plane of adherends
t,c,s	=	Tension, compression and shear with respect to applied load

SUMMARY

This report covers the analysis of adhesive-bonded double-lap joints by means
of elastic-plastic analytical techniques. Explicit solutions are derived. The
classical elastic analysis by Volkersen, which accounted for only adherend
stiffness imbalance, is extended to include adhesive plasticity and adherend
thermal mismatch. The formulas derived are sufficiently simple for design use,
yet account for more parameters than have been included in previous published
analyses.

Three important characteristics of double-lap joints are deduced. The first is
that there is a definite limit to the bond strength developable between specif-
ied adherends for a particular adhesive. The load capacity increases with over-
lap only until a defined value is attained. Beyond that overlap, no greater
load transfer can be effected. The load transfer is confined to two end zones
(only one in the case of severely dissimilar adherends) with a lightly-loaded
elastic trough in between. The extent of these end zones is limited and
expressed independently of the total overlap.

The second inherent characteristic of double-lap joints is that the maximum
potential bond shear strength is determined by the adhesive strain energy in
shear per unit bond area. This single adhesive parameter is the necessary and
sufficient characterization. That this is so has been established in terms of
a bi-elastic adhesive analysis in which it was demonstrated that all such
adhesive characterizations (two straight lines) having the same strain energy
(area under the stress-strain curve) and same failure stress and strain develop
precisely the same maximum bond strength between the same adherends. The
precise shape of the stress-strain curve has no effect on the limiting joint
strength. The shape can affect only the adhesive shear stress distribution
along the overlap.

The third feature of this analysis is that it shows precisely how much more of
a problem are the adhesive peel stresses at the ends of the overlap than are
the associated shear stresses. This peel problem is acute for thick composite
adherends and imposes an effective limit on the thickness of adherends which

1

can be bonded efficiently by means of a uniform double-lap joint. Beyond that thickness, it is necessary to use a more efficient tapered-lap joint, stepped-lap joint, or scarf joint.

Joint efficiency charts are provided for common adherend materials. Because it had not been anticipated hitherto that there was a need to characterize the adhesive film in peel as well as in shear, portions of these charts are speculative. The shear properties selected represent typical properties for the best 350 °F curing ductile and brittle (high-temperature) structural epoxy-base adhesives available. These charts show how, for thin adherends, the potential bond shear and peel strengths exceed by far the adherend strengths. Then, for moderate thicknesses, the limited shear strength of the adhesive may limit the joint strength. For thicker adherends, the limiting factor is invariably the peel strength of the adhesive for metal adherends or the interlaminar tension strength of the laminate for filamentary composite adherends.

1. INTRODUCTION

Adhesive bonded joints are already playing a significant role in the develop-
ment and production of metal aircraft structures and the indications are strong
that such joints will be of even greater importance in filamentary composite
structures. Various theoretical analyses have been performed, of which those
by Volkersen (Reference 1) in 1938 for double-lap joints and by Goland and
Reissner (Reference 2) in 1944 for single-lap joints are the classical refer-
ences. They provided considerable elucidations of the qualitative behavior of
joints under load. However, the theoretical analyses are based on certain
simplifications in order to achieve tractable results and the consequent quant-
itative agreement with experiment has hitherto been less than adequate to form
a basis for design without empirical modification. The objective of the pres-
ent formulation is to modify the theoretical analyses to the extent necessary
to achieve adequate correlation with experiment. Such new analyses must still
be sufficiently simple for use in design.

The key to the improvement of this work over that published previously is the
use of an elastic-plastic adhesive representation instead of either a purely-
elastic or mathematically intractable non-linear characterization. The justif-
ication for this is that the mathematically more complex arbitrary bi-elastic
representation is shown to predict the same joint strengths as the simpler
elastic-plastic analysis. It transpires that the adhesive strain energy in
shear per unit area of bond is the single necessary and sufficient adhesive
characterization to predict the potential shear strength of a bonded joint.
The rational basis for design, then, is the adhesive stress-strain curve in
shear, derived experimentally on either a torsion-ring or thick-adherend appar-
atus. The merit of the elastic-plastic formulation is that it permits explicit
analytical solutions to be derived for all the features of prime importance.
Other representations have not permitted this advantage.

The factors accounted for in this analysis include adhesive plasticity, adher-
end stiffness imbalance, adherend thermal mismatch, the nature of the load (be
it tensile lap-shear, compressive lap-shear or in-plane lap-shear), and the
effect of the peel stresses at the end(s) of the joint. Of these, only the

adherend stiffness imbalance had been accounted for explicity before. The peel stress problem, particularly characteristic of the failure modes for composite laminates, had been largely overlooked for double-lap joints, even though its importance had been realized for single-lap joints.

The understanding of the phenomena pertaining to double-lap bonded joints depends upon approaching the problem in terms of joint efficiency. The essence of the problem is depicted in Figure 1. A scarf joint between identical adherends has a nearly uniform shear stress (and strain) in the adhesive as a result of uniform stress throughout the adherends. However, in a uniform lap joint most of the load is transferred through narrow highly-stressed end zones separated by an inefficient lightly-stressed elastic trough. The riveted lap joint has the same non-uniform load transfer as the bonded lap joint; the outer rows of rivets are the most highly stressed. The analyses predict that practically all of the load transferred between these adherends passes through these effective end zones which are found to have a characteristic extent independent of the total overlap. The analyses cited above, like those of Plantema (Reference 3) and Szepe (Reference 4) also, are based on the assumption of linearly elastic materials. Therefore their analyses lack the plastic end zones inherent in the analysis presented herein, which establishes that much of the past discrepancy between theory and experiment may be ascribed to this factor. The influence of plasticity in the adhesive is revealed to be so great an increase in the potential shear strength of the bond that in many cases failure must be initiated in the adherends, as observed experimentally.

The technique of the present analysis is illustrated in the body of the report by considering one factor at a time. The completely general analysis is presented in Appendix Al. The report begins with the effect of adhesive plasticity on a balanced joint(Section 2). Next, (Section 3) the arbitrary bi-elastic adhesive characterization is shown to lead to the same result, justifying the use of the mathematically more convenient elastic-plastic formulation. Then, in turn, the strength reductions associated with adherend thermal and stiffness imbalances, acting independently, are explained in Sections 4 and 5 respectively. The problem of the peel stresses at the ends of the outer adherends follows, (Section 6), and it is found to dominate the behavior of the thicker composite adherends. Accounting for adhesive plasticity has raised the predict-

4

ed shear strength capacity of bonded joints to the level at which it becomes necessary to examine also adherend-induced failures of, or at the edge of, the joint (Section 7). The inclusion of thermal effects necessitates a distinction between compressive and tensile shear loading of a double-lap joint (Section 8). In-plane (edgewise) shear loading is shown in Section 9 to be governed by differential equations of the same form and the equivalent joint parameters are identified. Mixed-modulus adhesive-bonded joints are discussed in Section 10. The effects of the various joint parameters are elucidated in Section 11, while Section 12 explains how to use the design methods, and prepare design charts, for double-lap bonded joints. Conclusions are reached in Section 13 and the computer program developed is listed in Appendix A2, along with sample outputs and brief user instructions.

2. BALANCED DOUBLE-LAP JOINTS (ELASTIC-PLASTIC ANALYSIS)

The classical analysis by Volkersen (Reference 1) allows for only the stresses arising from the differential straining in lap joints and is restricted to elastic adhesive behavior. It forms the basis of the development here accounting for adhesive plasticity and thermal mismatch between the adherends, along with the adherend stiffness imbalance previously included. This section is restricted to consideration of adhesive non-linear behavior, independently of any adherend imbalance effects, to demonstrate the important conclusion that the maximum joint strength between given identical adherends is defined uniquely by the adhesive strain energy in shear. This conclusion is independent of the precise form of the stress-strain curve for the adhesive (as demonstrated by the bi-elastic solution in Section 3), and of any individual adhesive characteristic such as the initial elastic modulus.

Figure 2 depicts the geometry and nomenclature for the analysis of a symmetric double-lap joint. The conditions of longitudinal force-equilibrium for a differential element dx within the joint are

$$\frac{dT_o}{dx} + \tau = 0 \quad , \qquad \frac{dT_i}{dx} - 2\tau = 0 \quad , \tag{1}$$

where the subscripts o and i refer, respectively, to the outer and inner adherends, the inner adherend being acted on by the shear stresses in the adhesive on each side. The stress-strain relations for the assumed elastic adherend yield

$$\frac{d\delta_o}{dx} = \frac{T_o}{E_o t_o} \quad , \qquad \frac{d\delta_i}{dx} = \frac{T_i}{E_i t_i} \quad . \tag{2}$$

As a first approximation, the adhesive shear strain is taken as

$$\gamma = \frac{(\delta_i - \delta_o)}{\eta} \quad . \tag{3}$$

Within the elastic region (of length d), the adhesive shear stress is

7

assumed [*] to be

$$\tau = G\gamma = \frac{G}{\eta}(\delta_i - \delta_o) = f(x) \qquad (4)$$

while, throughout the remaining plastic region, the adhesive shear stress is taken as

$$\tau = \tau_p = \text{constant} . \qquad (5)$$

Eliminating δ_i and δ_o between equations (2) and (3) produces

$$\frac{d\gamma}{dx} = \frac{1}{\eta}\left(\frac{T_i}{E_i t_i} - \frac{T_o}{E_o t_o}\right) . \qquad (6)$$

The use of equations (1) to eliminate T_i and T_o then yields the governing differential equation

$$\frac{d^2\gamma}{dx^2} - \frac{1}{\eta}\left(\frac{1}{E_o t_o} + \frac{2}{E_i t_i}\right)\tau = 0 . \qquad (7)$$

Within the elastic region around the center of the joint, this equation becomes

---

[*] (The relation (4) used both by Volkersen (Reference 1) and by Goland and Reissner (Reference 2) implies not only a linear stress-strain relation in shear but also a uniform shear stress distribution across the thickness. It is this latter assumption which leads the theory to predict a non-zero shear stress at the load-free ends of the adhesive. However, the finite-element analyses of bonded joints by Teodosiadis (Reference 5) have revealed that this error affects the shear stress distribution only within a distance, from the ends, of a few times the adhesive layer thickness. This factor is important for the purely-elastic solution, with its characteristically sharp spikes at the ends of the shear stress distribution, which significantly over-estimates the shear stress at the ends of the joints. However, the practical adhesives all exhibit some non-linear behavior prior to failure and this proves to be a more powerful factor in softening the shear stress peaks at the ends of the joints than is inclusion of the variation of shear stress across the thickness of the bond line. For an elastic-plastic adhesive, it is slightly conservative to neglect this effect.)

$$\frac{d^2\tau}{dx^2} - \lambda^2\tau = 0 \quad , \qquad \left[\lambda^2 = \frac{G}{\eta}\left(\frac{1}{E_o t_o} + \frac{2}{E_i t_i}\right) = \frac{2G}{Et\eta} = \frac{2\tau_p}{Et(\eta\gamma_e)} \right] \tag{8}$$

and has the solution

$$\tau = A \cosh(\lambda x) + B \sinh(\lambda x) \quad . \tag{9}$$

The constant B is found to be identically zero for balanced joints ($2E_o t_o = E_i t_i$) since the adhesive shear stress distribution is necessarily symmetric about the x - origin adopted in Figure 2, being the mid-point of the joint.

In the plastic region, of length $(\ell - d)/2$ at each end of the joint, the solution of equations (5) and (6) is

$$\gamma = \left(\frac{\lambda^2}{2G}\right)\tau_p \xi^2 + C\xi + F \tag{10}$$

in which $dx \equiv d\xi$, the origin for ξ being at $x = +d/2$. The constants A, C, and F and the unknown d/ℓ are found by satisfying the boundary conditions

$$\gamma = \gamma_e \qquad \text{at} \qquad x = + d/2 \quad , \quad \xi = 0 \quad , \tag{11}$$

$$\gamma = \gamma_e + \gamma_p \qquad \text{at} \qquad \xi = + (\ell - d)/2 \quad , \tag{12}$$

$$\frac{d\gamma}{dx} = \frac{d\gamma}{d\xi} \qquad \text{at} \qquad x = + d/2 \quad , \quad \xi = 0 \quad , \tag{13}$$

and

$$\frac{d\gamma}{d\xi} = \frac{P}{E_i t_i \eta} = \frac{2\tau_{av}\ell}{E_i t_i \eta} = \frac{\lambda^2\tau_{av}\ell}{2G} \qquad \text{at} \quad \xi = (\ell - d)/2 \quad , \tag{14}$$

of which equation (13) ensures continuity in the adherend stresses. (Equation (14) could alternatively have been derived by consideration of gross horizontal equilibrium of the joint). Hence

$$F = \gamma_e = \tau_p / G \quad , \tag{15}$$

$$A = \tau_p / \cosh(\lambda d/2) \quad , \tag{16}$$

$$C = \left(\frac{\lambda\tau_p}{G}\right)\tanh(\lambda d/2) \quad , \tag{17}$$

9

$$\left[\lambda\left(\frac{\ell - d}{2}\right) + \tanh\left(\frac{\lambda d}{2}\right)\right]^2 = \tanh^2\left(\frac{\lambda d}{2}\right) + 2\frac{\gamma_p}{\gamma_e} \quad , \qquad (18)$$

and

$$\frac{\tau_{av}}{\tau_p} = \left(1 - \frac{d}{\ell}\right) + \frac{\tanh(\lambda d/2)}{(\lambda \ell/2)} \quad . \qquad (19)$$

The precise simultaneous solution of equations (18) and (19) in order to eliminate d is accomplished by a digital computer program (listed in Appendix A2) but, for sufficiently long overlaps, $\tanh(\lambda d/2) \to 1$, whence

$$\frac{\tau_{av}}{\tau_p}\left(\frac{\lambda\ell}{2}\right) \to \sqrt{1 + 2\frac{\gamma_p}{\gamma_e}} \quad , \qquad \left(\frac{\lambda\ell}{2} \to \infty\right) \quad . \qquad (20)$$

The left-hand side of equation (20) is proportional to the load ($P = 2\tau_{av}\ell$) so that the equation (20) indicates that increasing the overlap beyond an as yet undefined value yields no significant gain in strength. This is because the length of the plastic zone, $(\ell-d)/2$, is defined by equation (18) as

$$\lambda\left(\frac{\ell - d}{2}\right) \simeq \left[\sqrt{1 + 2\frac{\gamma_p}{\gamma_e}} - 1\right] \qquad (21)$$

and is defined by the material properties independently of the total overlap of the joint.

The non-dimensional equation (20) may be re-arranged in the form

$$P = 2\tau_{av}\ell = 4\sqrt{Et}\sqrt{\tau_p n\left(\frac{\gamma_e}{2} + \gamma_p\right)} \quad , \qquad (22)$$

in which the terms under the latter radical define the strain energy of unit area of the adhesive film. No other adhesive material properties are involved, so this establishes the adhesive strain energy in shear as the single necessary and sufficient characterization of the adhesive to define the maximum bond strength obtainable between given uniform adherends. While not so readily evident from the equations, the same holds true for joints between non-identical uniform adherends also. In the succeeding section the same conclusion is demonstrated for a bi-elastic adhesive representation. The grouping of terms is such that $n(\gamma_e + \gamma_p)$ is the maximum bond-line displacement, so the load can be

10

computed in terms of directly measurable quantities.

The maximum potential bond strength above requires at least a moderately long overlap, with an elastic trough in the middle of the joint. For sufficiently short overlaps, the joint will be fully plastic throughout and d will be zero. The limiting overlap, beyond which some elastic adhesive strain must be present follows from equation (18) by setting d equal to zero.

$$\frac{\lambda\ell}{2}\bigg|_{transition} = \sqrt{2\frac{\gamma_p}{\gamma_e}} \ . \tag{23}$$

In the fully-plastic case, equation (19) predicts that

$$\frac{\tau_{av}}{\tau_p} \to 1 \ , \qquad (\frac{\lambda\ell}{2} \to 0) \ . \tag{24}$$

Even in the fully-elastic case, $d = \ell \to 0$, equation (19) leads to the results (24). For long overlaps with a purely-elastic adhesive, equation (20) reduces to the Volkersen solution

$$\frac{\tau_{av}}{\tau_p}\left(\frac{\lambda\ell}{2}\right) \to 1 \ , \qquad (\gamma_p \equiv 0 \ , \ \frac{\lambda\ell}{2} \to \infty) \ , \tag{25}$$

showing a constant load capacity for long overlaps and a steadily decreasing average shear stress as the overlap increases. It should be noted, however, that for a long overlap the end stresses (and strains) are invariant with the length of the overlap; an increase in overlap merely relieves the already low stresses in the central portion of the joint, whether the adhesive be purely-elastic or elastic-plastic, and any such increase in overlap in no way affects the critical stresses and strains in the adhesive.

The solution above is depicted in non-dimensional form in Figures 3 and 4, while some of the corresponding stress and strain distributions within the joint are illustrated in Figure 5.

The failure criterion assumed in the analysis above is that of the total shear strain in the adhesive. The joint failure strengths so predicted should be checked against the criterion for bond failure in peeling, rather than in shear, and against the adherend failure (or yield) criteria. These other joint

strength cutoffs are discussed in Sections 6 and 7.

3. BALANCED DOUBLE-LAP JOINTS (BI-ELASTIC ANALYSIS)

The preceding section demonstrated a versatile technique for characterizing the adhesive non-linear behavior by representing the actual characteristic as an equivalent elastic-plastic formulation, as depicted in Figure 6. The question arises as to whether any different possible characterization would still have led to the conclusion that the adhesive strain energy in shear is the single necessary and sufficient quantity defining the maximum potential joint strength. This issue is resolved in the affirmative here by showing that any arbitrary bi-elastic representation (Figure 6) leads to the same result. It is evident, consequently, that there is little accuracy to be gained by more complex representations of the adhesive characteristics. Furthermore, the mathematical convenience of standardizing on the elastic-plastic formulation rather than to add another parameter to the adhesive characterization is thereby justified.

The joint analysis begins in much the same way with equations (1) through (3) of Section 2. The bi-elastic adhesive characterization, illustrated in Figure 6, is expressed mathematically by the relations

$$\tau = G_e \gamma = \frac{G_e}{\eta}(\delta_i - \delta_o) = f(x) \tag{26}$$

for the central elastic trough and

$$\tau = \tau_p + G_p(\gamma - \gamma_e) = (G_e - G_p)\gamma_e + G_p\gamma$$

$$= \tau_p + G_p\left[\frac{(\delta_i - \delta_o)}{\eta} - \gamma_e\right] \tag{27}$$

for the end zones of the joint. (The precise form of these equations was arrived at by eliminating others which did not yield an explicit formulation to demonstrate the desired objective. Alternative formulations tried proved the point at issue only implicitly rather than explicitly).

As for the elastic-plastic adhesive, the governing differential equation proves to be

$$\frac{d^2\gamma}{dx^2} = \frac{1}{\eta}\left(\frac{1}{E_o t_o} + \frac{2}{E_i t_i}\right)\tau = \frac{\lambda_e^2}{G_e}\tau \qquad (28)$$

where, for conformity with equation (8), λ_e^2 is defined here as

$$(\lambda_e)^2 = \frac{G_e}{\eta}\left(\frac{1}{E_o t_o} + \frac{2}{E_i t_i}\right) \quad . \qquad (29)$$

The solution of equations (26) and (28) for the central region (of length d) of the joint follows from

$$\frac{d^2\gamma}{dx^2} - \lambda_e^2\gamma = 0 \qquad (30)$$

as

$$\gamma = A\cosh(\lambda_e x) + B\sinh(\lambda_e x) \qquad (31)$$

in which B is set equal to zero by the choice of the origin of the x-coordinate. For the outer ends, each of extent $(\ell - d) / 2$, the solution proceeds from the substitution of equation (27) into equation (28). Thus

$$\frac{d^2\gamma}{dx^2} - \lambda_p^2\gamma = \lambda_e^2\left(1 - \frac{G_p}{G_e}\right)\gamma_e = \text{constant} \quad , \qquad (32)$$

where

$$(\lambda_p)^2 = \frac{G_p}{\eta}\left(\frac{1}{E_o t_o} + \frac{2}{E_i t_i}\right) \quad . \qquad (33)$$

The solution is

$$\gamma = C\cosh(\lambda_p x) + F\sinh(\lambda_p x) - \left(\frac{G_e}{G_p} - 1\right)\gamma_e \quad . \qquad (34)$$

The integration constants A, C and F and the unknown d/ℓ are found by satisfying the boundary conditions

$$\gamma = \gamma_e = \tau_p / G_e \quad \text{at} \quad x = d / 2 \; , \; \xi = 0 \; , \qquad (35)$$

$$\gamma = \gamma_e + \gamma_p \quad \text{at} \quad \xi = (\ell - d) / 2 \; , \qquad (36)$$

$$d\gamma / dx = d\gamma / d\xi \quad \text{at} \quad x = d / 2 \; , \; \xi = 0 \; , \qquad (37)$$

14

and

$$\frac{d\gamma}{d\xi} = \frac{P}{E_i t_i \eta} = \frac{2\tau_{av}\ell}{E_i t_i \eta} = \frac{\lambda_e^2}{2G_e}\tau_{av}\ell \quad \text{at} \quad \xi = \frac{(\ell - d)}{2} \quad . \tag{38}$$

For the elastic solution, condition (35) converts equation (31) to the form

$$\gamma = [\gamma_e / \cosh(\lambda_e d/2)]\cosh(\lambda_e x) \quad . \tag{39}$$

Hence, at the transition in adhesive behavior,

$$\left.\frac{d\gamma}{dx}\right|_{\frac{d}{2}} = \gamma_e \lambda_e \tanh\left(\frac{\lambda_e d}{2}\right) . \tag{40}$$

while

$$\left.\frac{d\gamma}{d\xi}\right|_0 = F\lambda_p \quad . \tag{41}$$

Therefore,

$$F = \gamma_e \frac{\lambda_e}{\lambda_p} \tanh\left(\frac{\lambda_e d}{2}\right) \quad . \tag{42}$$

Since $\gamma = \gamma_e$ at $\xi = 0$ [condition (35)],

$$C = \left(\frac{G_e}{G_p}\right)\gamma_e \quad . \tag{43}$$

From the remaining boundary conditions,

$$\left(\frac{\gamma_p}{\gamma_e}\right) + \left(\frac{G_e}{G_p}\right) = \left(\frac{G_e}{G_p}\right)\cosh\left[\lambda_p\left(\frac{\ell-d}{2}\right)\right] + \left(\frac{\lambda_e}{\lambda_p}\right)\tanh\left(\frac{\lambda_e d}{2}\right)\sinh\left[\lambda_p\left(\frac{\ell-d}{2}\right)\right] \tag{44}$$

and

$$\left(\frac{\tau_{av}}{\tau_p}\right)\left(\frac{\lambda_e \ell}{2}\right)\left(\frac{\lambda_e}{\lambda_p}\right) = \left(\frac{G_e}{G_p}\right)\sinh\left[\lambda_p\left(\frac{\ell-d}{2}\right)\right] + \left(\frac{\lambda_e}{\lambda_p}\right)\tanh\left(\frac{\lambda_e d}{2}\right)\cosh\left[\lambda_p\left(\frac{\ell-d}{2}\right)\right] . \tag{45}$$

These equations can be solved simultaneously to deduce d and τ_{av}. The process is somewhat tedious but, in view of its important ramifications, it is summarized as follows. Equations (44) and (45) have the form

$$A = B \cosh\theta + C \sinh\theta \quad ,$$

15

$$F = B \sinh\theta + C \cosh\theta \quad ,$$

$$\theta = \lambda_p \left(\frac{\ell - d}{2}\right) \quad ,$$

where

$$A = \left(\frac{\tau_{av}}{\tau_p}\right)\left(\frac{\lambda_e \ell}{2}\right)\left(\frac{\lambda_e}{\lambda_p}\right) \quad , \quad B = \frac{G_e}{G_p} \quad ,$$

$$C = \left(\frac{\lambda_e}{\lambda_p}\right)\tanh\left(\frac{\lambda_e d}{2}\right) \quad , \quad F = \left(\frac{\gamma_p}{\gamma_e} + \frac{G_e}{G_p}\right) \quad . \right\} \qquad (46)$$

Therefore,

$$\sinh\theta = (AC - BF) / (C^2 - B^2) \quad , \quad \cosh\theta = (AB - FC) / (B^2 - C^2) \quad .$$

The hyperbolic functions are eliminated through use of the identity

$$\cosh^2\theta - \sinh^2\theta = 1 \quad ,$$

leading to

$$(AB - FC)^2 - (AC - BF)^2 = (B^2 - C^2)(C^2 - B^2)$$

whence

$$A^2 - F^2 = C^2 - B^2 \quad .$$

Reverting now to the expressions (46) it is found that precisely

$$\left[\left(\frac{\tau_{av}}{\tau_p}\right)\left(\frac{\lambda_e \ell}{2}\right)\right]^2 = \tanh^2\left(\frac{\lambda_e d}{2}\right) + 2\frac{\gamma_p}{\gamma_e} + \frac{G_p}{G_e}\left(\frac{\gamma_p}{\gamma_e}\right)^2 \quad . \qquad (47)$$

For the long overlaps of interest at the maximum potential joint strength (the asymptotes in Figure 3),

$$\tanh\left(\frac{\lambda_e d}{2}\right) \simeq 1 \quad , \qquad (48)$$

whence

$$\left(\frac{\tau_{av}}{\tau_p}\right)\left(\frac{\lambda_e \ell}{2}\right) \rightarrow \sqrt{1 + 2\frac{\gamma_p}{\gamma_e} + \frac{G_p}{G_e}\left(\frac{\gamma_p}{\gamma_e}\right)^2} \quad . \qquad (49)$$

Thus

16

$$P = 2\tau_{av}\ell \rightarrow 4\sqrt{Et}\sqrt{\eta\frac{\tau_p\gamma_e}{2}\left[1 + 2\frac{\gamma_p}{\gamma_e} + \frac{G_p}{G_e}\left(\frac{\gamma_p}{\gamma_e}\right)^2\right]} \quad . \tag{50}$$

Now, the area under the bi-elastic stress-strain curve, Figure 6, is

$$\text{Area} = \frac{1}{2}[G_e(\gamma_e)^2 + G_p(\gamma_p)^2] + G_e\gamma_e\gamma_p \tag{51}$$

which can be easily re-arranged into the form of the second radical in equation (50). This explicit solution therefore demonstrates that, for any arbitrary bi-elastic representation of the shear behavior of an adhesive film, its strain energy per unit bond area is the unique necessary and sufficient characterization defining the maximum attainable bond strength between two adherends.

4. EFFECT OF THERMAL MISMATCH BETWEEN ADHERENDS

Metal and composite adherends are frequently bonded together because of the high stress concentrations associated with bolt holes in composite laminates. On the other hand, the normally high characteristic bond strengths cannot always be realized because of the differences in coefficients of thermal expansion between dissimilar adherends. This is particularly marked in graphite/ epoxy - to - aluminum bonds because of the great disparity between the respective coefficients of thermal expansion. Since the adherends are usually bonded together at 250 °F or 350 °F and the joints are required to withstand loading at as low as -67 °F, there are significant "no-load" strains induced in the adhesive which detract from the load potential of the joint. This phenomenon is illustrated in Figure 7, showing how the bond at one end of the joint is more severely strained than at the other end.

The complete analysis is presented in Appendix A1, so it suffices here to discuss the highlights of the solution (A.61). In the absence of any adherend stiffness imbalance ($E_i t_i = 2E_o t_o$), the exact solution derives from the following pair of equations for $\alpha_o > \alpha_i$ and $\Delta T < 0$ (where $\Delta T = T_{operating} - T_{cure}$):

$$\frac{\tau_{av}}{\tau_p} = 1 - \frac{d}{\ell} + \frac{\tanh\left(\frac{\lambda d}{2}\right)}{(\lambda \ell/2)} \tag{52}$$

and

$$\left(\frac{\tau_{av}}{\tau_p}\right)\left(\frac{\lambda \ell}{2}\right) = \sqrt{\tanh^2\left(\frac{\lambda d}{2}\right) + 2\frac{\gamma_p}{\gamma_e} - \frac{(\alpha_i - \alpha_o)\Delta T \lambda}{\tau_p\left(\frac{1}{E_o t_o} + \frac{2}{E_i t_i}\right)}} \; . \tag{53}$$

The notation is defined in Figure 8.

For the case $\alpha_o < \alpha_i$, the sign of the second term is changed to reflect the shift, from one end of the joint to the other, of the maximum adhesive shear strain. In the absence of any adherend stiffness imbalance, a change in load from tension to compression merely shifts the critical end of the joint from one end to the other, as shown in Figure 7, and does not need a change in sign of the thermal mismatch term. (Note, however, that when peel stresses dominate

the ultimate strength of a uniform double-lap joint a change in load direction does have a significant effect on the joint strength because what are critical tensile peel stresses at the ends of the outer adherends in the tensile loading case become inconsequential compressive transverse stresses for compressive loading).

In the general case, for the long overlaps associated with the "plateau" load levels of Figure 3, the asymptotic joint strength is given by the lesser value of

$$\left(\frac{\tau_{av}}{\tau_p}\right)\left(\frac{\lambda\ell}{2}\right) \rightarrow \left[\sqrt{1 + 2\frac{\gamma_p}{\gamma_e}} + CTHERM(1)\right]\left[\frac{1 + ETR(1)}{2}\right] , \quad (54)$$

and

$$\left(\frac{\tau_{av}}{\tau_p}\right)\left(\frac{\lambda\ell}{2}\right) \rightarrow \left[\sqrt{1 + 2\frac{\gamma_p}{\gamma_e}} + CTHERM(2)\right]\left[\frac{1 + ETR(2)}{2}\right] , \quad (55)$$

where the adherend stiffness imbalances are

$$ETR(1) = \frac{E_i t_i}{2E_o t_o} , \quad ETR(2) = \frac{2E_o t_o}{E_i t_i} \quad (56)$$

and the adherend thermal mismatches are

$$CTHERM(1) = \frac{(\alpha_o - \alpha_i)\Delta T\lambda}{\tau_p\left(\frac{1}{E_o t_o} + \frac{2}{E_i t_i}\right)} , \quad CTHERM(2) = \frac{(\alpha_i - \alpha_o)\Delta T\lambda}{\tau_p\left(\frac{1}{E_o t_o} + \frac{2}{E_i t_i}\right)} . \quad (57)$$

A negative value for either equation (54) or (55) indicates that the thermal mismatch is so severe that the joint would break apart due to thermal effects alone without the application of any mechanical load. Equations (54), (55), and (57) reveal that any adherend thermal mismatch effectively reduces the available adhesive strain energy to resist the applied load. That this is so is best illustrated by re-arrangement of the first square bracket term in equation (54) into the form

$$\sqrt{\frac{2}{\gamma_e\tau_p n}}\left[\sqrt{n\tau_p\left(\frac{\gamma_e}{2} + \gamma_p\right)} + \frac{(\alpha_o - \alpha_i)\Delta T}{\sqrt{\left[2\left(\frac{1}{E_o t_o} + \frac{2}{E_i t_i}\right)\right]}}\right] \quad (58)$$

in which the first radical in the square brackets defines the adhesive film

shear strain energy per unit area of bond while the second term characterizes exclusively adherend properties. Not surprisingly, if adherend thermal mismatch is associated with thick (stiff) adherends, the joint strength degradation is more pronounced.

Figure 9 shows the reduction in the asymptotic (or plateau) strengths of stiffness balanced joints, as defined by equations (54) and (55), due to the presence of thermal mismatch between the adherend materials.

The temperature differential ΔT is introduced above as the difference between the adhesive cure temperature and the operating temperature of the joint. Strictly, the reference temperature should be defined as the stress-free temperature of the joint. Because adhesives are long-chain polymers with viscoelastic properties, a fraction of the residual bond stresses can be dissipated by creep. Obviously the theory is general enough to cope with any known stress-free temperature, but the precise determination of the latter may be very complex. The available evidence on this matter indicates the following: (1) some joints do break apart while cooling down in the autoclave (particularly with a brittle adhesive bonding graphite-epoxy to aluminum) as a result of the load being induced at a greater rate than that at which the adhesive can creep, (2) curvature measurements on long hybrid strips indicate that the stress-free temperature is close to the normal cure temperature of the adhesive (curing a 250 °F adhesive at 350 °F induces thermal stresses characteristic of 250 °F because the adhesive polymerizes at this temperature even if it may subsequently be heated up to higher temperatures, (3) long boron-epoxy reinforced aluminum extrusions cured and aged at room-temperature and subsequently post-cured at elevated temperature have a stress-free temperature essentially of room temperature because, during the post-curing, the only locations at which the adhesive (or resin matrix) is stressed highly enough to induce creep are confined to narrow zones at each end of the reinforcement while the lightly-stressed bulk of the adhesive (resin matrix) serves as a "memory" for the stress-free state on cooling down, and (4) strength tests on some short-overlap hybrid composite joints have not revealed any adverse effect from thermal mismatch. It seems self-evident that creep can alleviate thermal stresses only within the ultimate strain capacity of an adhesive, so the observations above are compatible.

21

5. EFFECT OF STIFFNESS IMBALANCE BETWEEN ADHERENDS

Whenever the net stiffness at one end of a joint differs from that at the other end, the adhesive shear strain distribution is rendered non-symmetric. This phenomenon is depicted in Figure 10 for stiffness imbalance alone, showing how the adhesive strains are more severe at that end from which the "soft" adherend extends than at the other end from which the "stiff" adherends extend. The full potential strength of the adhesive bond is therefore not being realized at this latter end. The simultaneous presence of thermal mismatch between the adherends will either aggravate or alleviate the effects of stiffness imbalance. A comprehensive analysis of this phenomenon is presented in Appendix A1, so only the results will be discussed here. The pertinent equations (A.5) and (A.61) are that

$$\left(\frac{\tau_{av}}{\tau_p}\right)\left(\frac{\lambda \ell}{2}\right) \rightarrow \left[\sqrt{1 + 2\frac{\gamma_p}{\gamma_e}} + \frac{(\alpha_o - \alpha_i)\Delta T \lambda}{\tau_p\left(\frac{1}{E_o t_o} + \frac{2}{E_i t_i}\right)}\right]\left[\frac{1 + \frac{E_i t_i}{2E_o t_o}}{2}\right] , \quad (59)$$

$$\text{for } E_i t_i < 2E_o t_o .$$

With respect to the symmetric solution (20), and omitting consideration of thermal effects, it is apparent that the limiting strength of the joint is simply scaled up or down by an elasto-geometric factor. Since

$$\lambda = \sqrt{\frac{G}{\eta}\left(\frac{1}{E_o t_o} + \frac{2}{E_i t_i}\right)} , \quad (60)$$

the effects of stiffness imbalance are manifest in both sides of equation (59). Isolating out the influence of thermal imbalance, and using the outer adherends as reference for a balanced joint, it can be shown that the stiffness unbalanced joint is weaker than the balanced joint by the factor

$$\sqrt{\left(\frac{E_i t_i}{2E_o t_o}\right)\left[1 + \frac{E_i t_i}{2E_o t_o}\right]}\Bigg/ 2 \qquad \left(\begin{array}{c} E_o t_o \text{ reference} \\ E_i t_i \leq 2E_o t_o \end{array}\right) . \quad (61)$$

This factor is illustrated in Figure 11 and applies whether the adhesive shear stress distribution be all-elastic or contain one or two plastic zones. Naturally it does not apply for fully-plastic joints which are not on the "plateau" strengths established in Figure 3. It is evident that the softer (thinner)

23

adherend(s) lose strength more rapidly with stiffness imbalance than do the bonds. In other words, if the bond is strong enough to fail outside a balanced joint, it will inevitably be strong enough to fail any unbalanced joint outside the bond provided that the stiffer adherend is no stiffer than that in the balanced joint.

In the case of the splice plates bonded to plates butted together, it is more informative to use the inner adherend(s) as reference to illustrate the relative efficiencies of splice plates of different thicknesses. Using $E_i t_i$ as the reference for a balanced joint, the unbalanced joint is weaker by the factors

$$\sqrt{\left(\frac{2E_o t_o}{E_i t_i}\right)\left[1 + \frac{2E_o t_o}{E_i t_i}\right]\bigg/ 2} \qquad \left(\begin{array}{c} E_i t_i \text{ reference} \\ 2E_o t_o \leq E_i t_i \end{array}\right) , \qquad (62)$$

and

$$\sqrt{\left[1 + \left(\frac{2E_o t_o}{E_i t_i}\right)\right]\bigg/ 2\left(\frac{2E_o t_o}{E_i t_i}\right)} \qquad \left(\begin{array}{c} E_i t_i \text{ reference} \\ 2E_o t_o \geq E_i t_i \end{array}\right) . \qquad (63)$$

Figure 12 depicts this strength reduction with respect to balanced joints. At first sight it would seem that stiffer splices would increase the load transferred at the outer ends of the splices and that, therefore, the joint strength would be raised. Actually, while more load is transferred at the outer ends of the unbalanced splice, the differential adherend stresses at the inner ends (of the plates) are thereby so greatly reduced that the adhesive shear strains there are greatly diminished. Effectively, therefore, the inner ends of the unbalanced splice can be only lightly loaded prior to failure of the bonds at the outer ends. Such a failure occurs at a lower load level than could be carried by a stiffness-balanced joint.

It is evident that significant penalties are associated with adherend stiffness imbalance. Except for such thin (or weak) adherends that joint efficiency is not necessary, it may well be desirable to locally build up the adherends to match stiffnesses along the bond length. Indeed, still further (balanced) reinforcement enhances the joint strength. Such reinforcement is readily incorporated in a composite panel during layup. In metal structures one can either bond on a local doubler or selectively chem-mill the panel away from the joint areas.

(A word of caution is warranted over the use of reinforcement in the joint area for uniform double-lap joints in practice. For thick adherends, the increase in thickness may well do more harm to the resistance to peel loads than it does to enhance the shear strength. This will be particularly so for composite adherends. In order to take advantage of this increase in shear strength in practice, it is usually necessary to taper the splice plates at their outer ends in conjunction with a build-up in thickness over the ends of the butted plates.)

6. PEEL STRESSES IN DOUBLE-LAP JOINTS

The analyses in the preceding sections, and in Appendix A1, deal with the shear
stresses in the bond line. As a prelude to this section, it is appropriate to
examine the progression of failure modes as the adherend thickness is increased.
For very thin adherends, the potential bond strength is so far in excess of the
adherend strength that failures occur consistently outside the joint. For some-
what thicker adherends, a situation is reached in which bond failure in shear
is initiated at the ends of the joint as the result of yielding of the (metal)
adherends. The yielding causes displacement differentials across the bond line
which are in excess of the capacity of the adhesive. Even though the after-the-
fact examination reveals an adhesive failure, this should be more properly
thought of as an adherend failure because it is governed almost entirely by
adherend properties. For slightly thicker (stronger) adherends, the bond is
failed in shear according to the analyses of the preceding sections at loads
less than sufficient to yield (or break) the adherends. At first sight, it may
seem that this mode is the last of the sequence but the experimental evidence
indicates that this is not the case. The last link in the chain is failures
induced by peel forces for still thicker adherends. The characteristic failure
mode for thick composite bonded joints is illustrated in Figure 13. The analo-
gous mode for metal adherends is failure of the bond in peel before its shear
strength potential could be reached.

The reason for these two seemingly physically distinct manifestations for the
metal and composite adherends is simply that the interlaminar tension strength
of the laminates is lower than that of most adhesives. Their mathematical
formulation is the same.

The geometry and nomenclature for this analysis are illustrated in Figure 14
for a double-lap joint in which the extensional stiffness of the inner adherend
need not be twice that of each outer adherend. This failure mode is governed
essentially by the outer adherend(s) alone, even though the observed failure is
in the inner adherend. The differential equilibrium equations for the element
of outer adherend are

$$\frac{dM}{dx} = V - \tau \frac{t_o}{2} \qquad (64)$$

and

$$\frac{dV}{dx} = -\sigma_c \quad . \qquad (65)$$

The characteristic equation of the outer adherend undergoing plate bending is

$$\frac{d^2 w_o}{dx^2} = -\frac{M}{D} \quad . \qquad (66)$$

The assumed elastic peel stress is defined as

$$\frac{\sigma_c}{E_c{}'} = -\frac{w_o}{\eta} \qquad (67)$$

in which $E_c{}'$ is the "effective" tensile modulus of the adhesive, subject to Poisson effects from in-plane constraints of the adherends and including an allowance for the transverse deformations of the adherends under the peel stresses. An approximate representation of the phenomena is provided in Figure 14. On this basis, it is evident that

$$\frac{1}{E_c{}'} = \frac{1}{E_c} + \frac{k_1}{E_{in}} + \frac{k_2}{E_{on}} \quad , \qquad (68)$$

where E_{in} and E_{on} are the transverse tensile moduli of the inner and outer adherends respectively. The constants k_1 and k_2 refer to the number (or fraction) of adhesive layer thicknesses for which the adherends are affected by the peel stresses. In contradistinction to the elastic-plastic formulation of the shear behavior of the adhesive, it is appropriate to confine attention to elastic peel stress behavior, for two reasons. First, in the case of composite adherends, the inner laminate will fail by interlaminar tension (in conjunction with a negative influence from the concurrent interlaminar shear) at that load level at which the adhesive peel stress just exceeds the laminate interlaminar strength. The failure will initiate at the very end of the joint between the first and second layers of fibers adjacent to the bond. It is immaterial that, were the laminate stronger, a ductile adhesive could have developed that same peel stress over a larger area in association with higher average bond stresses. Second, for metal adherends, the Poisson effects of in-plane adhesive constraint

on the very thin (typically 0.005 inch) bond line so greatly modify the apparent adhesive behavior that it no longer represents the ductile characteristics of the bulk adhesive. The reason for this is that, like many long-chain polymer materials, adhesives are practically incompressible. It is an easily deduced characteristic of such materials that their strength under hydrostatic tension or compression is theoretically infinite and so are their elastic moduli. The relatively stiff metal adherends enforce biaxial in-plane tension into the thin adhesive film as the adherends try to peel apart. This so enhances the peel strength potential of the adhesive film as to effectively prevent "yielding" and to increase the load level for potential peel failure. (For this reason, the tensile modulus E_c of the adhesive film in equation (68) must be determined by transverse loading of an adhesive film bonded to blocks rather than on a bulk adhesive specimen. A compression test is recommended for determining the modulus, since such a tension test is prone to premature failure.) The net result is that shear failure of the adhesive prevails up to those adherend thicknesses for which the adhesive bond is unable to develop sufficient strength to fail the adherends. It is necessary, when bonding still thicker adherends, to change the geometry to a more efficient form (such as a tapered-lap, stepped-lap , or scarf joint) which is not subject to critical peel stresses at the ends of the joint. While an elastic-plastic (or even bi-elastic) peel stress analysis can be readily formulated (and may even be solvable explicitly), it appears to be of academic interest only for the material systems now available. Perhaps in case of a major breakthrough in interlaminar strength improvement of composites by some technique not suitable for similarly benefiting adhesives because of associated intolerable adverse effects on the adhesive shear properties, such an elastic-plastic peel stress analysis may become worthwhile.

Returning now to the analysis, in equation (64) the adhesive shear stress τ is set constant in order to uncouple the differential equations governing the peel and shear stresses. The justification for doing this is that, since most structural adhesives exhibit at least some plasticity (while the best ones exhibit considerable ductility), the shear stress is constant over a significant distance from the critical end at which the peel stress peaks. Subject to this assumption, the governing differential equation for the deflection of an outer adherend is

$$\frac{d^4w_o}{dx^4} - \frac{E_c'}{D\eta} w_o = 0 \qquad (69)$$

and, introducing the notation

$$\chi^4 = E_c' / 4D\eta \quad , \qquad (70)$$

the solution is

$$w_o = A \sin\chi x \cosh\chi x + B \cos\chi x \sinh\chi x + C \sin\chi x \sinh\chi x + F \cos\chi x \cosh\chi x \quad . \qquad (71)$$

The boundary conditions defining the constants A, B, C, and F are

$$\int_{-\frac{\ell}{2}}^{+\frac{\ell}{2}} \sigma_c dx = 0 = \int_{-\frac{\ell}{2}}^{+\frac{\ell}{2}} w_o dx \quad , \qquad (72)$$

$$M = -D\frac{d^2w_o}{dx^2} = 0 \quad \text{at} \quad x = \pm\frac{\ell}{2} \quad , \qquad (73)$$

and

$$V = 0 \quad , \quad \text{whence} \quad \frac{dM}{dx} = -\tau\frac{t_o}{2} = -D\frac{d^3w_o}{dx^3} \quad \text{at} \quad x = \frac{\ell}{2} \quad . \qquad (74)$$

Of these, the equation (73) requires that

$$\frac{d^2w_o}{dx^2} = 2\chi^2[A \cos\chi x \sinh\chi x - B \sin\chi x \cosh\chi x$$

$$+ C \cos\chi x \cosh\chi x - F \sin\chi x \sinh\chi x] = 0 \quad \text{at} \quad x = \pm\frac{\ell}{2} \quad . \qquad (75)$$

Hence

$$C = F = 0 \qquad (76)$$

which simultaneously satisfies equation (72). Since the concern is for overlaps sufficiently long to preclude inadequate shear strength, it is appropriate to set

$$\cosh\left(\frac{\chi\ell}{2}\right) \simeq \sinh\left(\frac{\chi\ell}{2}\right) \simeq \frac{1}{2}e^{\left(\frac{\chi\ell}{2}\right)} \quad , \qquad (77)$$

so that

$$A \cos \left(\frac{\chi \ell}{2}\right) \simeq B \sin \left(\frac{\chi \ell}{2}\right) \quad . \tag{78}$$

Equation (74) then requires that

$$-\frac{\tau t_o}{2D} = 2\chi^3 \left[-(A+B)\sin \left(\frac{\chi \ell}{2}\right) \sinh \left(\frac{\chi \ell}{2}\right) + (A-B)\cos \left(\frac{\chi \ell}{2}\right) \cosh \left(\frac{\chi \ell}{2}\right) \right] \tag{79}$$

so, for large $(\chi \ell / 2)$,

$$A \simeq -\frac{\tau t_o}{2D} \sin \left(\frac{\chi \ell}{2}\right) \bigg/ \left[2\chi^3 \cdot \frac{1}{2} e^{\left(\frac{\chi \ell}{2}\right)} \right] \quad , \tag{80}$$

$$B \simeq -\frac{\tau t_o}{2D} \cos \left(\frac{\chi \ell}{2}\right) \bigg/ \left[2\chi^3 \cdot \frac{1}{2} e^{\left(\frac{\chi \ell}{2}\right)} \right] \quad . \tag{81}$$

Hence,

$$w_o \bigg|_{\ell/2} \simeq -\frac{\tau t_o}{2D} \cdot \frac{1}{2\chi^3} \left[\sin^2 \left(\frac{\chi \ell}{2}\right) + \cos^2 \left(\frac{\chi \ell}{2}\right) \right] \quad , \tag{82}$$

whence the maximum peel stress in the adhesive, and adjacent adherend (laminate) at the end of the joint, is

$$\sigma_{c_{max}} \simeq \frac{E_c'}{\eta} \cdot \frac{\tau t_o}{2D} \cdot \frac{1}{2\chi^3} = \tau \left(\frac{3E_c'(1-\nu^2)t_o}{E_o \eta} \right)^{\frac{1}{4}} \quad . \tag{83}$$

It is evident that the peel stresses at the end of the joint are not a problem if the thickness of the outer adherends is small enough and that the use of a low modulus and/or thick adhesive film is advantageous. As explained above, the precise effective value of E_c' is difficult to establish theoretically. Equation (83) affords a means of establishing the effective value from tests having this mode of failure, since all other quantities involved can be measured readily. The use of an experimental basis for E_c' could also eliminate the effect of the simplifying assumptions made in deriving this result, by providing an empirical correction.

The result (83) is depicted in Figure 15 in non-dimensional form for physically realizable ranges of the parameters involved. An assessment of these confirms that peel stress is not a problem for very thin laminates but that it is so for thicknesses within the normal range of constructional practice.

31

Having established the mathematical nature of the peel stress problem above, it becomes possible to recommend geometric as well as material techniques to alleviate the problem. Recognizing that the peel stress is only a problem when it prevents the development of the full potential shear strength of the joint, it becomes obvious to sacrifice some of the unattained shear potential in exchange for a reduction in the peel stress. The simplest technique for accomplishing this is by scarfing off the ends of the joint, as shown in Figure 13. The small reduction in shear strength is caused by increasing the adherend stress in the scarfed-off ends, thereby decreasing the displacement differential across the bond-line and, with it, the effectiveness of one end zone of the joint in transferring shear load. A quantitative examination of this peel-stress relief problem, in Reference 6, has established that it is quite straightforward to introduce a compensating stiffness imbalance at the other end of the joint so as to make both ends of the tapered-lap joint equally effective in transferring shear loads. With this modification in optimized form, indeed, the theory predicts that the shear stress transfer may be increased by as much as 24 per cent above the potential which the uniform adherends could have developed had not the peel stress failure cut-off prevented it. With regard to adhesive material properties, the nature of the problem suggests that, if a brittle adhesive must be used to effect the shear transfer because of a high-temperature environment, the use of a ductile adhesive to soften the peel-stress spikes at the end of the overlap will be very advantageous for thick adherends.

7. ADHEREND INDUCED FAILURES

For certain geometry and material combinations, the potential adhesive shear strength predicted in Sections 2 through 5 may not be developed prior to adherend-induced failure. One such instance is the interlaminar tension failure of composite laminates induced by excessive peel stresses at the end of the joint, as elucidated in Section 6. This applies particularly for the thicker adherend sections. For very thin (weak) adherends, on the other hand, the potential shear strength of the adhesive may greatly exceed the tensile (or compressive) strength of the laminate outside the joint. This adherend strength cut-off is readily seen to be governed by the criteria

$$\sigma_{o_{max}} t_o \; < \; (\tau_{av})_{potential} \ell \; , \tag{84}$$

or

$$\sigma_{i_{max}} t_i \; < \; 2(\tau_{av})_{potential} \ell \; , \tag{85}$$

for adherend failures instead of adhesive failures.

A related failure mode, prevalent with ductile adherends, such as aluminum, is that of yielding the adherend just outside the joint. As the adherend yields, the adhesive at the end of the joint is subjected to bond-line differential displacements beyond its shear strain capability. The problem is aggravated by squeeze-out around the periphery of the bond area during curing, which results in the thinnest bond in the most critical location(s). This adherend yielding induces a failure which progresses along the joint, starting from either end, as long as the load is maintained. Although it is the adhesive that is observed to have failed after test, this failure is governed principally by the adherend.

8. CHANGE IN JOINT STRENGTH BETWEEN TENSILE AND COMPRESSIVE SHEAR LOADING

The discussion of the influence on joint strength of simultaneous adherend stiffness and thermal imbalances is best deferred until after explanation of the effect of changing the load direction from tensile shear to compressive shear. The differential equilibrium equations (A.1) through (A.7) were set up for tensile load application to the adherends. Maintaining the same sign convention, the effect of reversal of the load direction is to change the signs of T_1, T_2, δ_1, δ_2, τ and γ. Indeed, everything is changed but for the thermal stress term $(\alpha_i - \alpha_o)\Delta T$. Thus, the solution for compressive shear loading is deduced from that for tensile shear loading by reversing the sign of the thermal mismatch coefficient CTHERM and leaving all else the same. It is apparent therefore that, in the presence of thermal mismatch between adherends, compressive shear loads may fail the joint at a different load from the tensile shear failure load. In addition to these different potential shear strengths of the bonded uniform double-lap joint in the two load directions, it is necessary to consider also the peel stresses. The peel stresses will always be harmful at one end of the joint for tensile shear loading but will frequently not be of concern for compressive shear loading. This anomaly arises as the result of the reversal in sign of the peel stresses in going from one end of the joint to the other, in conjunction with the much higher compressive interlaminar strength of adherends and adhesives than the corresponding tensile values.

9. IN-PLANE (EDGEWISE) SHEAR LOADING

Not many joints in an aircraft structure transfer pure tensile lap shear, even though this load is the basic test situation and the standard analysis case to be found in the literature. In most cases the load transferred is predominantly in-plane (edgewise) shear. Just as with tensile, or compressive, lap shear joints, the load is transferred effectively through narrow strips of a defined width independent of the total overlap, as shown in Figure 16. These strips are typically narrower than for tensile lap shear and the design of such a joint is more critical. This problem has been investigated elastically by SAAB (Reference 7), in Sweden, but has received less attention than it merits elsewhere.

The analysis of in-plane shear loading on a double-lap joint (or on a single-lap joint restrained against transverse deflection) proves to be governed by differential equations of basically the same form as for tensile (or compressive) shear loading derived in Sections 2 through 5 and the Appendices. The only parameter having a different mathematical influence is that of thermal imbalance, which is discussed below after the derivation of the equations accounting for adhesive plasticity and any adherend shear stiffness imbalance present.

Figure 17 depicts the geometry and nomenclature pertaining to the analysis of in-plane (edgewise) shear loading on a double-lap joint. The symbol S represents the adherend shear stress resultant or shear flow ($\tau_{xy}t$), while the other symbols remain the same as those used in Section 2 and Appendix A.1. In order to eliminate edge effects, one postulates an infinitely wide joint closing upon itself around the circumference of an infinite cylinder. Horizontal (circumferential) force equilibrium of the differential element dx within the joint requires that

$$\frac{dS_o}{dx} + \tau = 0 \quad , \quad \frac{dS_i}{dx} - 2\tau = 0 \quad . \tag{86}$$

The shear-stress/shear-strain relations for the adherends yield

37

$$\frac{d\delta_o}{dx} = \frac{S_o}{G_o t_o} \quad , \quad \frac{d\delta_i}{dx} = \frac{S_i}{G_i t_i} \quad , \tag{87}$$

where G_o and G_i are the shear moduli of the adherends. As a first approximation the adhesive shear strain is taken as

$$\gamma = \frac{(\delta_i - \delta_o)}{\eta} \quad . \tag{88}$$

Within the elastic region (of length d to be determined), the adhesive shear stress is assumed to be

$$\tau = G\gamma = \frac{G}{\eta}(\delta_i - \delta_o) = f(x) \tag{89}$$

(in which the unsubscripted G refers to the adhesive shear modulus) while, throughout the remaining (plastic) region, the adhesive shear stress is taken as

$$\tau = \tau_p = \text{constant} \quad . \tag{90}$$

Elimination of δ_i and δ_o, and S_i and S_o, in turn between equations (86) through (88) yields the boundary conditions

$$\frac{d\gamma}{dx} = \frac{1}{\eta}\left(-\frac{S_o}{G_o t_o} + \frac{S_i}{G_i t_i}\right) \tag{91}$$

and governing differential equation

$$\frac{d^2\gamma}{dx^2} - \frac{1}{\eta}\left(\frac{1}{G_o t_o} + \frac{2}{G_i t_i}\right)\tau = 0 \quad . \tag{92}$$

These equations have precisely the same form as equations (6) and (7), indicating that the same solutions may be employed with the equivalent parameters defined in Table I on the next page.

It follows, then, from equation (59) that the limiting strength for long overlap joints under in-plane shear loading is given by the lesser of

$$\left(\frac{\tau_{av}}{\tau_p}\right)(\lambda_s \ell) \rightarrow \sqrt{1 + 2\frac{\gamma_p}{\gamma_e}\left(1 + \frac{G_i t_i}{2G_o t_o}\right)} \tag{93}$$

and

38

$$\left(\frac{\tau_{av}}{\tau_p}\right)\left(\lambda_s \ell\right) \;\to\; \sqrt{1 + 2\,\frac{\gamma_p}{\gamma_e}\left(1 + \frac{2G_o t_o}{G_i t_i}\right)} \quad . \tag{94}$$

These equations may be re-arranged into the form of equation (22). That is, for stiffness-balanced adherends,

$$Q \;=\; 2\tau_{av}\ell \;=\; 4\sqrt{G_{adherend}t}\,\sqrt{n\tau_p\left(\frac{\gamma_e}{2} + \gamma_p\right)} \quad . \tag{95}$$

Since the shear modulus of conventional materials is less than the extensional moduli, the in-plane shear load capacity of a double-lap bonded joint is usually less than that for tensile shear. The exception is predominantly $\pm 45°$ cross-plied composite laminate adherends, for which G_{xy} is greater than E_x. Any adherend stiffness imbalance reduces the joint shear strength via the $(1 + GTR)$ / 2 factor equivalent to the $(1 + ETR)$ / 2 factor for tensile and compressive shear loading.

TABLE I. EQUIVALENT PARAMETERS FOR DIFFERENT LOAD CONDITIONS

Tensile/Compressive Shear Loading	In-Plane (Edgewise) Shear Loading
$\tau \;,\; \tau_p$	$\tau \;,\; \tau_p$
$\gamma \;,\; \gamma_e \;,\; \gamma_p$	$\gamma \;,\; \gamma_e \;,\; \gamma_p$
$G \;,\; n$	$G \;,\; n$
$\delta_i \;,\; \delta_o$	$\delta_i \;,\; \delta_o$
$E_i \;,\; E_o$	$G_i \;,\; G_o$
$T_i \;,\; T_o$	$S_i \;,\; S_o$
$\lambda^2 \;=\; \dfrac{G}{n}\left(\dfrac{1}{E_o t_o} + \dfrac{2}{E_i t_i}\right)$	$(\lambda_s)^2 \;=\; \dfrac{G}{n}\left(\dfrac{1}{G_o t_o} + \dfrac{2}{G_i t_i}\right)$
ℓ	ℓ
$\lambda\ell$	$\lambda_s\ell$
$ETR(i) \;=\; E_i t_i \;/\; 2E_o t_o$	$GTR(i) \;=\; G_i t_i \;/\; 2G_o t_o$
$ETR(o) \;=\; 2E_o t_o \;/\; E_i t_i$	$GTR(o) \;=\; 2G_o t_o \;/\; G_i t_i$

It is relatively simple to generalize the analysis above to the situation where simultaneously applied tensile (or compressive) and edgewise shear loads exist together. The former will develop a maximum bondline displacement of, say, $n(\gamma_{t,c})_{max}$ while the latter induces an orthogonal displacement of $n(\gamma_s)_{max}$. In the absence of any adherend thermal mismatch, these maximum bondline displacements will occur at the same end of the joint. Failure will occur when the RMS resultant exceeds the capacity of the adhesive. That is, when

$$n(\gamma_e + \gamma_p) = \sqrt{[n(\gamma_{t,c})_{max}]^2 + [n(\gamma_s)_{max}]^2} \, , \tag{96}$$

where the subscripts t and c refer to tension or compression, as appropriate.

Equation (96) affords a means of accounting for the influence of adherend thermal mismatch. For the postulated infinite cylinder, the thermal mismatch manifests itself exclusively in the adhesive axial shear strain $\gamma_{t,c}$. The magnitude of $\gamma_{t,c}$ derives from the general tensile/compressive shear analysis (Sections 2 through 5 and Appendix A.1) on setting $\tau_{av} \equiv 0$. That is, a given value of CTHERM will cause a certain value of $\gamma_{t,c}$, replacing the γ_p in formula (A.61). For moderately long overlaps, and sufficient thermal mismatch to induce plastic adhesive shear strain,

$$\left| \frac{(\alpha_i - \alpha_o)\Delta T \lambda}{\tau_p \left(\frac{1}{E_o t_o} + \frac{2}{E_i t_i} \right)} \right| = \left| CTHERM \right| \simeq \sqrt{1 + 2\frac{(\gamma_{t,c})_{max}}{\gamma_e}} \tag{97}$$

For only sufficient thermal mismatch to remain within the elastic capability of the adhesive, equation (97) is replaced by

$$\left| CTHERM \right| \simeq \sqrt{\frac{(\gamma_{t,c})_{max}}{\gamma_e}} \tag{98}$$

In combining $(\gamma_{t,c})_{max}$ with $(\gamma_s)_{max}$ it is necessary to check at both ends of the joint separately for the most severe resultant adhesive shear strain.

If the "cylinder" be slit, so as not to exclude edge effects from the problem, it is immediately apparent that any adherend thermal mismatch induces adhesive shear strains in both the "axial" and "circumferential" directions. It is quite straightforward to set up equations equivalent to (86) through (98) including thermal effects in both directions and the solution is readily deduced, along

40

the lines presented above. In this case, it is one of the four corners of the
bond which becomes critical, not an entire edge. The average bond stress which
can be carried may well be reduced significantly by any thermal mismatch effects
rendering one corner of the joint critical. The analysis necessarily includes
the thermal distortion of the adherends outside the joint area because such
thermal effects influence the adherend stresses at the boundary of the bond.
Consequently, no universal solutions can be produced. With the large variety
of locations possible for the critical bond shear strain in conjunction with the
large number of possibilities for plastic and/or elastic adhesive behavior in
the orthogonal directions, it is inappropriate to set up the differential
equations here.

10. MIXED-MODULUS ADHESIVE JOINTS

A significant effort has been devoted to the concept (Figure 18) of using a high-modulus adhesive in the central region of the joint and a low-modulus adhesive in the outer regions where the relative displacements between the adherends exceed the strain capabilies of the high-modulus adhesives. The aim is to stress the adhesive more highly in the relatively unloaded central region of the joint. The achievements hitherto have not been great in view of the expectations. In view of the predictions of the present analysis that practically all of the load is transferred in two narrow strips at the ends of the joint, it is worth examining this problem with the present mathematical model. An elastic analysis is presented in Reference 8 by Raphael.

In the ideal situation, one could consider that the use of mixed-modulus adhesives is equivalent to using a single hypothetical adhesive possessing the initial modulus of the stiff adhesive and the plastic strain capability of the ductile adhesive. For identical failure stresses, this analogy is precise if the stiff adhesive extends exactly to that position in the joint at which the ductile adhesive is just plastic. Under such conditions, since γ_p/γ_e is large in this application, increasing the shear modulus G has but a small effect on the strain energy and even less on the joint strength, since the respective joint strengths are shown in equation (22) to be proportional to $\sqrt{[\frac{1}{2}\gamma_e + \gamma_p]}$. The total displacement $n(\gamma_e + \gamma_p)$ remains unchanged. The effect of replacing the low-modulus inefficient elastic trough in the joint by another such trough with a higher modulus is minimal. Therefore, the use of a stiff adhesive in the center of the joint can improve the joint strength only little above that of which the ductile adhesive alone is capable. Indeed, during bonding, there is an inevitable tendency for the stiff adhesive to squeeze out and displace the ductile adhesive, to the extent that the effective strips may be less than dictated by equation (23). It is well nigh probable that a strength reduction will have been achieved. Such appears to have been the situation in the experiments reported in Reference 9.

In short, in comparison with a ductile adhesive, the small potential added strength to be achieved by use of the mixed-modulus adhesive concept appears

to be inadequate in the light of the production difficulties involved. Variable thickness adhesives or adherends seem to represent a more profitable approach to pursue. One seeks an adhesive film thickness approximately proportional to the adherend relative displacement (i.e., very thin in the middle where the displacement is least).

While the mixed-modulus adhesive concept has no practical merit in comparison with a ductile adhesive alone, it does offer advantages over a brittle adhesive alone. By softening the end zones of the joint, a strength increase must be obtained and a marked improvement derived with respect to the peel stress problem at the end of the joint (see Section 6). Therefore, in those high-temperature environments which preclude the efficient use of ductile adhesives, a brittle adhesive (which retains its strength at high temperature) may serve to transfer effectively all the shear load while the weaker ductile adhesive protects the ends of the overlap, enabling the brittle adhesive to develop a higher stress prior to failure than it could when acting alone.

11. PARAMETRIC EFFECTS AND JOINT EFFICIENCY CHARTS

The dominant characteristic of the load versus bond overlap relation for double-lap joints is the asymptotic strength for moderate to long overlaps, for which the joint strength is essentially constant. For short overlaps, the bond is uniformly stressed and the load is proportional to the overlap. For brittle adhesives there is a significant transition between these two limits, but most good structural adhesives have sufficient ductility for the transition to be ignored. Confining attention to the asymptotic solution clarifies the assessment of the influence of the various parameters.

From equation (A.61), the asymptotic joint strength is the lesser of

$$\left(\frac{\tau_{av}}{\tau_p}\right)\left(\frac{\lambda \ell}{2}\right) = \left[\sqrt{1 + 2\frac{\gamma_p}{\gamma_e}} + CTHERM(1)\right]\left[\frac{1 + ETR(1)}{2}\right] \tag{99}$$

and

$$\left(\frac{\tau_{av}}{\tau_p}\right)\left(\frac{\lambda \ell}{2}\right) = \left[\sqrt{1 + 2\frac{\gamma_p}{\gamma_e}} + CTHERM(2)\right]\left[\frac{1 + ETR(2)}{2}\right] . \tag{100}$$

These equations are expressed in non-dimensional form because of computational convenience and mathematical generality of the solutions so obtained. It is appropriate here to re-dimensionalize the equations. The joint strength can be shown to be the lesser of

$$P = 2\tau_{av}\ell = \sqrt{2\eta\tau_p(\tfrac{1}{2}\gamma_e + \gamma_p)2E_i t_i\left(1 + \frac{E_i t_i}{2E_o t_o}\right)} + (\alpha_o - \alpha_i)\Delta TE_i t_i \tag{101}$$

and

$$P = 2\tau_{av}\ell = \sqrt{2\eta\tau_p(\tfrac{1}{2}\gamma_e + \gamma_p)4E_o t_o\left(1 + \frac{2E_o t_o}{E_i t_i}\right)} + (\alpha_i - \alpha_o)\Delta T2E_o t_o . \tag{102}$$

In these equations, the quantity $2\tau_p\eta(\tfrac{1}{2}\gamma_e + \gamma_p)$ denotes the adhesive strain energy in shear per unit projected bond area. (There are two layers for a double-lap joint). No other adhesive property is involved in the strength expressions. This is why the precise shape of the stress-strain curve of the adhesive is relatively unimportant (see Section 3). Likewise, the thermal

mismatch and stiffness imbalance terms are confined to a single location. It is noteworthy that the length of the joint does not appear explicitly on the right hand side of equations (101) and (102). Its effect is implied in the restriction that the overlaps for which equations (101) and (102) apply exceed the transitional overlaps for fully-plastic behavior. The transitional overlap is, for all practical purposes,

$$\ell_{transitional} \simeq \frac{P}{2\tau_p} \tag{103}$$

for ductile adhesives. For brittle adhesives it is somewhat less than predicted by equation (103), but the overlap at which the asymptote is effectively reached is somewhat greater for brittle adhesives. The precise value of the transitional overlap is given by the lesser of equations (A.74) and (A.76).

It is interesting to observe that, in no place in equations (101) and (102) does the adhesive shear strain appear separately from the bond-line thickness. They always appear as a product. The important conclusion to be deduced from this is that it is the relative displacement across the bond-line which is most important and that the difficult-to-measure bond-line thickness need not be measured precisely at all. The appropriate characterization for an adhesive is a shear stress versus displacement record. This is not to imply that the thickness η is unimportant. Inasmuch as it influences the bond-line displacement at failure, η must be controlled. The stress-displacement curve for the adhesive must be derived from a torsion-ring or thick-adherend specimen simulating closely the thickness and processing (particularly cure temperature and pressure and heat-up rate) applicable to any design being investigated. The optimum bond-line thickness appears to be in the range 0.004 to 0.006 inch for ductile adhesives and 0.007 to 0.010 inch for brittle adhesives. For starved glue-lines, the loss in shear displacement restricts the strength while, for excessively thick glue-lines, the bond properties are usually deteriorated by voids. Nevertheless, if the voids are excluded by suitable processing and the stress-displacement record is obtained for the appropriate thickness of bond, there is no inherent physical reason prohibiting successful design and application of thick bond-lines.

Figure 3 shows the influence of adhesive ductility on the strength of balanced double-lap joints. Figures 11 and 12 quantify the reduction in the asymptotic

46

bond strengths due to adherend stiffness imbalance in the absence of thermal mismatch, while Figure 9 reveals how thermal mismatch between the adherends reduces the asymptotic strength of stiffness-balanced bonded joints. Figure 19 completes the characterization of the influence of the joint parameters by portraying the complete load versus overlap curves, in non-dimensional form, for selected cases including the transitional behavior.

The influence of the various parameters in dimensionalized form, accounting for the various possible modes of failure, is illustrated in Figures 20 and 21. The first pertains to 7075-T6 aluminum, while the second applies to high-strength graphite-epoxy (HTS or MODMOR II fibers). Both charts eliminate stiffness and/or thermal imbalance from consideration because their purpose is to reveal, without ambiguity, the interaction of the three basic failure modes. The inclusion of these omitted parameters is straightforward. The various material properties on which these charts are based are enumerated in Table II (p. 80). Unidentified idealized adhesives are used because of the lack of precise tension properties for thin films to quantify the peel-stress failure mode(s). The shear properties are representative of the best of 350 °F curing adhesives. Figures 20 and 21 are presented in terms of both maximum obtainable joint strength (with adequate overlap) and the joint efficiency defined as the ratio of joint strength to adherend strength. The minimum overlaps shown should be increased by an amount $3/\lambda$ to account for the elastic trough in the middle of the bonded joint. In addition, provision should be made for manufacturing tolerances. The overlaps shown actually define the extent of the effective end-zones in the adhesive.

The acute peel-stress problem with composite adherends is dramatically emphasized in Figure 21. For all but thin laminates, the ends of the outer adherends must be scarfed off to try to approach the bond shear strength potentials, The analysis method needs to be modified to account for the change in joint geometry (see Reference 6). Both Figures 20 and 21 confirm the merits of using ductile adhesives whenever the environment permits. (Plasticized adhesives show markedly inferior strengths to the unplasticized adhesives at temperatures above about 250 °F). It is obvious that, in assessing fatigue test data on the relative merits of ductile and brittle adhesives, one must make the comparison in terms of cycles to failure at a common adherend stress level, using identical

adherends, rather than in terms of percentage of static joint strength. The static strengths are too dissimilar to provide a meaningful reference for comparing fatigue test data.

The influence of temperature on the strength of bonded joints is manifest in changing adhesive characteristics. The same formulas apply, with the values of τ_p, γ_e, γ_p, $\sigma_{c_{max}}$, E_c etc., determined for the particular operating temperature. Briefly, as the temperature is reduced towards -67 °F, the adhesive becomes more brittle. However, the peak shear stress is increased also, so the change in shear strain energy is small. On the other hand, the peel-stress problem is aggravated by a reduction in operating temperature. An increase in temperature induces more ductility in an adhesive, with an associated reduction in peak shear stress. Again, the effect on strain energy is small for temperatures in the range 70 °F to 160 °F and the change in peel-stress phenomena is beneficial. The change in adhesive shear stress-strain curves with temperature is typified by the characteristics in Figure 22. Eventually, as the temperature is increased further, each adhesive suffers a rapid drop-off in strength, over a narrow temperature range, at a characteristic temperature. Examples of this are shown in Figure 23, using standard lap-shear data to characterize the strength losses. It is evident that the unplasticized adhesives exhibit superior strength retention in the range 200 °F to 400 °F. (Polyimides extend this range still higher, but with even less peel strength than the brittle epoxies).

The analysis of bonded joints at partial loads is accomplished by an inverse method. Instead of straining the bond-line to the maximum shear strain $(\gamma_e + \gamma_p)$, a lower maximum strain is adopted which permits sufficient extent of the plastic end zones to precisely balance the lesser load applied. This procedure is illustrated in Figure 24.

The various considerations above serve to identify the influence of the parameters governing the joint strength. The next section explains how to prepare charts for general use in double-lap bonded joint design. The information contained therein can be plotted in the form of P versus t diagrams, or η versus t diagrams such as Figures 20 and 21, for a specific design. Since the length of the joint is important only inasmuch as that a determinable minimum must be exceeded for given adherends, plots of load capacity versus overlap

48

become unnecessary. The various computations are based on the formulas

$$P = \sigma_y t \qquad \text{for adherend tensile failure outside the joint,} \qquad (104)$$

$$P = \sqrt{8E\tau_p \eta\left(\frac{\gamma_e}{2} + \gamma_p\right)t} \quad \propto \sqrt{t} \quad \text{for adhesive shear stress failure,} (105)$$

and

$$t \geq \left(\frac{\sigma_p}{\tau_p}\right)^4\left(\frac{2E\eta}{3(1 - \nu^2)E_c{}'}\right) \qquad \text{for adhesive (or adherend) peel} \qquad (106)$$
$$\text{stress failure.}$$

In these equations, t is the thickness of the inner adherend of stiffness-balanced joints made from the same adherend material throughout.

12. DESIGN METHOD

The objective of design in bonded joints should be to obtain the maximum possible bond strength from the minimum overlap, since this represents the least weight design. For maximum strengths which are governed by bond shear failures, this means effectively designing for the asymptotic (or plateau) strength levels and seeking the minimum length for obtaining a given percentage (say 99%) of that strength potential. It is evident from Figure 3 that this overlap is given by the non-dimensionalized overlap

$$(\lambda\ell)_{\text{practical design}} = (\lambda\ell)_{\text{transitional}} + 2 \; . \tag{107}$$

To this must be added a small tolerance for fabrication considerations and to provide adequate residual strength after long-term environmental exposure has destroyed the effectiveness of a narrow strip around the periphery of the bond but, in no circumstances, can any greater overlap be considered significantly more effective in transferring shear load. It should be self-evident from Figure 4 that the concept of designing by means of an average allowable bond shear stress (whether derived from single-lap shear tests or arrived at as an empirical low stress value) is at best cumbersome, because of the complex dependence of the average bond stress on the governing joint parameters, and probably unreliable because of frequent failure to account properly for all the variables. The alternative concept, advocated here, of designing in terms of running load in pounds per inch width of joint provides a simple and reliable technique when employed in conjunction with a check on ensuring the minimum adequate overlap. (In addition to this, for thicker adherends, it is necessary to check against peel-stress induced failures which represent another factor not covered by any average allowable shear stress method.)

The basis of the design method for shear is equations (101) and (102), re-arranged into the form

$$[2\tau_{av}\ell - (\alpha_o - \alpha_i)\Delta T E_i t_i] = \sqrt{2k\tau_p n(\gamma_e + \gamma_p)2E_i t_i\left(1 + \frac{E_i t_i}{2E_o t_o}\right)} \; , \tag{108}$$

and

51

$$[2\tau_{av}\ell - (\alpha_i - \alpha_o)\Delta T 2E_o t_o] = \sqrt{2k\tau_p n(\gamma_e + \gamma_p)4E_o t_o\left(1 + \frac{2E_o t_o}{E_i t_i}\right)} \quad , \qquad (109)$$

where

$$k = (\tfrac{1}{2}\gamma_e + \gamma_p) / (\gamma_e + \gamma_p) \qquad (110)$$

is determined from the adhesive stress-strain (or stress-displacement) characteristic. The same formula

$$(P - A)^2 = B \qquad (111)$$

is evaluated in turn for each end of the joint being assumed critical. The lower positive value of P is adopted and, if either estimate of P is negative, it must be concluded that the joint will break apart because of excessive internal thermal stresses. The necessary minimum overlap then follows from the approximation

$$\ell_{practical\ design} = \frac{P}{2\tau_p} + \frac{2}{\lambda} \quad , \qquad (112)$$

where

$$\lambda = \sqrt{\frac{G}{\eta}\left(\frac{1}{E_o t_o} + \frac{2}{E_i t_i}\right)} = \sqrt{\frac{\tau_p}{n\gamma_e}\left(\frac{1}{E_o t_o}\right)\left(1 + \frac{2E_o t_o}{E_i t_i}\right)} \quad . \qquad (113)$$

The elastic bond-line displacement $n\gamma_e$ can be estimated with sufficient accuracy from the adhesive shear-stress versus bond-line displacement characteristic. This potential bond shear strength should exceed by 50 per cent the adherend strength (or the design ultimate load for stiffness-critical structures).

The joint efficiency charts (Figures 20 and 21) indicate a need to ensure also that the adherends being joined are not so thick that peel stresses become a problem. The governing equation (83) is re-arranged to read

$$t_{o_{max}} = \frac{E_o \eta}{3(1 - \nu^2)}\left[\frac{1}{E_c} + \frac{k_1}{E_{in}} + \frac{k_2}{E_{on}}\right]\left(\frac{\sigma_p}{\tau_p}\right)^4 \qquad (114)$$

in which σ_p is the adhesive (or interlaminar tension) allowable peel stress. The thickness $t_{o_{max}}$ refers to the maximum thickness of the outer adherends which will not be associated with peel problems. For design purposes, in order to maintain a potential strength margin of 50 per cent for the bond or 25 per cent

for the laminate, major reductions are necessary. The factors are $(2/3)^4 = 0.198$ for adhesive-governed failures and $(4/5)^4 = 0.419$ for inter-laminar tension failures. The effect of such reduction factors, which account principally for manufacturing deviations and environmental degradation, is to restrict the thickness of the ends of the outer adherends. Even within the confines of a basic double-lap configuration (and without the expense of a true scarf joint) a superior joint can be formed by tapering the ends of the outer adherends (see Figure 13) to alleviate the potential peel-stress problems.

13. CONCLUSIONS

The behavior of adhesive-bonded double-lap joints under static load is found to be amenable to an analytic solution encompassing the effects of adhesive plasticity, adherend thermal mismatch and adherend stiffness imbalance. In addition, the failure mode associated with peel stresses rather than shear stresses in the adhesive is analyzed and an explicit solution derived. All the physical material properties needed to employ these analyses as a basis for rational design have been identified explicitly. They include stress-strain curves for adhesive films in shear bonded to torsion-ring or thick-adherend specimens, obtained for a range of temperatures covering the operating environment. The need for the tensile characteristics for the same constrained films becomes apparent when potential peel-stress failure modes are examined. Much of the past discrepancy between theory and experiment can be ascribed to having omitted consideration of adhesive plasticity and peel stresses.

While the analysis is concerned significantly with adding adhesive plasticity to published linear elastic solutions, it becomes evident that the mathematical ease of omitting the elastic portion of the characteristic completely and obtaining upper- and lower-bound solutions associated with the equivalent adhesive characteristics shown in Figure 25 has considerable merit. This is particularly so for the ductile adhesives used in subsonic airframe manufacture because such a great fraction of the load is carried by the plastic part of the adhesive behavior.

It is shown that the appropriate basis for design is the average bond stress for very short overlaps only, and is the joint strength for longer overlaps because the strength becomes independent of overlap rapidly as the overlap increases. A direct simple technique is presented based on three simple computations: the first provides the joint strength for balanced joints, the second a strength increment (usually negative) for thermal effects, while the third completes the design with a factor (usually a reduction) accounting for adherend stiffness imbalance. An unbalanced joint must be inherently weaker than a joint between identical adherends for at least one load direction, be it tensile or compressive lap shear.

The key concept of the analysis and design method is the limited effective zones at the ends of the joint, through which most of the load is transferred, while the remainder of the bond is relatively inefficient. An assessment of the efficiency of bonded double-lap joints must conclude that they are 100 per cent efficient for thin adherends, becoming less so for thicker adherends, particularly for the case of brittle adhesives. The analyses provide the means for identifying unambiguously at what thickness the loss of efficiency is sufficient to justify the use of the more efficient tapered-lap joint and even the more difficult to manufacture stepped-lap or scarf joints. Even the latter is not perfectly efficient for unbalanced adherends, as is discussed in Reference 10.

More work remains to be done on this problem, particularly experimental work on the peel-stress problem. It is hoped that these explicit analytical solutions may serve as a reference to direct the experimental effort along a fruitful path now that the quantities needed for rational design have been positively identified.

REFERENCES

1. Volkersen, O., "Die Nietkraftverteilung in Zugbeanspruchten Nietverbindungen mit Konstanten Laschen-querschnitten," Luftfahrtforschung 15, 4-47 (1938).

2. Goland, M. and Reissner, E., "The Stresses in Cemented Joints," J. Appl. Mech. 11, A17-A27 (1944).

3. Plantema, F. J., Nat. Luchtavaartlaboratorium, Amsterdam, Report 1181.

4. Szepe, F., "Strength of Adhesive-Bonded Lap Joints with Respect to Change of Temperature and Fatigue," Experimental Mechanics 6, 280-286 (1966).

5. Teodosiadis, R., "Plastic Analysis of Bonded Composite Lap Joints," Douglas Aircraft Company Report No. DAC-67836, May 1969.

6. Hart-Smith, L. J., "Non-Classical Adhesive-Bonded Joints in Practical Aerospace Construction," Douglas Aircraft Co., NASA Langley Report CR-112238, January 1973.

7. Ljungstrom, O., "Design Aspects of Bonded Structures I," Bonded Aircraft Structures, CIBA (A.R.L.) Conference, Duxford, Cambridge, 1957, pp. 11-32.

8. Raphael, C., "Variable-Adhesive Bonded Joints," Applied Polymer Symposia No. 3, Structural Adhesives Bonding, (Editor, Bodnar, M. J.), pp. 99-108, Interscience (1966).

9. Clark, G. A. and Clayton, K. I., "Fabrication Techniques for Advanced Composite Attachments and Joints," North American Rockwell Corp., Technical Report AFML-TR-69-151, pp. 36-38, May 1969.

10. Hart-Smith, L. J., "Adhesive-Bonded Scarf and Stepped-Lap Joints," Douglas Aircraft Co., NASA Langley Report CR-112237, January 1973.

11. de Bruyne, N. A., "The Strength of Glued Joints," Aircraft Engineering 16, 115-118, 140 (1944).

UNLOADED JOINT

JOINT GEOMETRY

LOADED JOINT WITH INEXTENSIBLE ADHERENDS

ADHESIVE SHEAR STRESS

LOADED JOINT WITH ELASTIC ADHERENDS

ADHESIVE SHEAR STRAIN
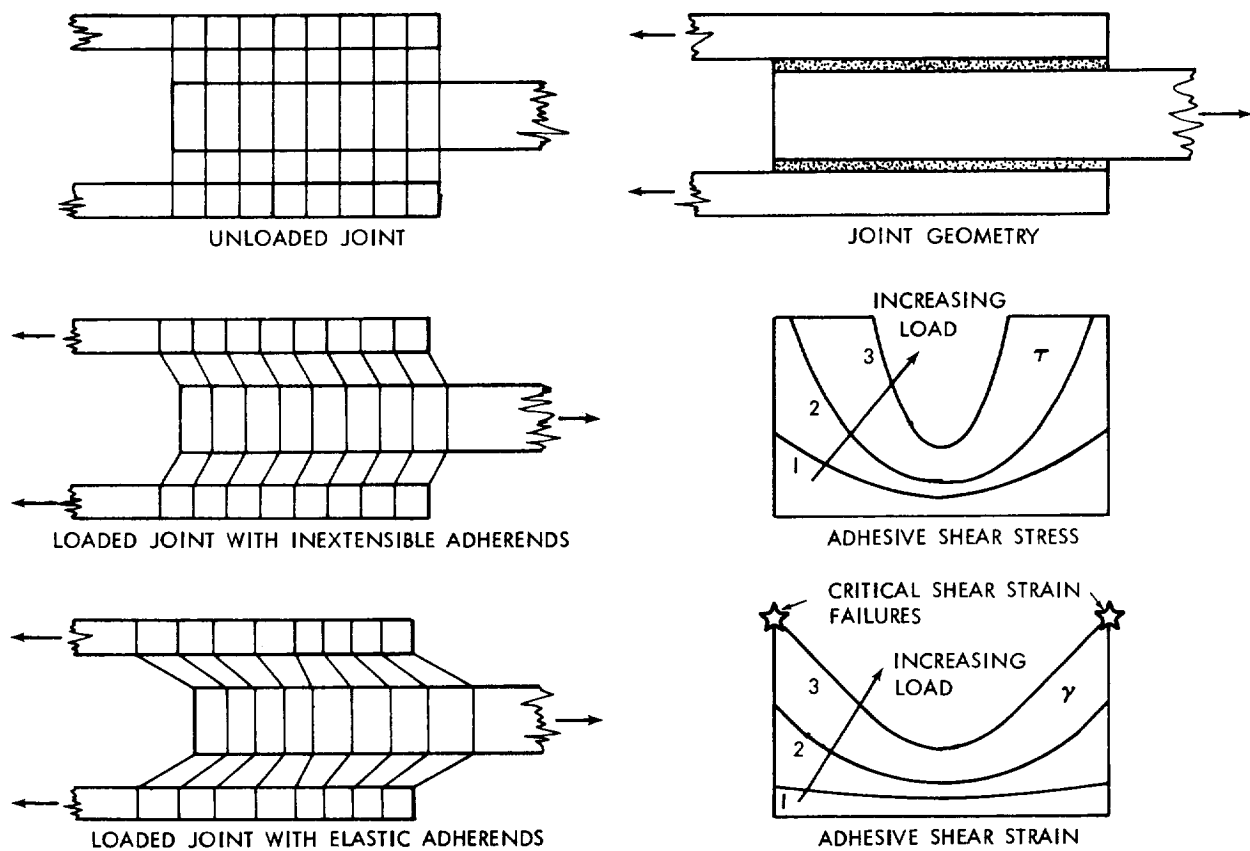
FIGURE 1.   SCHEMATIC EXPLANATION OF SHEARING IN ADHESIVE

GEOMETRY

YOUNG'S MODULUS E

$\frac{P}{2}$

$\frac{P}{2}$

$(=\tau_{av}l)$

SHEAR MODULUS G

2τ

ADHESIVE BEHAVIOUR

PLASTIC | ELASTIC | PLASTIC

d

l

Δx (REFERENCE)

δ_0

$\left(1 + \frac{T_0}{E_0 t_0}\right)\Delta x$

$\delta_0 + \left(\frac{d\delta_0}{dx}\right)\Delta x$

$T_0 \longleftarrow \qquad \longrightarrow T_0 + \left(\frac{dT_0}{dx}\right)\Delta x$

$\tau \Delta x$

$\tau \Delta x$

$T_i \longleftarrow \qquad \longrightarrow T_i + \left(\frac{dT_i}{dx}\right)\Delta x$

$\tau \Delta x$

$\left(1 + \frac{T_i}{E_i t_i}\right)\Delta x$

δ_i

$\delta_i + \left(\frac{d\delta_i}{dx}\right)\Delta x$

Δx (REFERENCE)
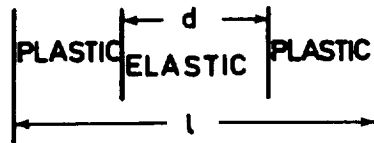
DISPLACEMENTS AND FORCES

FIGURE 2.   CO-ORDINATE SYSTEM AND DEFORMATIONS IN BONDED JOINTS
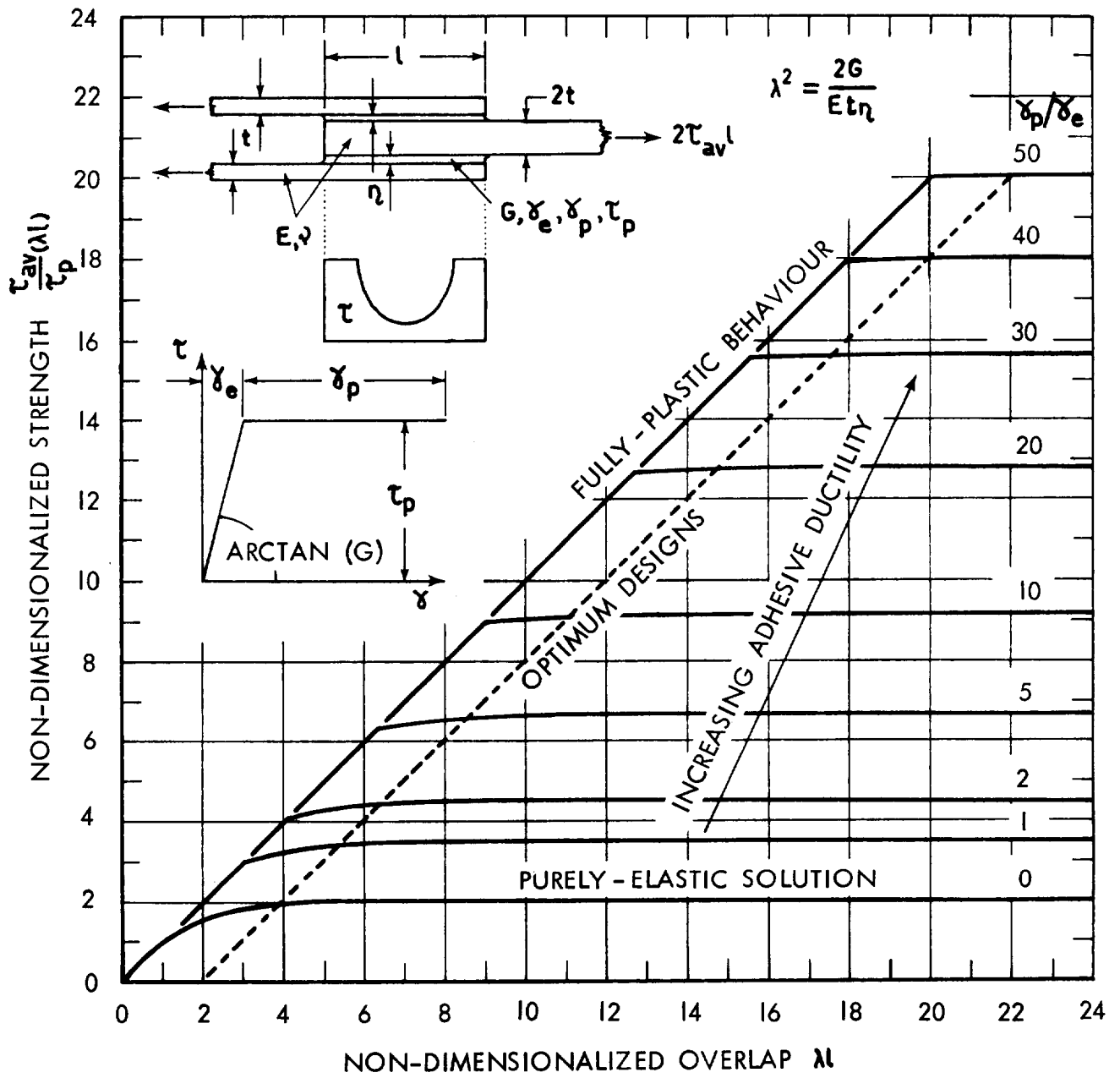
FIGURE 3. SHEAR STRENGTH OF DOUBLE-LAP BONDED JOINTS
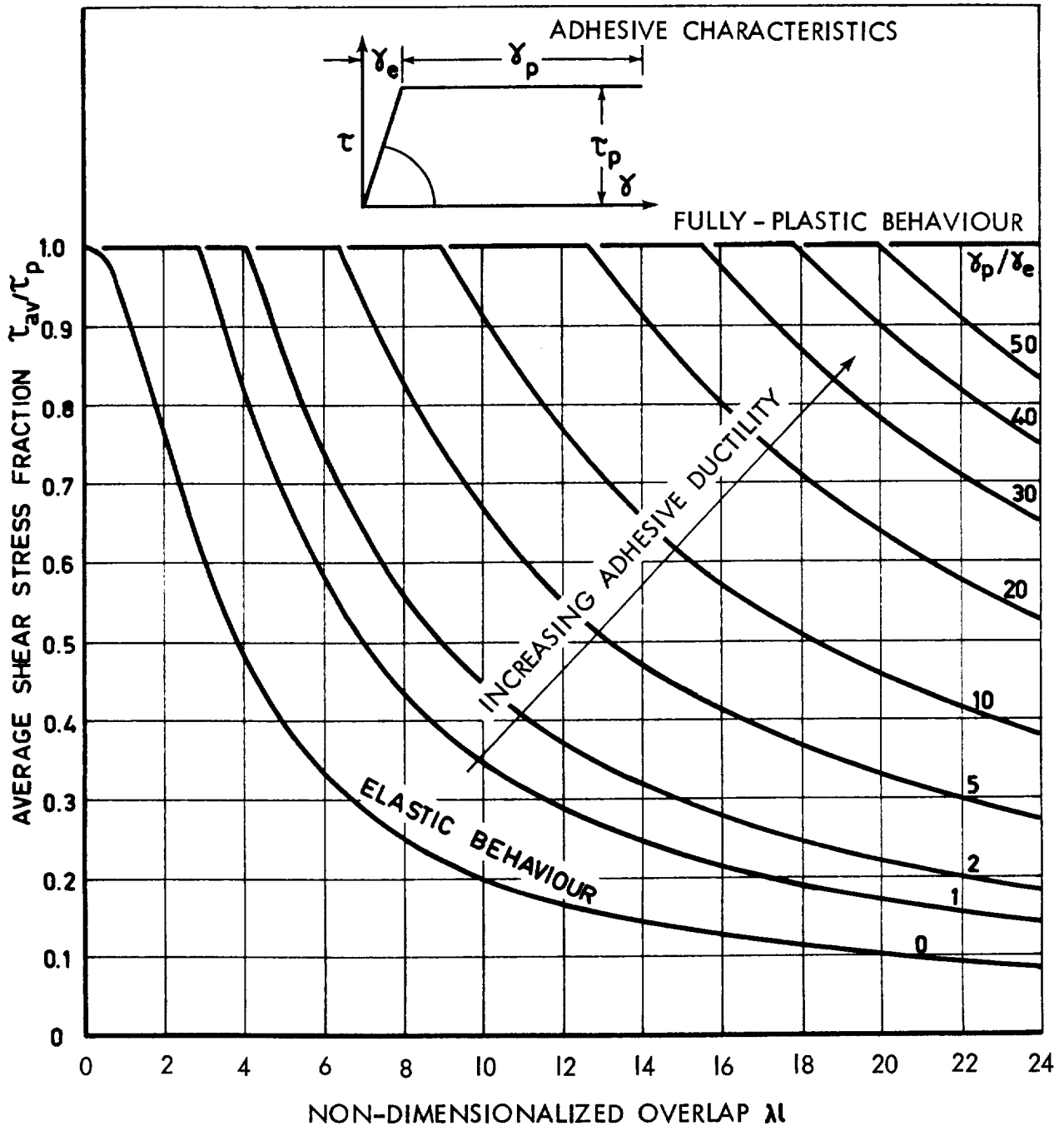
FIGURE 4. AVERAGE SHEAR STRESSES IN DOUBLE-LAP ADHESIVE BONDS
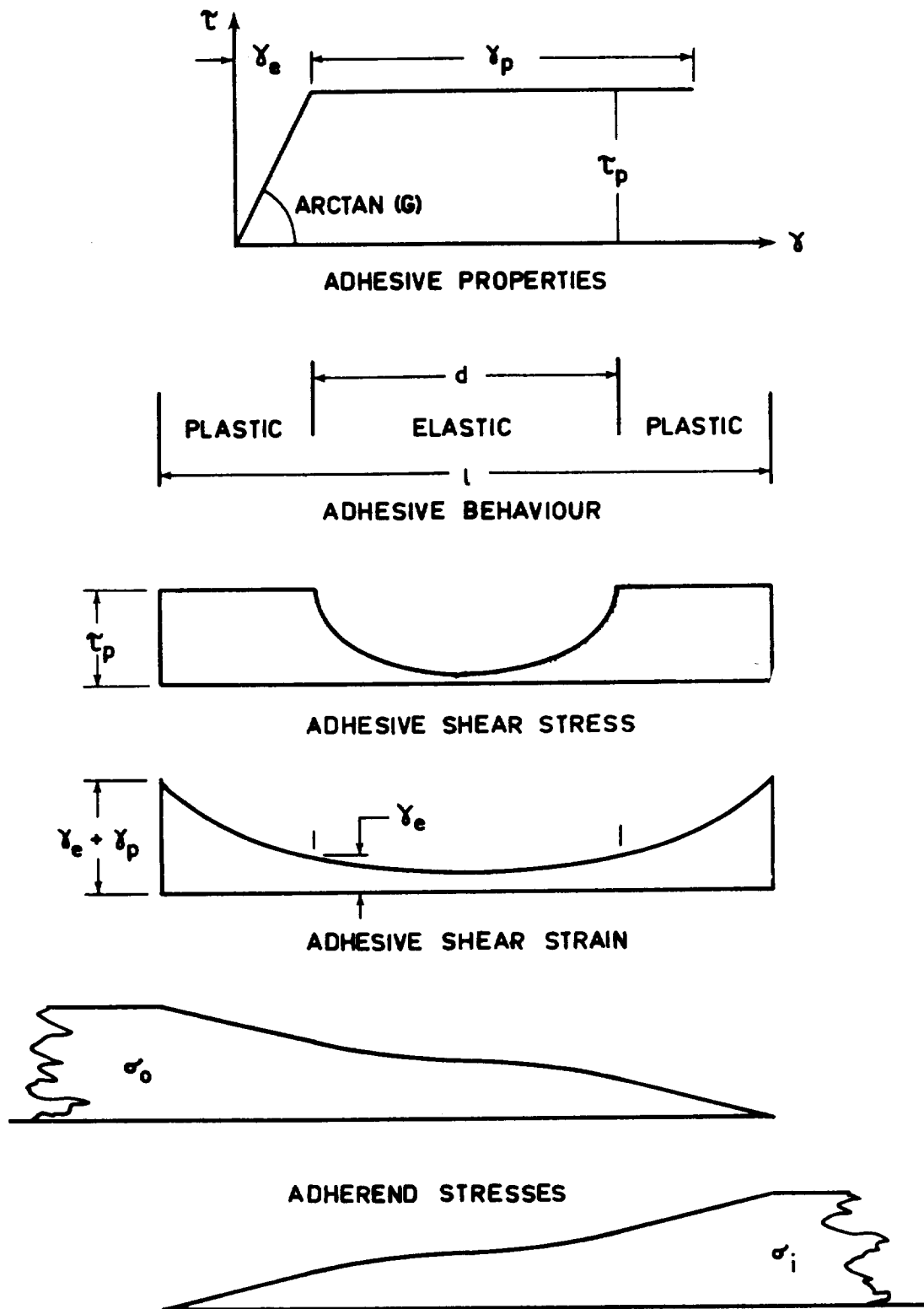
FIGURE 5. STRESSES AND STRAINS IN BONDED JOINTS
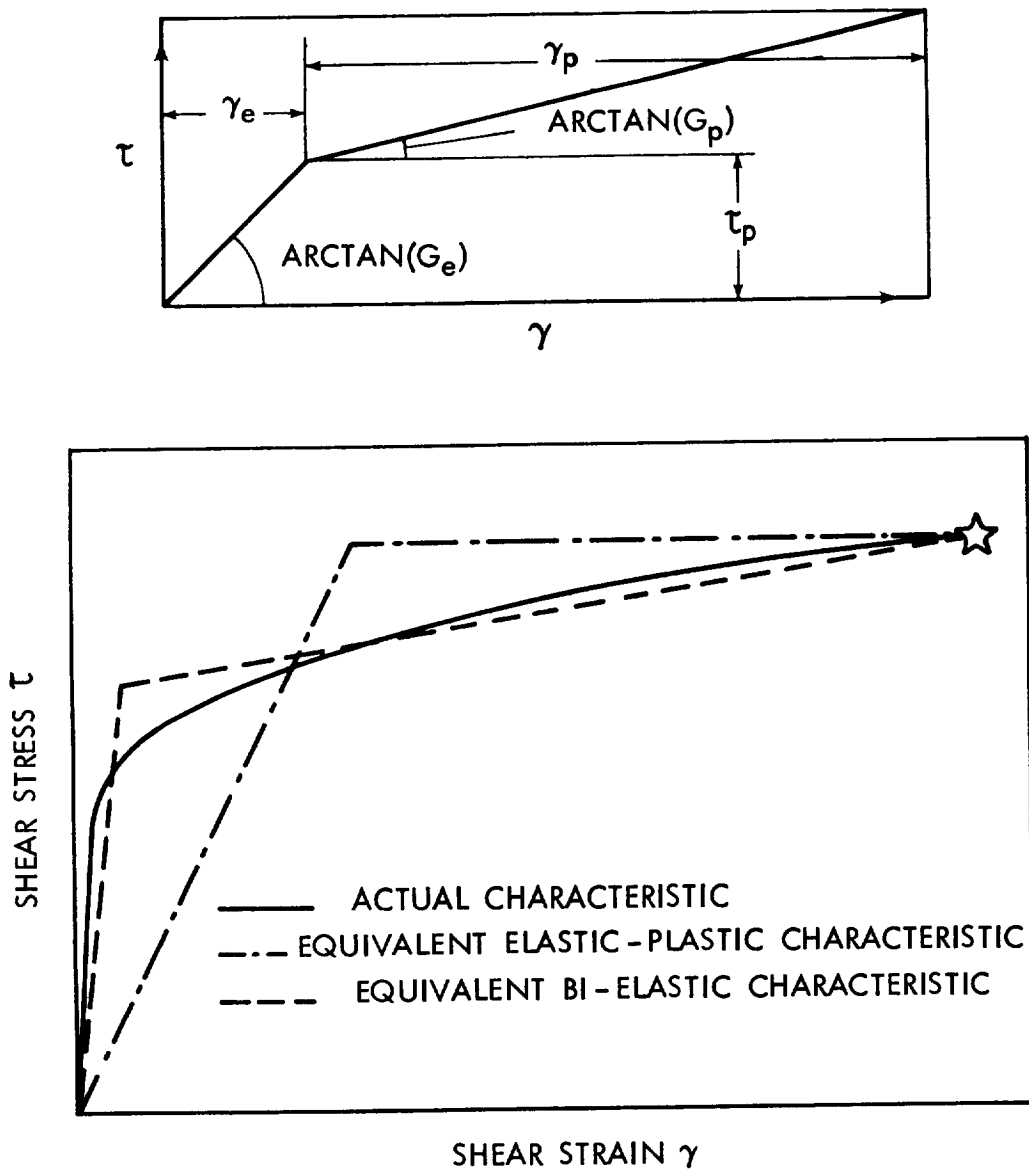
FIGURE 6. ANALYTICAL REPRESENTATIONS FOR ACTUAL ADHESIVE
CHARACTERISTICS

COMPOSITE

METAL

COMPOSITE

UNLOADED JOINT
(SHOWING RESIDUAL DEFORMATIONS
DUE TO THERMAL MISMATCH)

TENSILE SHEAR LOAD
(LEFT END CRITICAL)

COMPRESSIVE SHEAR LOAD
(RIGHT END CRITICAL)

JOINT GEOMETRY

τ

RESIDUAL STRESSES

γ

RESIDUAL STRAINS

INCREASING LOAD

1 2 3

τ

ADHESIVE SHEAR STRESS

CRITICAL SHEAR STRAIN FAILURE

INCREASING LOAD

3

2

1

γ

ADHESIVE SHEAR STRAIN
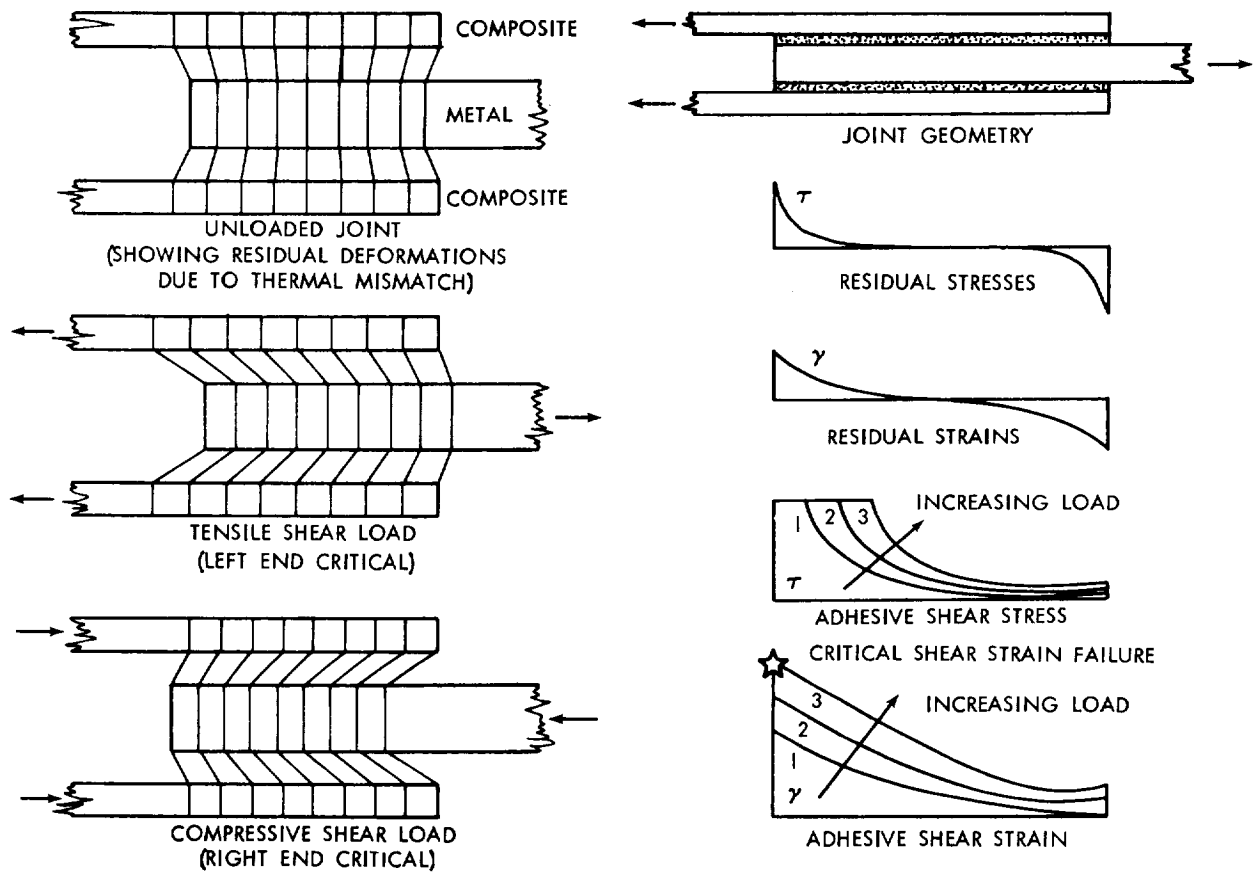
FIGURE 7.   DEFORMATIONS AND ADHESIVE SHEAR STRAINS IN THERMALLY-
MISMATCHED BONDED JOINTS
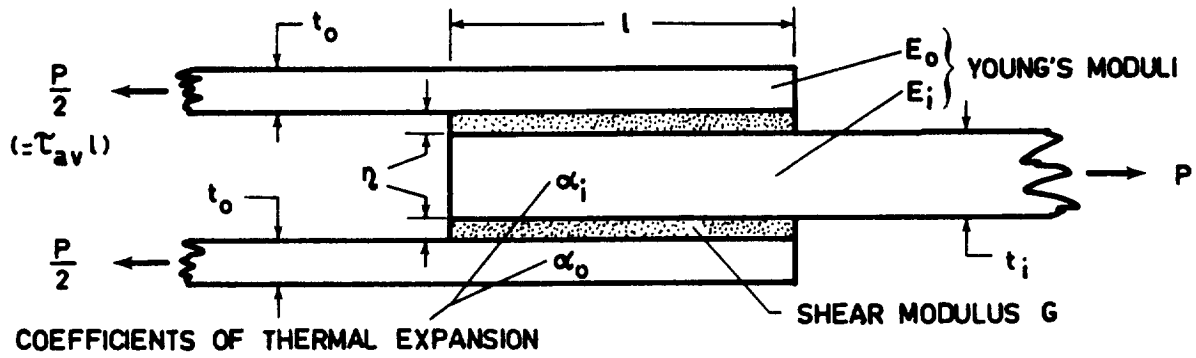
GEOMETRY

ADHESIVE BEHAVIOUR

$$\left(1 + \frac{T_o}{E_o t_o} + \alpha_o \Delta T\right)\Delta x$$

$$\delta_o + \left(\frac{d\delta_o}{dx}\right)\Delta x$$

$$T_o \quad T_o + \left(\frac{dT_o}{dx}\right)\Delta x$$

$$\tau \Delta x$$

$$\tau \Delta x$$

$$T_i \quad T_i + \left(\frac{dT_i}{dx}\right)\Delta x$$

$$\tau \Delta x$$

$$\left(1 + \frac{T_i}{E_i t_i} + \alpha_i \Delta T\right)\Delta x$$

$$\delta_i + \left(\frac{d\delta_i}{dx}\right)\Delta x$$

DISPLACEMENTS AND FORCES
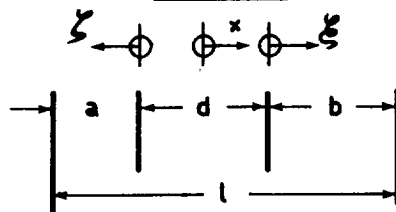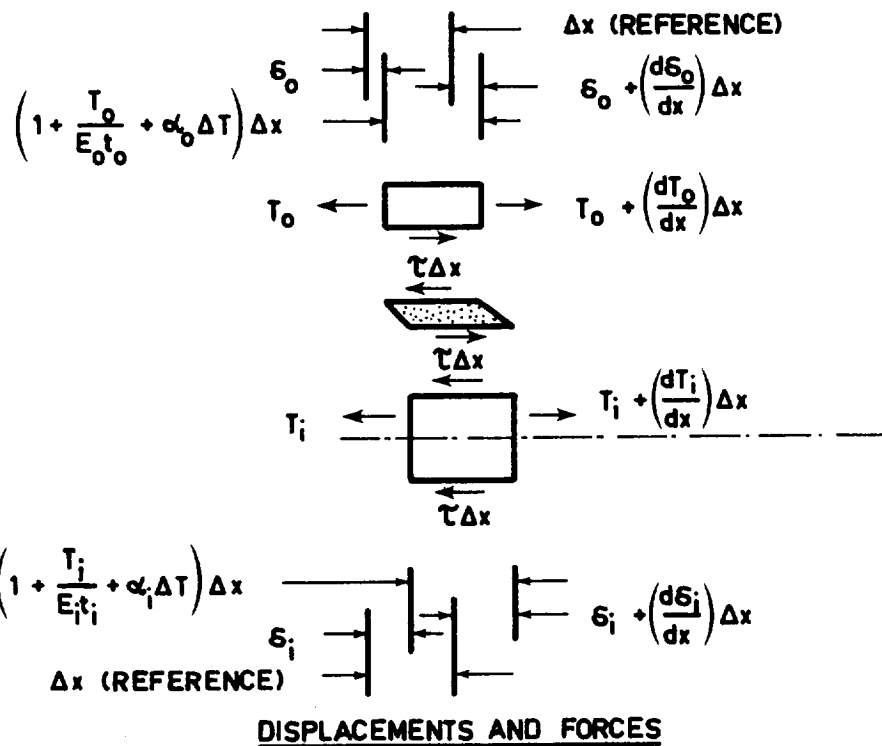
FIGURE 8. CO-ORDINATE SYSTEM AND DEFORMATIONS IN BONDED JOINTS (DISSIMILAR ADHERENDS)
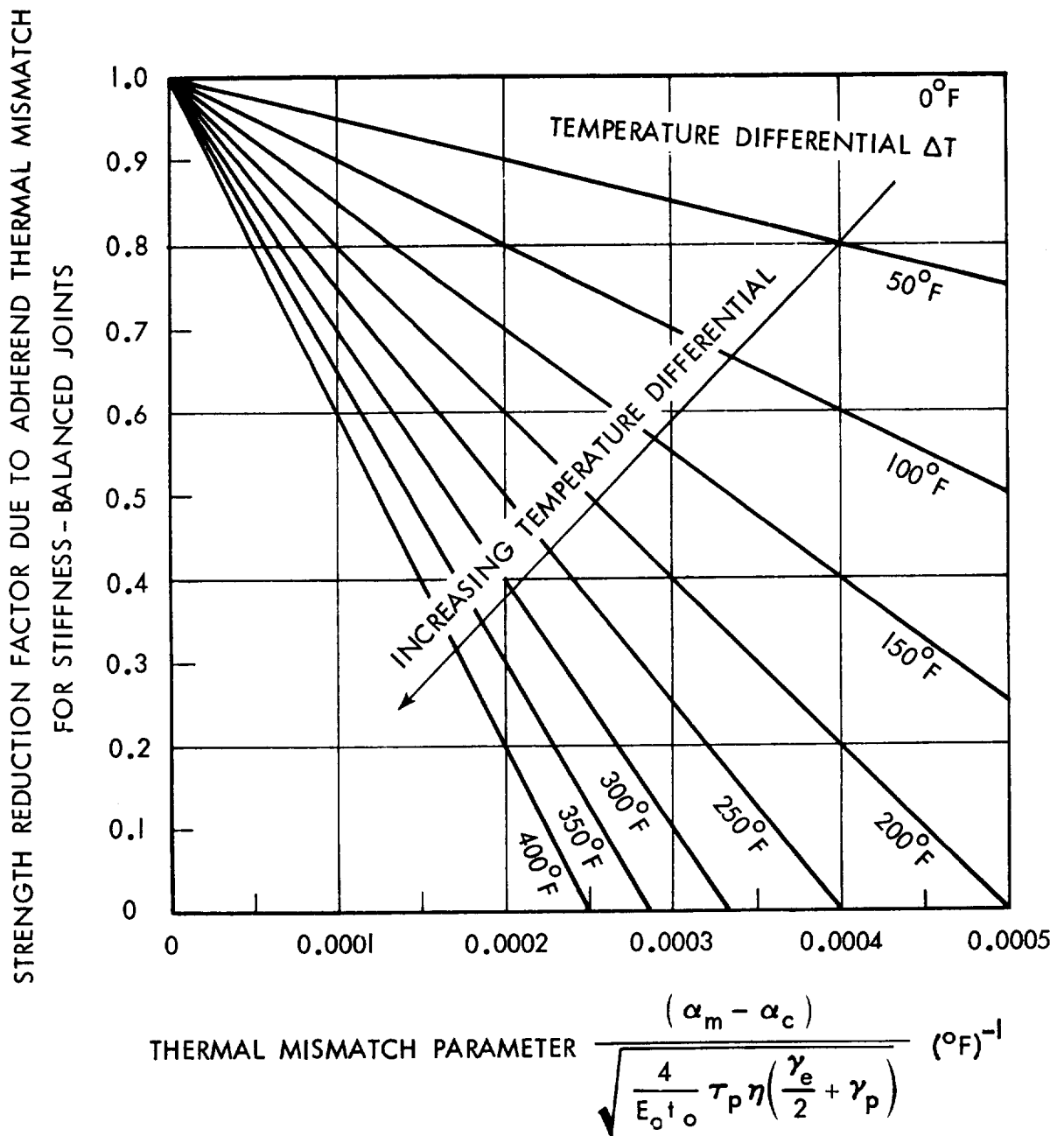
FIGURE 9. STRENGTH REDUCTION FACTOR IN DOUBLE-LAP BONDED JOINTS, DUE TO ADHEREND THERMAL MISMATCH

67

UNLOADED JOINT

JOINT GEOMETRY

TENSILE SHEAR LOAD

INCREASING LOAD

3

2

τ

1

ADHESIVE SHEAR STRESS

RIGHT END CRITICAL
FOR BOTH CONDITIONS

CRITICAL SHEAR STRAIN FAILURE

INCREASING LOAD

3

2

γ

1

COMPRESSIVE SHEAR LOAD

ADHESIVE SHEAR STRAIN
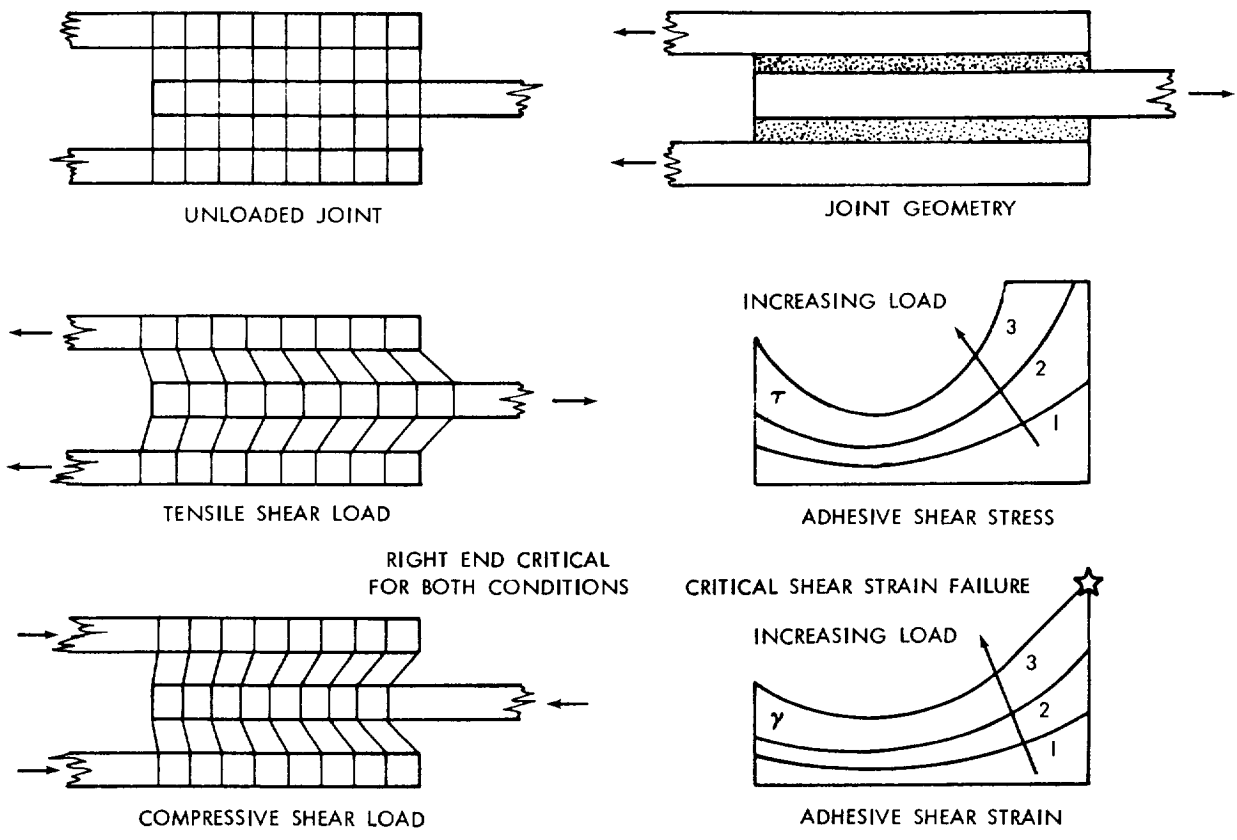
FIGURE 10. DEFORMATIONS AND ADHESIVE SHEAR STRAINS IN STIFFNESS-
UNBALANCED BONDED JOINTS
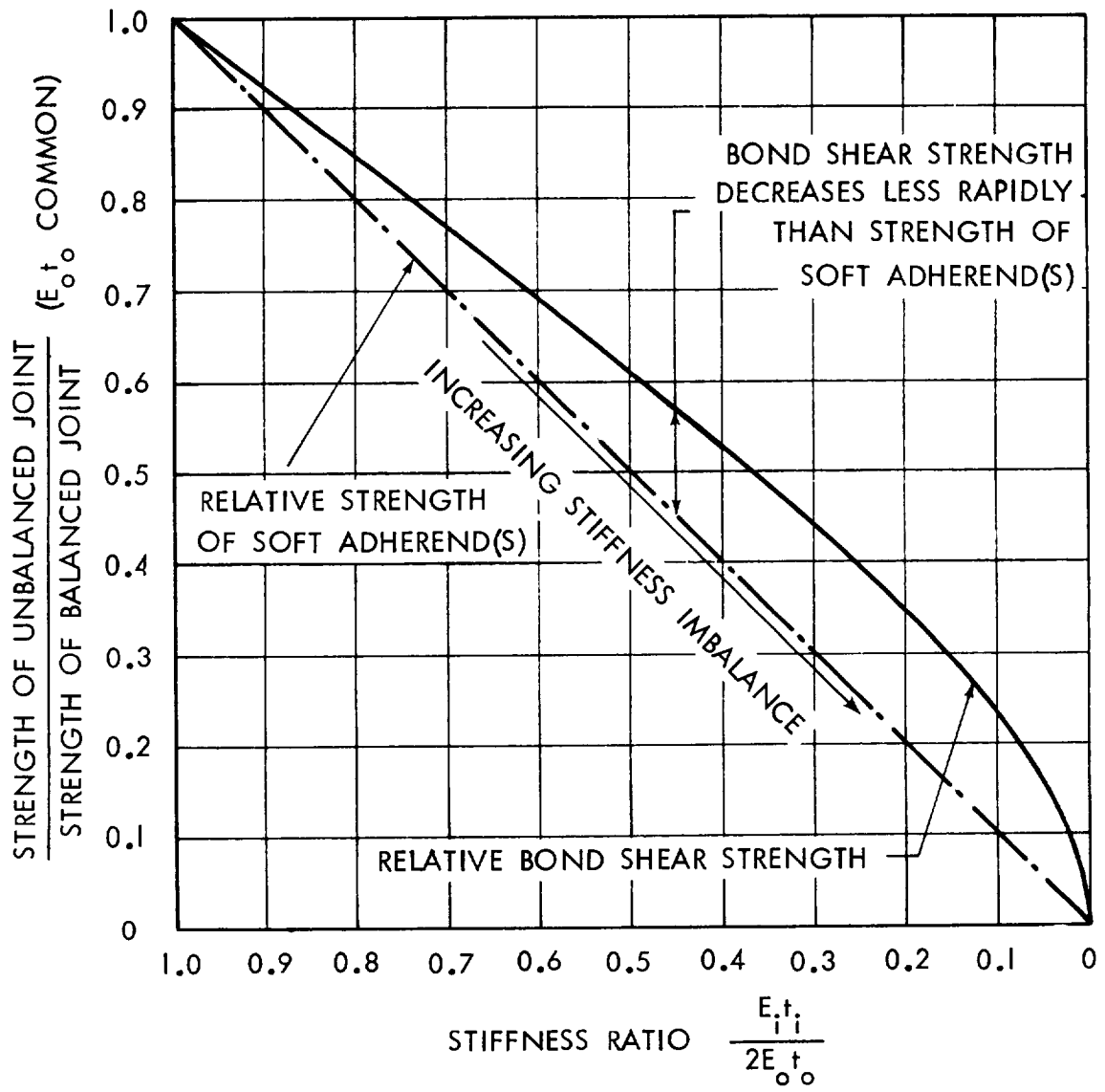
FIGURE II. STRENGTH REDUCTION FACTOR IN DOUBLE-LAP BONDED JOINTS, DUE TO ADHEREND STIFFNESS IMBALANCE
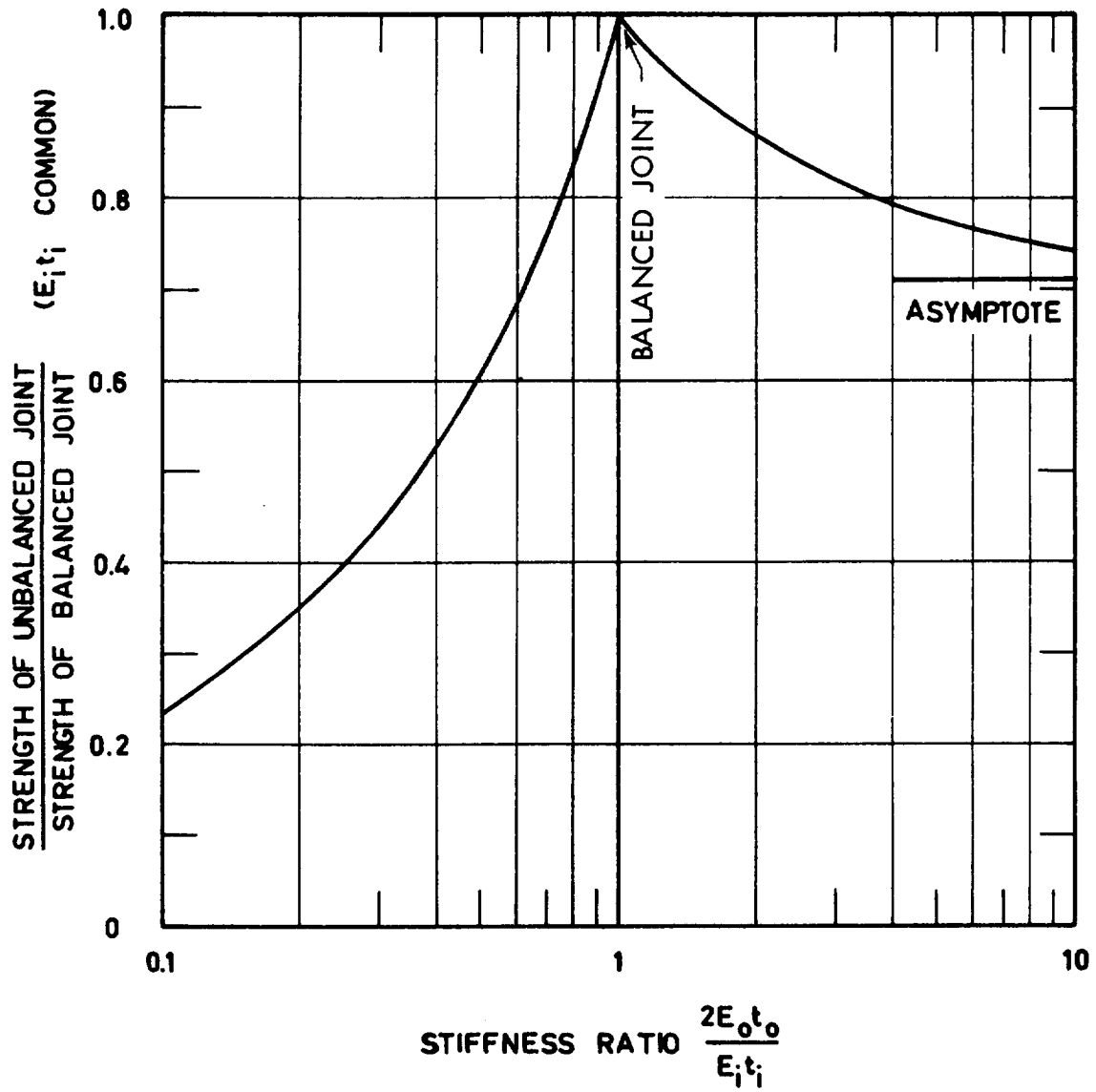
FIGURE 12. STRENGTH REDUCTION IN BONDED JOINTS DUE TO ADHEREND
STIFFNESS IMBALANCE

CHARACTERISTIC FAILURE MODE
FOR THICK COMPOSITE ADHERENDS

ALTERNATIVE PEEL STRESS
RELIEF TECHNIQUES

BOND PEEL STRESSES

REDUCED BOND PEEL STRESSES

ASSOCIATED SHEAR STRESSES

HIGHER AVERAGE SHEAR STRESS
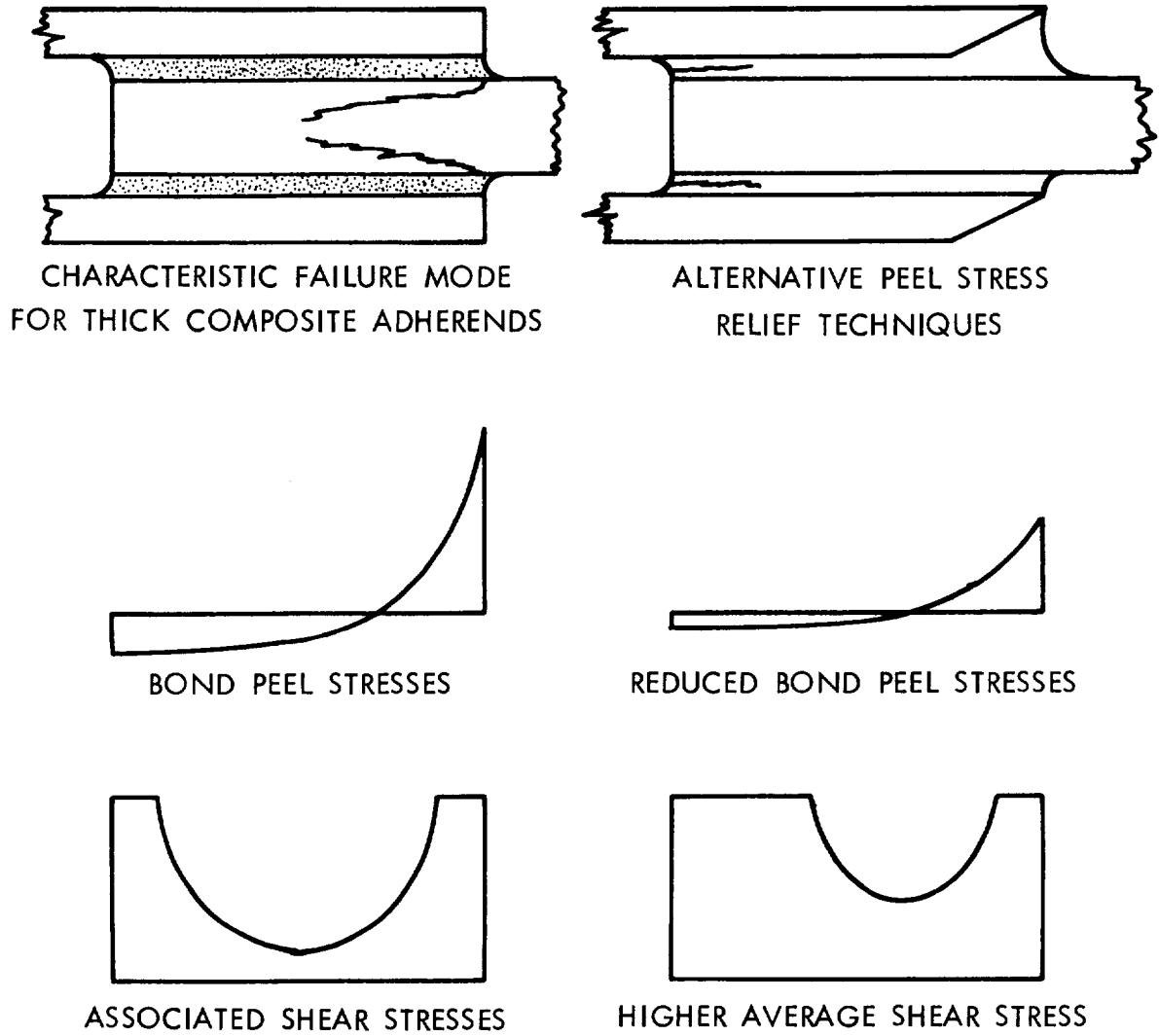
FIGURE 13. PEEL-STRESS FAILURE OF THICK COMPOSITE BONDED JOINTS
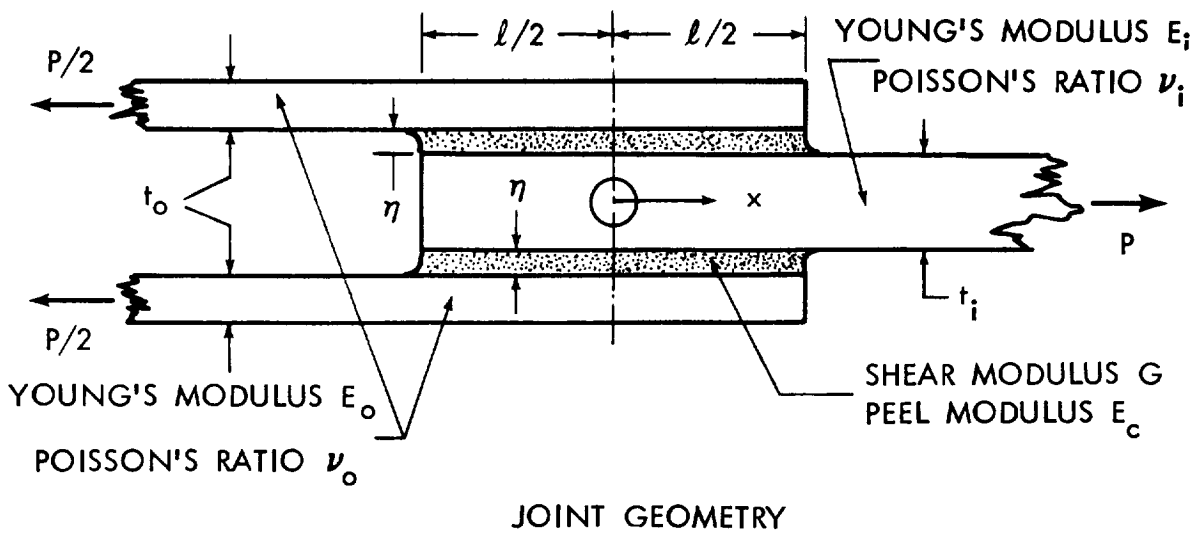
JOINT GEOMETRY
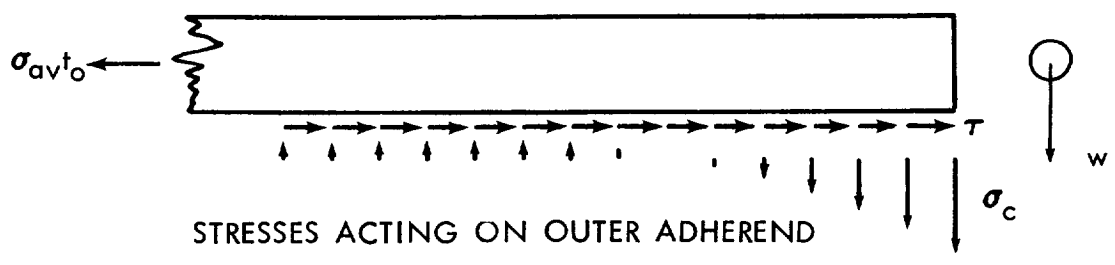
STRESSES ACTING ON OUTER ADHEREND
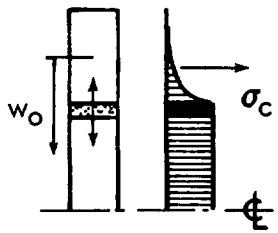
PEEL STRESS
DISTRIBUTION
THROUGH THICKNESS
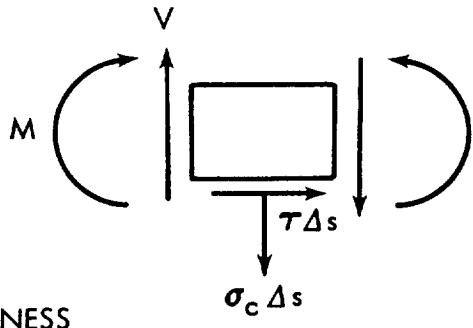
ELEMENT LOADS FOR OUTER ADHEREND

FIGURE 14. CO-ORDINATE SYSTEM AND PEEL DEFORMATIONS IN DOUBLE-LAP
BONDED JOINTS
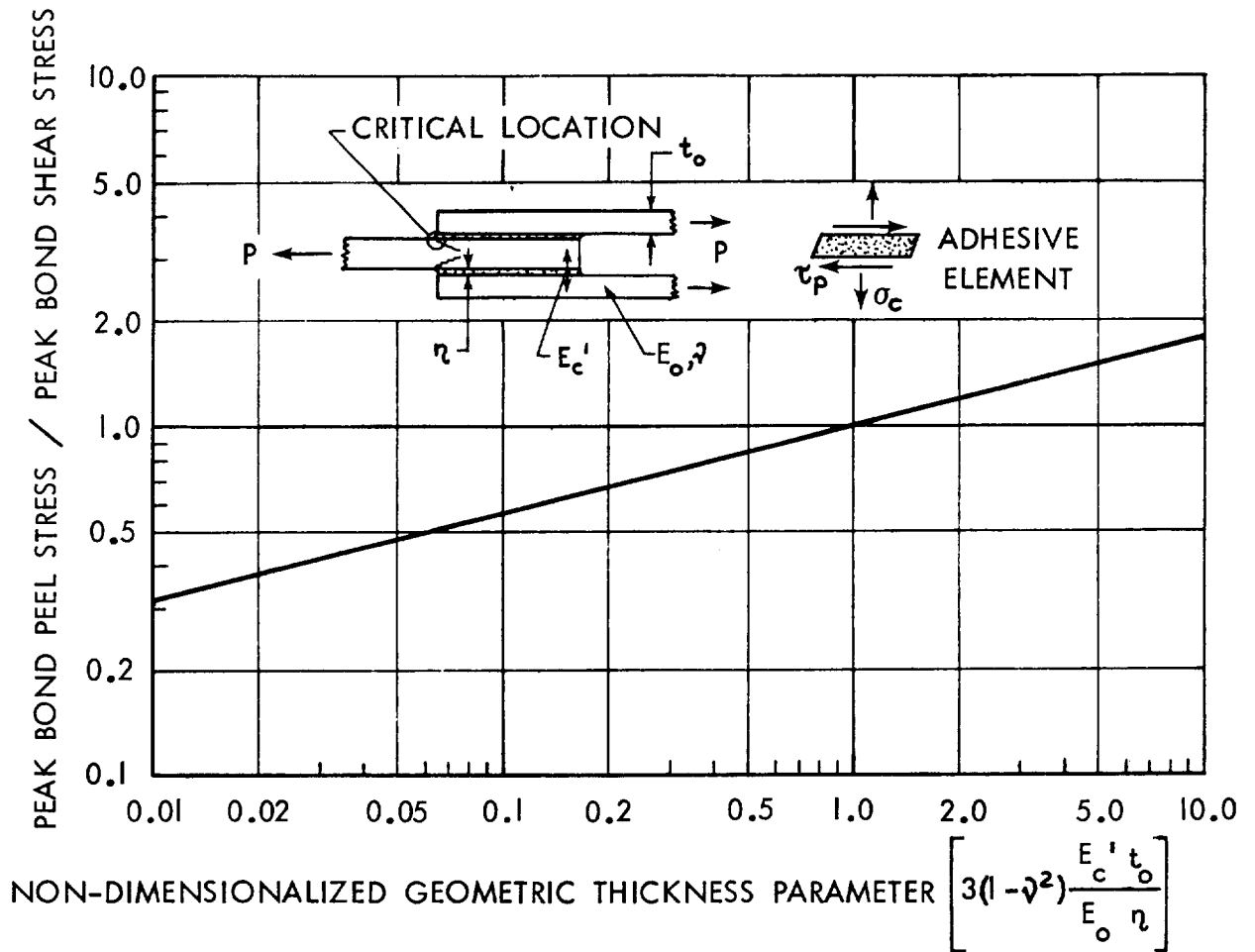
FIGURE 15. ELASTIC PEEL STRESSES IN DOUBLE-LAP BONDED JOINTS
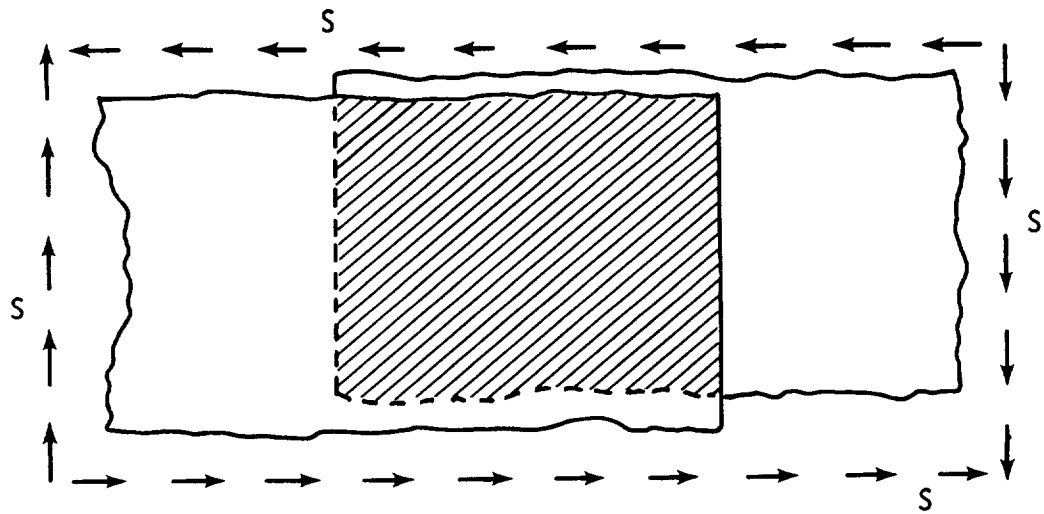
LAP JOINT IN EDGEWISE SHEAR

ADHESIVE SHEAR STRAIN DISTRIBUTION
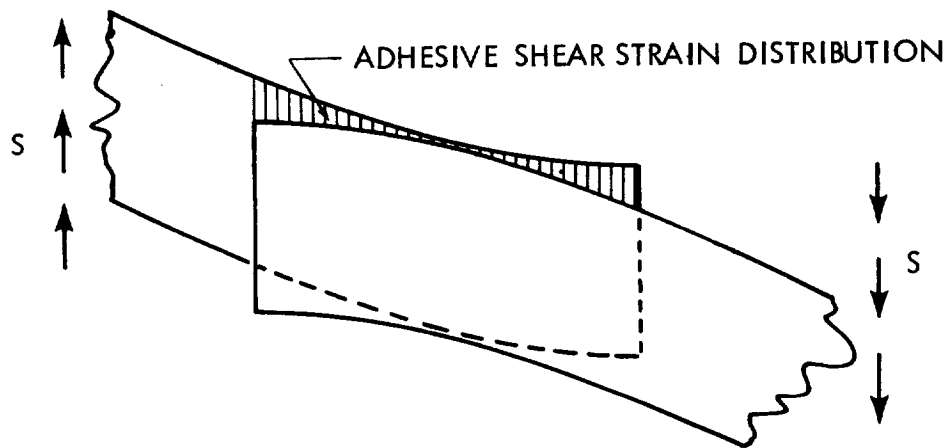
SHEAR DEFORMATION (EXAGGERATED)

σ

ADHEREND SHEAR STRESS DISTRIBUTION

τ

ADHESIVE SHEAR STRESS DISTRIBUTION

FIGURE 16. ADHESIVE-BONDED JOINT LOADED BY IN-PLANE SHEAR

JOINT GEOMETRY

REFERENCE

$$\delta_o + \left(\frac{d\delta_o}{dx}\right)\Delta x$$

REFERENCE

δ_o

E = YOUNG'S MODULUS
OF ADHEREND(S)
G = SHEAR MODULUS
OF ADHESIVE

Δx

$S_o \quad S_o + \left(\frac{dS_o}{dx}\right)\Delta x$

$\tau \Delta x$

$\tau \Delta x \quad \tau \Delta x$

I UNIT

$\tau \Delta x$

$S_i \quad S_i + \left(\frac{dS_i}{dx}\right)\Delta x$

REFERENCES

$$\delta_i + \left(\frac{d\delta_i}{dx}\right)\Delta x$$

δ_i

ELEMENT FORCES AND DISPLACEMENTS
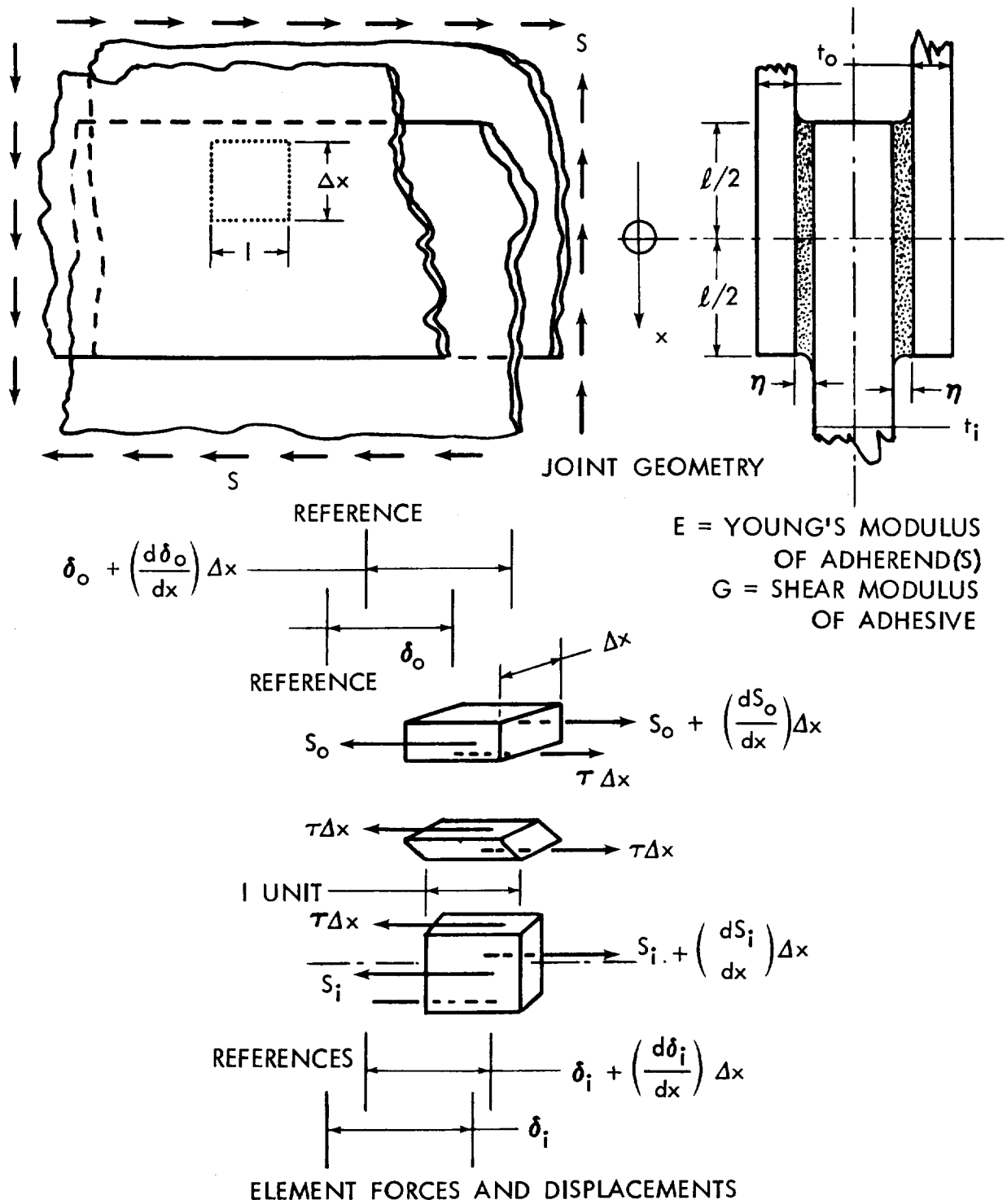
FIGURE 17.   CO-ORDINATE SYSTEM AND SHEAR DEFORMATIONS IN BONDED
JOINT UNDER IN-PLANE SHEAR

SINGLE DUCTILE ADHESIVE

MIXED-MODULUS ELASTIC ADHESIVES

HIGH-MODULUS
LOW-MODULUS

MIXED-MODULUS
ELASTIC AND PLASTIC ADHESIVES

ELASTIC
PLASTIC

MIXED-MODULUS
INSUFFICIENT LOW-MODULUS
ADHESIVE — JOINT STRENGTH
DEGRADED
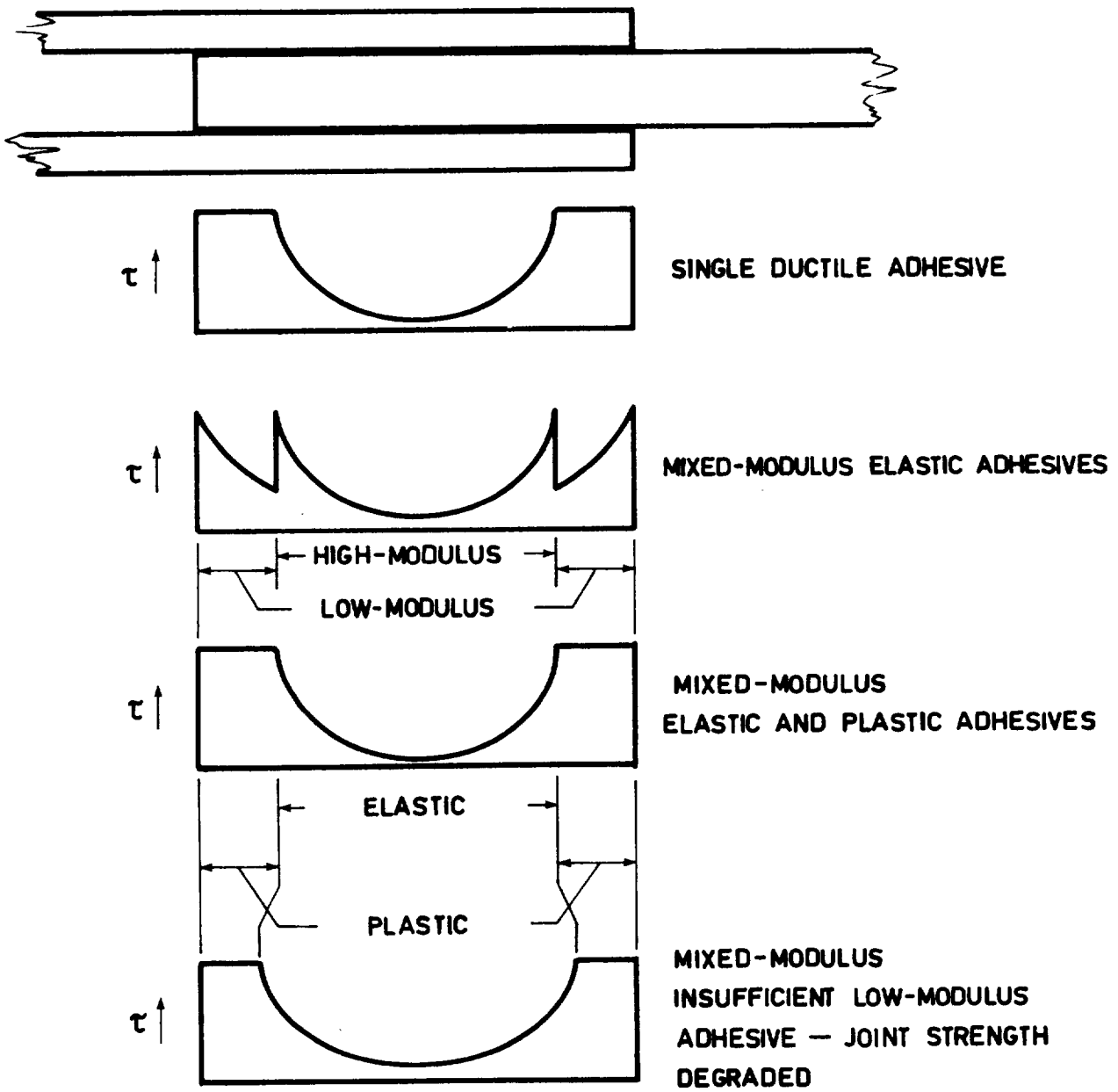
FIGURE 18. MIXED-MODULUS ADHESIVE BONDED JOINTS (SHEAR STRESS
DISTRIBUTIONS)
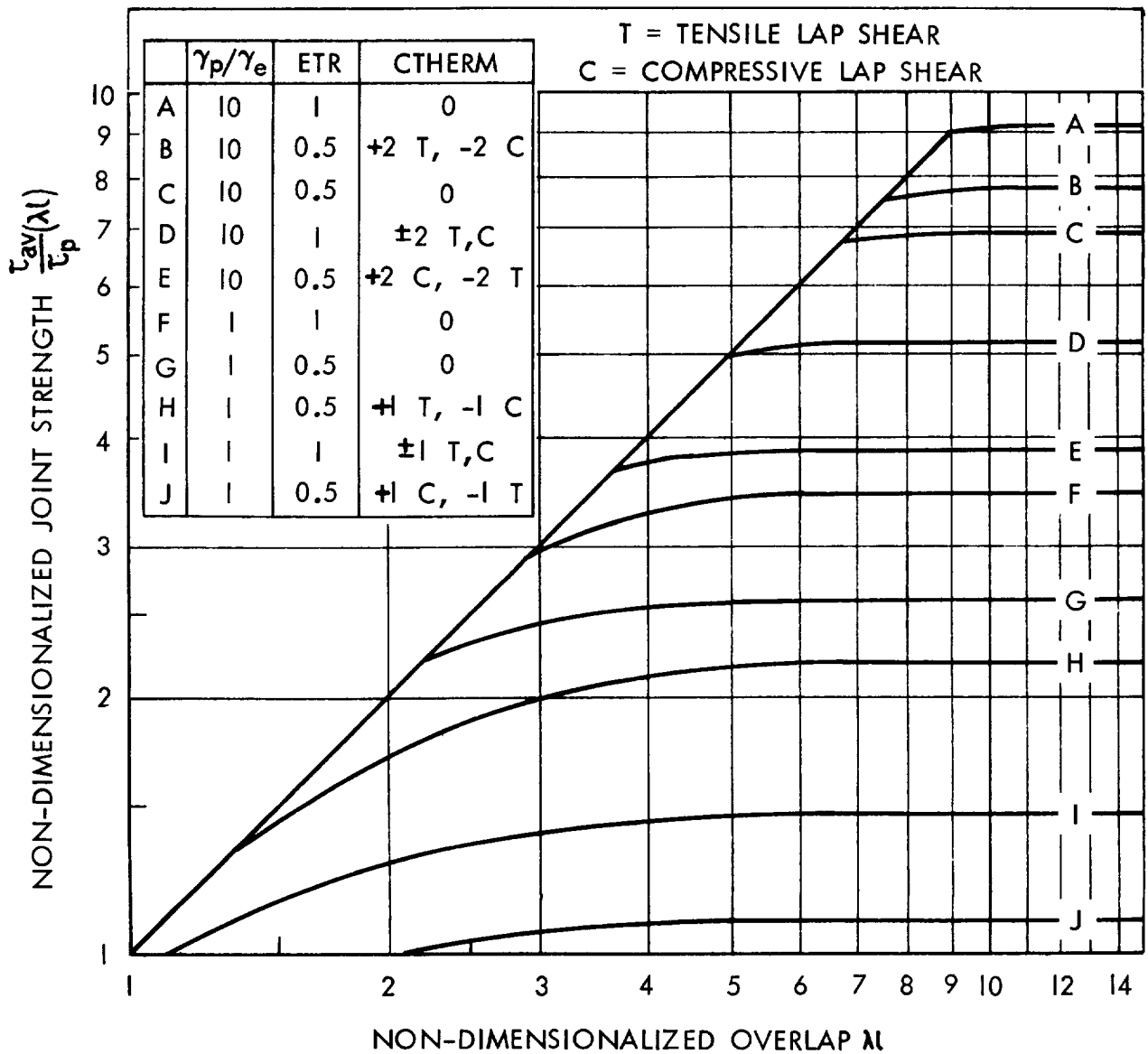
FIGURE 19. INFLUENCE OF GOVERNING PARAMETERS ON SHEAR STRENGTH OF DOUBLE-LAP JOINTS
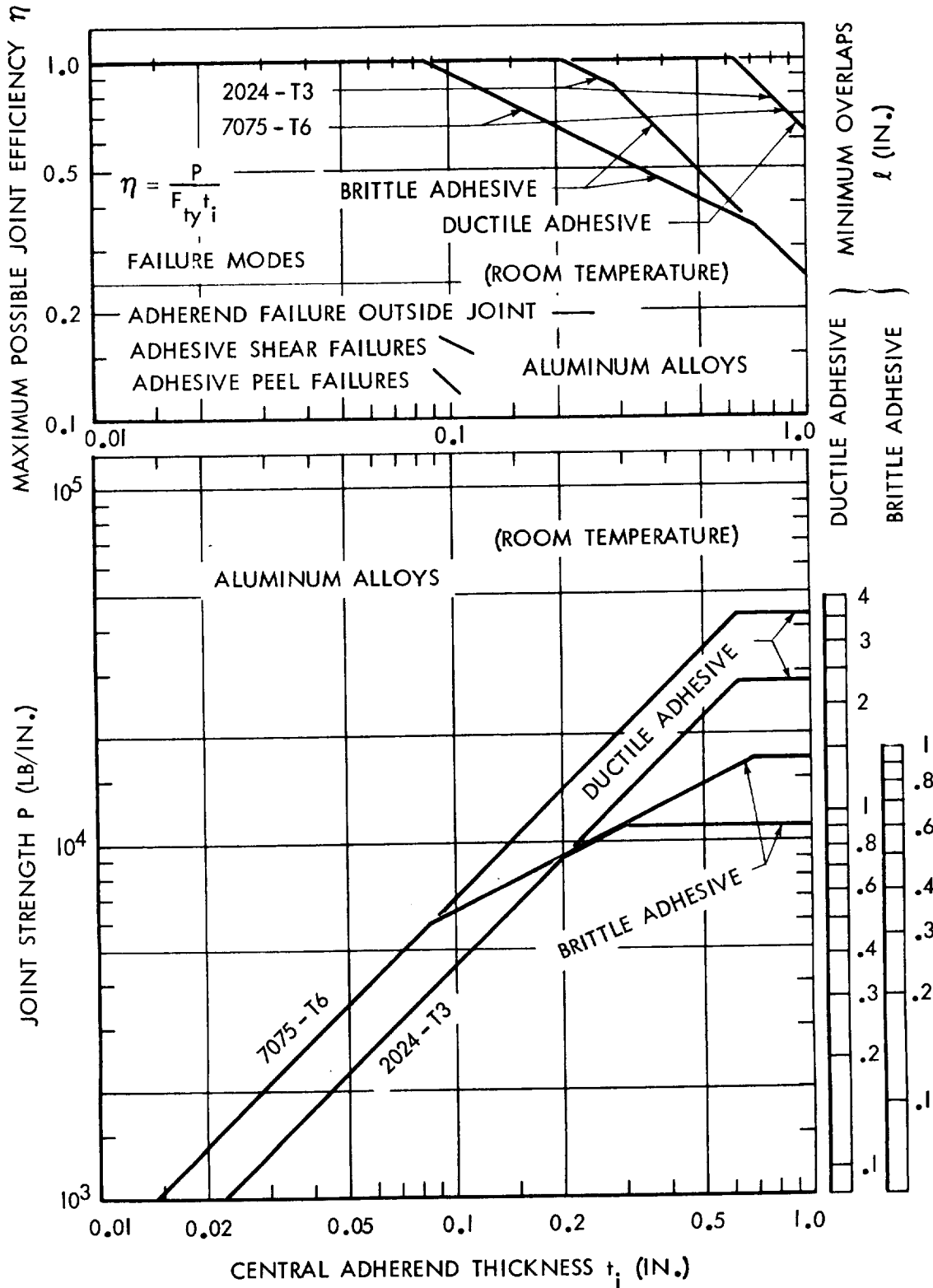
FIGURE 20. MAXIMUM EFFICIENCY AND JOINT STRENGTH FOR METAL ADHERENDS. (REFER TO TABLE 2 FOR PROPERTIES)
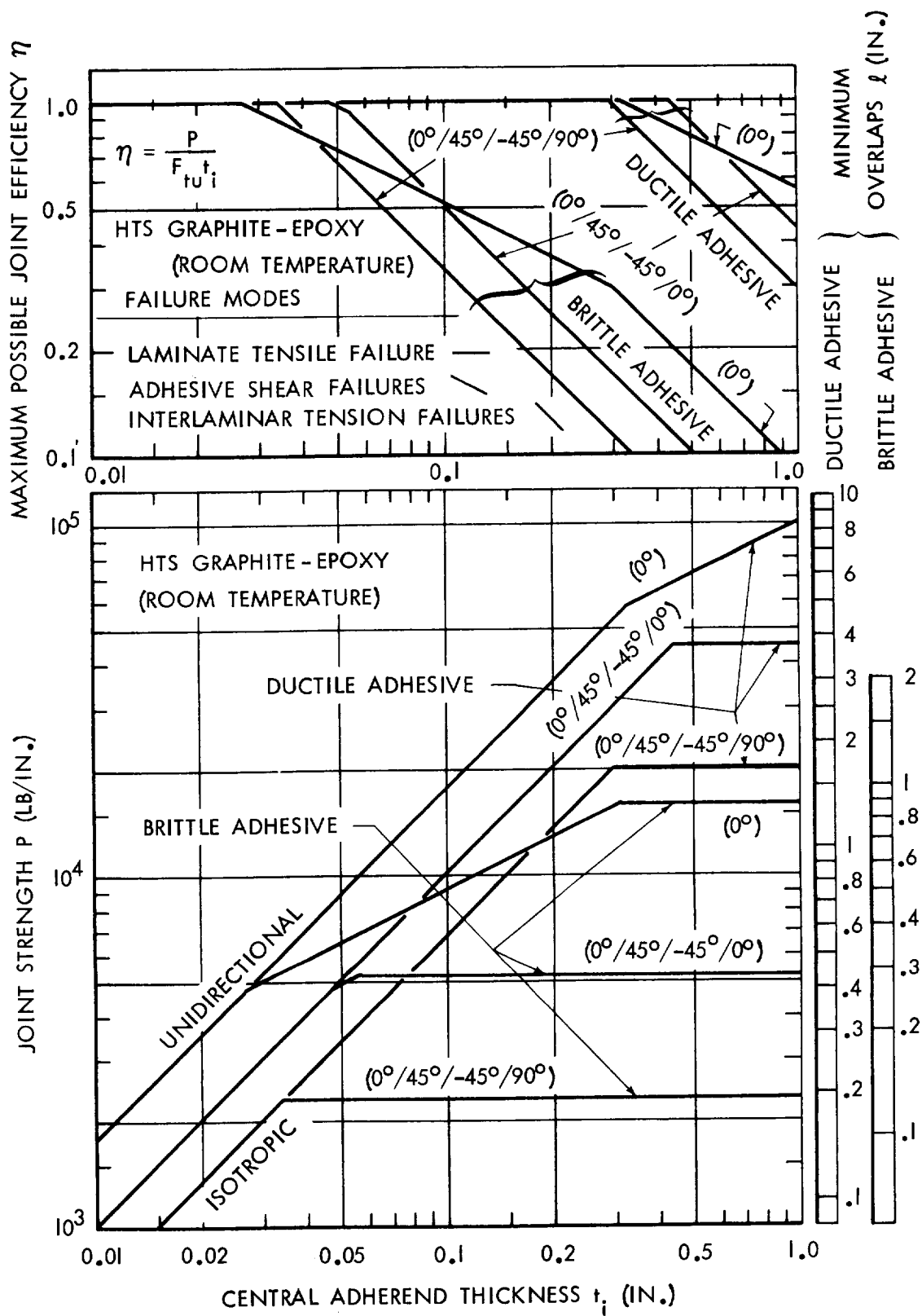
FIGURE 21. MAXIMUM EFFICIENCY AND JOINT STRENGTH FOR COMPOSITE ADHERENDS. (REFER TO TABLE 2 FOR PROPERTIES)

TABLE II. MATERIAL PROPERTIES FOR FIGURES 20 AND 21

2024-T3 ALUMINUM ALLOY:

$E = 10.5 \times 10^6$ psi, $F_{ty} = 47$ ksi, $F_{tu} = 65$ ksi.

7075-T6 ALUMINUM ALLOY:

$E = 10.3 \times 10^6$ psi, $F_{ty} = 70$ ksi, $F_{tu} = 80$ ksi.

HIGH-STRENGTH GRAPHITE-EPOXY:

$(0°/+45°/90°/-45°)_s$ pattern:

$E_L^t = 8.0 \times 10^6$ psi, $E_N^t = 1.7 \times 10^6$ psi,

$F_L^{tu} = 69$ ksi, $F_N^{tu} = 8$ ksi,

$(0°/+45°/0°/-45°)_s$ pattern:

$E_L^t = 11.9 \times 10^6$ psi, $E_N^t = 1.7 \times 10^6$ psi,

$F_L^{tu} = 103$ ksi, $F_N^{tu} = 8$ ksi,

$(0°)$ unidirectional laminate:

$E_L^t = 21.0 \times 10^6$ psi, $E_N^t = 1.7 \times 10^6$ psi,

$F_L^{tu} = 180$ ksi, $F_N^{tu} = 8$ ksi,

(in which the subscript N refers to properties in the thickness direction).

DUCTILE ADHESIVE:

$\tau_p = 6$ ksi, $\eta = 0.005$ in., $\gamma_p/\gamma_e = 20$,

$\eta(\frac{1}{2}\gamma_e + \gamma_p) = 0.0102$ in., $E_c \simeq 500$ ksi, $\sigma_{c_{max}} \simeq 10$ ksi.

BRITTLE ADHESIVE:

$\tau_p = 9$ ksi, $\eta = 0.005$ in., $\gamma_p/\gamma_e = 1.5$,

$\eta(\frac{1}{2}\gamma_e + \gamma_p) = 0.00042$ in., $E_c \simeq 1500$ ksi, $\sigma_{c_{max}} \simeq 17$ ksi.
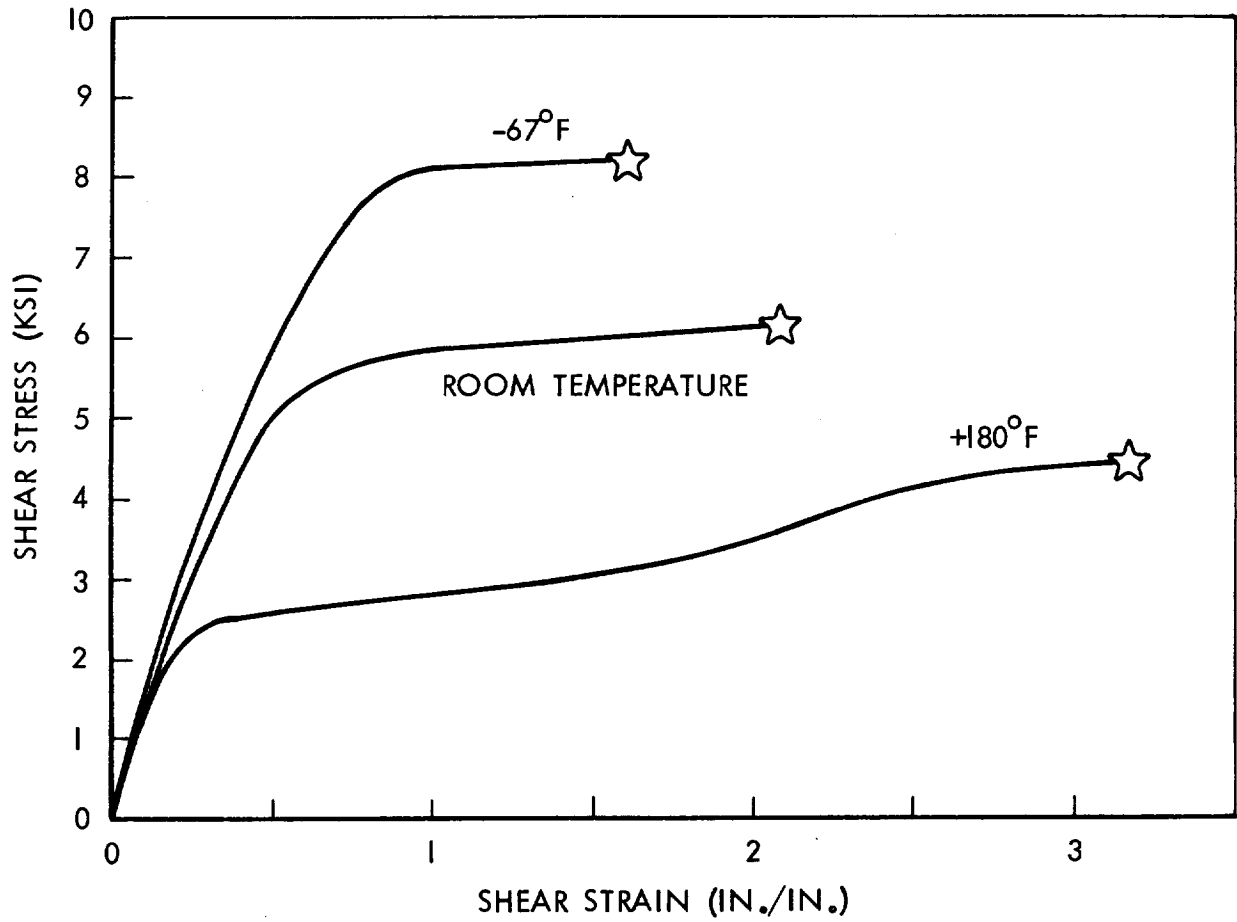
FIGURE 22. STRESS-STRAIN CHARACTERISTICS OF ADHESIVE FILM IN SHEAR, SHOWING TEMPERATURE DEPENDENCE
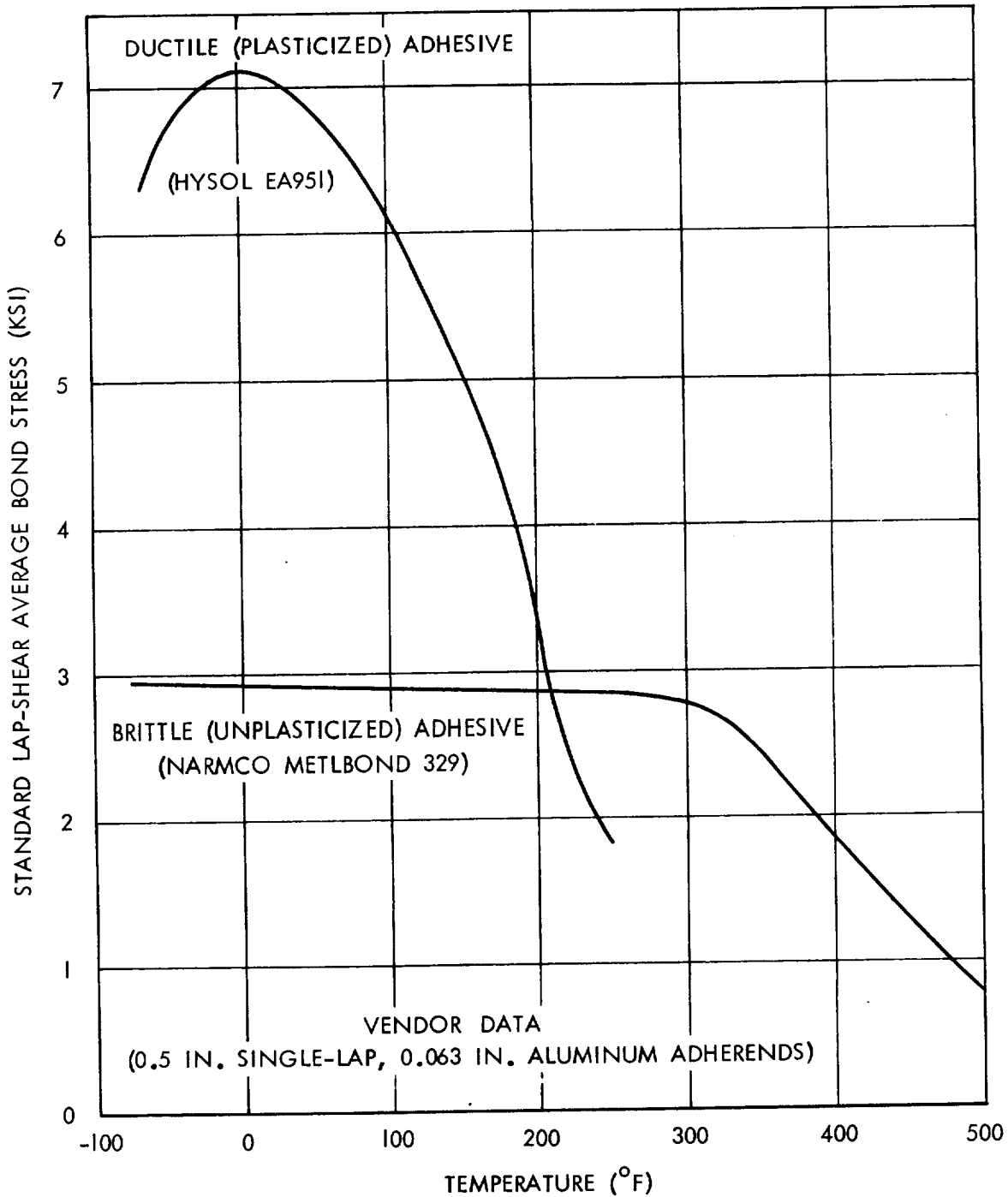
FIGURE 23. COMPARISON OF DUCTILE AND BRITTLE ADHESIVE STRENGTHS AT VARIOUS TEMPERATURES
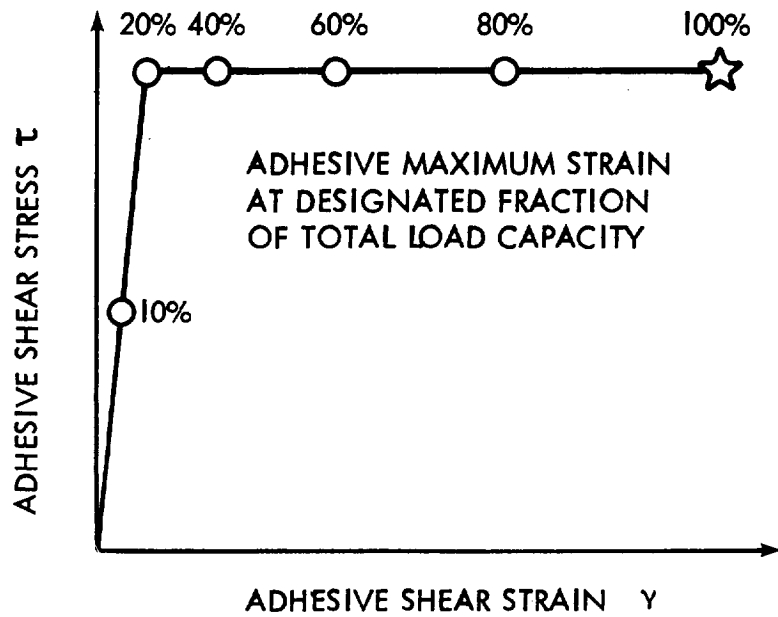
DUCTILE ADHESIVE SHEAR CHARACTERISTIC UNDER PARTIAL LOADS
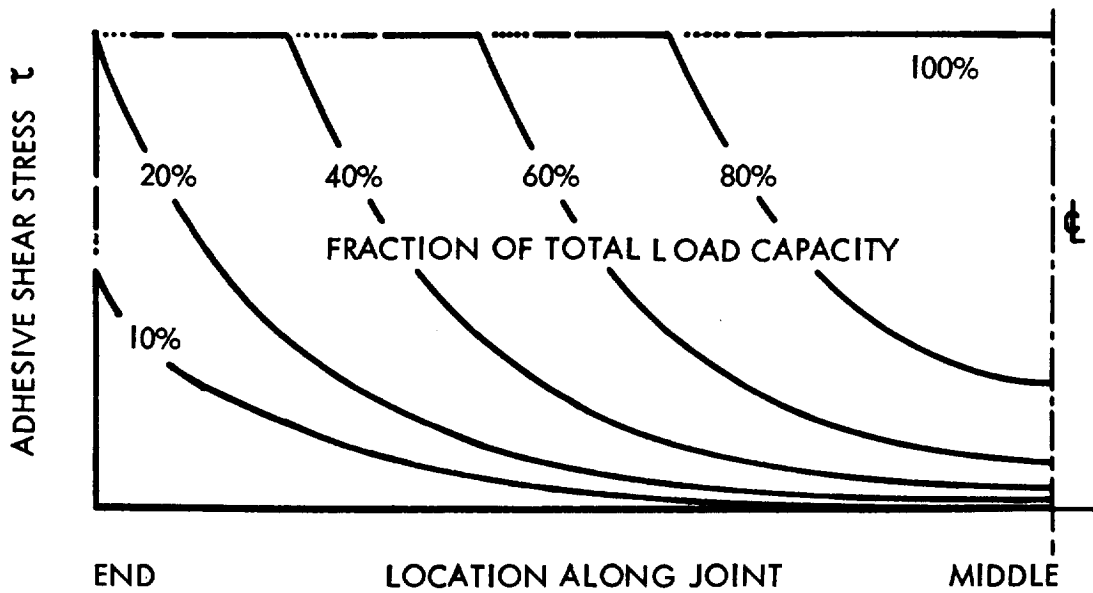
FIGURE 24. DOUBLE-LAP BONDED JOINTS UNDER PARTIAL LOADS
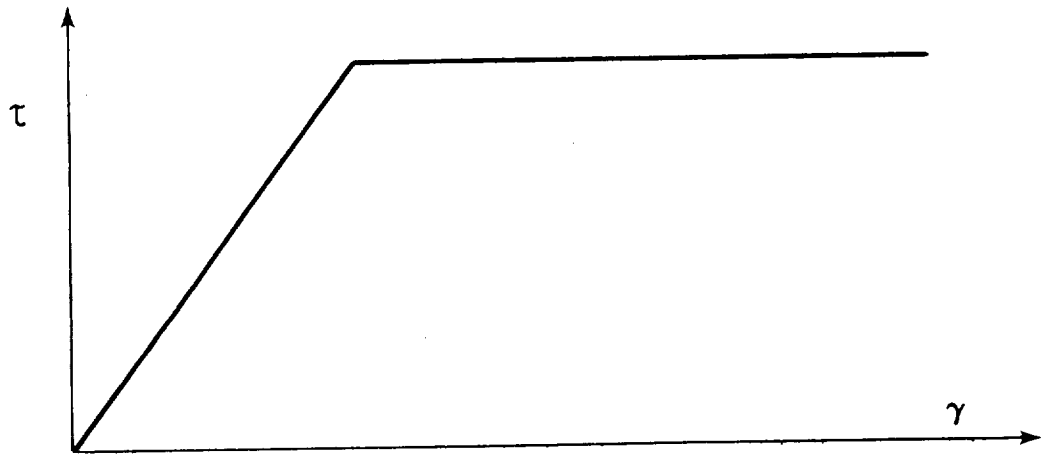
EQUIVALENT ELASTIC-PLASTIC CHARACTERIZATION
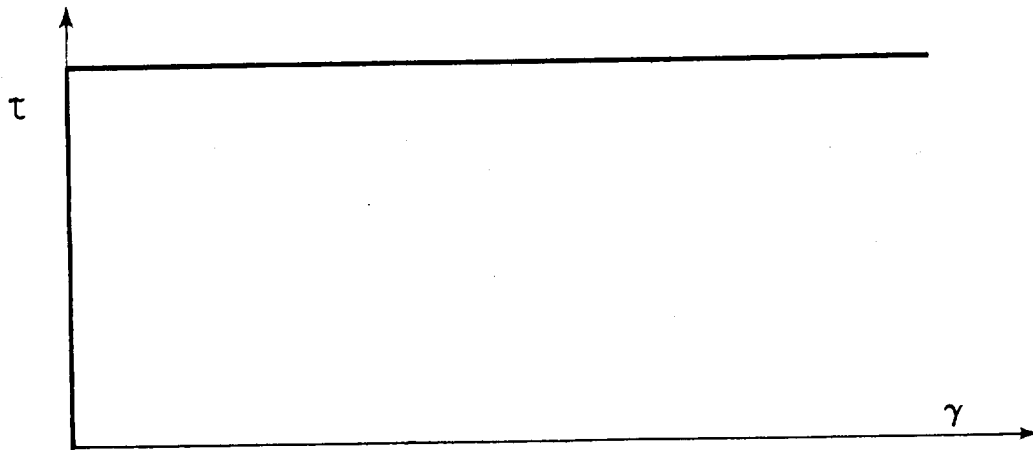
PURELY-PLASTIC UPPER BOUND REPRESENTATION
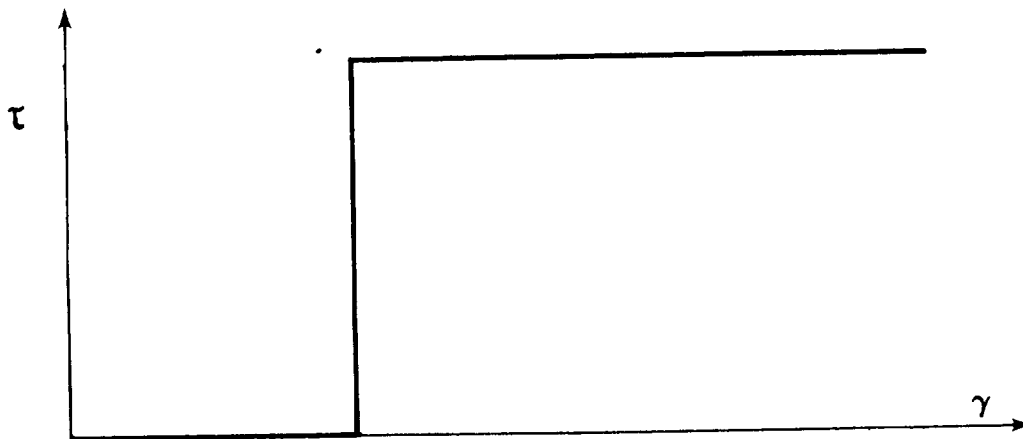
PURELY-PLASTIC LOWER BOUND REPRESENTATION

FIGURE 25. BONDED JOINT ANALYSIS IN TERMS OF UPPER AND LOWER BOUNDS THROUGH FULLY-PLASTIC ANALYSIS

APPENDICES

A. 1 General Analysis Including Adherend Imbalances

In some cases, design requirements other than the optimization of a specific bonded joint dictate that the net stiffnesses on each side of a bonded joint need to be unbalanced. In other instances, thermally dissimilar materials must be bonded together. Such situations accentuate the adhesive strain concentrations at one end of the joint, thereby reducing the average adhesive failing stress for intermediate and long overlaps. The appropriate analysis follows the approach used in Section 2, but the simplifications ensuing from symmetry of the adhesive strains about the mid-point can no longer be utilized. The same basic differential equations apply, but different boundary conditions hold. There are three mathematically distinct cases: (1) fully elastic adhesive throughout, (2) adhesive strained into the plastic state at one end only, and (3) plastic adhesive behavior at both ends of the joint and the associated special case of fully-plastic behavior throughout the joint. Those analyses are presented in turn below.

A.1.1 Fully-Elastic Analysis

This problem, first analyzed by Volkersen (Reference 1), is solved by de Bruyne (Reference 11). Referring to Figure 8, the basic differential equations are:

Horizontal force equilibrium

$$\frac{dT_o}{dx} + \tau = 0 \quad , \qquad \frac{dT_i}{dx} - 2\tau = 0 \quad , \tag{A.1}$$

Adherend stress-strain relations

$$\frac{d\delta_o}{dx} = \frac{T_o}{E_o t_o} + \alpha_o \Delta T \quad , \qquad \frac{d\delta_i}{dx} = \frac{T_i}{E_i t_i} + \alpha_i \Delta T \quad , \tag{A.2}$$

Adhesive elastic stress-strain relation

$$\tau = G\gamma = \frac{G}{\eta}(\delta_i - \delta_o) \quad . \tag{A.3}$$

The differential equation governing the adhesive shear-stress distribution follows by differentiation and elimination as

$$\frac{d^2\tau}{dx^2} - \lambda^2\tau = 0 \quad , \tag{A.4}$$

where

$$\lambda^2 = \frac{G}{\eta}\left(\frac{1}{E_o t_o} + \frac{2}{E_i t_i}\right) \quad . \tag{A.5}$$

The general solution of equation (A.4) is

$$\tau = A \sinh(\lambda x) + B \cosh(\lambda x) \quad . \tag{A.6}$$

The constants A and B are evaluated from the boundary conditions on $d\tau/dx$. Thus

$$\frac{d\tau}{dx} = A\lambda \cosh(\lambda x) + B\lambda \sinh(\lambda x) = \frac{G}{\eta}\left(\frac{T_i}{E_i t_i} - \frac{T_o}{E_o t_o} + (\alpha_i - \alpha_o)\Delta T\right) \quad . \tag{A.7}$$

Satisfaction of this condition at both ends of the joint automatically ensures that gross horizontal equilibrium is maintained. Choosing the origin of the x - co-ordinate as the middle of the joint, gross horizontal equilibrium requires

that

$$\tau_{av}\ell = \int_{-\frac{\ell}{2}}^{+\frac{\ell}{2}} \tau dx = \frac{2B}{\lambda} \sinh\left(\frac{\lambda\ell}{2}\right) \quad . \tag{A.8}$$

Substitution of this condition into equation (A.7) evaluated at one or other end of the joint provides

$$A = \frac{\tau_{av}\left(\frac{\lambda\ell}{2}\right)\left(1 - \frac{E_i t_i}{2E_o t_o}\right)}{\cosh\left(\frac{\lambda\ell}{2}\right)\left(1 + \frac{E_i t_i}{2E_o t_o}\right)} + \frac{(\alpha_i - \alpha_o)\Delta T\lambda}{\left(\frac{1}{E_o t_o} + \frac{2}{E_i t_i}\right)\cosh\left(\frac{\lambda\ell}{2}\right)} \quad , \tag{A.9}$$

$$B = \tau_{av}\left(\frac{\lambda\ell}{2}\right) \bigg/ \sinh\left(\frac{\lambda\ell}{2}\right) \quad . \tag{A.10}$$

The maximum value of τ will occur at one end or other, determined by the relative magnitudes of the adherend imbalances. The adhesive shear stress at the right end of the joint (Figure 8), $x = \ell/2$, (from which adherend i extends) is

$$\tau_{max} = \tanh\left(\frac{\lambda\ell}{2}\right)\left[\tau_{av}\left(\frac{\lambda\ell}{2}\right)\left(\frac{1 - \text{ETR}(1)}{1 + \text{ETR}(1)}\right) - \tau_{max} \text{CTHERM}(1)\right] + \frac{\tau_{av}\left(\frac{\lambda\ell}{2}\right)}{\tanh\left(\frac{\lambda\ell}{2}\right)} \quad , \tag{A.11}$$

in which the notation

$$\text{ETR}(1) = E_i t_i \big/ 2E_o t_o \tag{A.12}$$

and

$$\text{CTHERM}(1) = (\alpha_o - \alpha_i)\Delta T\lambda \bigg/ \left[\tau_{max}\left(\frac{1}{E_o t_o} + \frac{2}{E_i t_i}\right)\right] \tag{A.13}$$

has been introduced to characterize adherend stiffness and thermal imbalances, respectively. Re-arrangement of equation (A.11) yields

$$\frac{\tau_{av}}{\tau_{max}} = \frac{[1 + \tanh\left(\frac{\lambda\ell}{2}\right)\text{CTHERM}(1)]}{\left(\frac{\lambda\ell}{2}\right)\left[\left(\frac{1 - \text{ETR}(1)}{1 + \text{ETR}(1)}\right)\tanh\left(\frac{\lambda\ell}{2}\right) + \frac{1}{\tanh\left(\frac{\lambda\ell}{2}\right)}\right]} \tag{A.14}$$

in the event that the maximum shear stress τ_{max} $(= \tau_p)$ is at $x = +\ell/2$. Were the other end of the joint $(x = -\ell/2)$ critical, similar manipulations lead to the result

$$\tau_{max} = \tanh\left(\frac{\lambda\ell}{2}\right)\left[\tau_{av}\left(\frac{\lambda\ell}{2}\right)\left(\frac{ETR(1)-1}{ETR(1)+1}\right) + \tau_{max} \; CTHERM(1)\right] + \frac{\tau_{av}\frac{\lambda\ell}{2}}{\tanh\left(\frac{\lambda\ell}{2}\right)} \quad . \qquad (A.15)$$

The similarity of form between equations (A.11) and (A.15) suggests the introduction of the notation

$$ETR(2) = 2E_o t_o \; / \; E_i t_i = 1 \; / \; ETR(1) \qquad (A.16)$$

and

$$CTHERM(2) = (\alpha_i - \alpha_o)\Delta T\lambda \; / \; \left[\tau_{max}\left(\frac{1}{E_o t_o} + \frac{2}{E_i t_i}\right)\right] = - CTHERM(1) \quad . \; (A.17)$$

These convert equation (A.15) for τ_{max} at $x = -\ell/2$ to the form

$$\frac{\tau_{av}}{\tau_{max}} = \frac{[1 + \tanh\left(\frac{\lambda\ell}{2}\right)CTHERM(2)]}{\left(\frac{\lambda\ell}{2}\right)\left[\frac{1 - ETR(2)}{1 + ETR(2)}\tanh\left(\frac{\lambda\ell}{2}\right) + \frac{1}{\tanh\left(\frac{\lambda\ell}{2}\right)}\right]} \quad . \qquad (A.18)$$

Equations (A.14) and (A.18) are thus cyclic with respect to the end of the joint. The joint strength is identified simply by the lesser of equations (A.14) and (A.18). The non-dimensionalized adherend imbalances ETR and CTHERM conveniently lack any influence of the joint length which is confined to the nondimensionalized overlap $(\lambda\ell)$. Equations (A.14) and (A.18) therefore serve as the characterization of the elastic double-lap joint. For long overlaps, $\tanh(\lambda\ell/2) \to 1$, so that the non-dimensionalized joint strength $(\tau_{av} \; / \; \tau_p)(\lambda\ell)$ approaches the lesser of the two constant values

$$\left(\frac{\tau_{av}}{\tau_p}\right)\left(\frac{\lambda\ell}{2}\right) \to [1 + CTHERM(1)]\left[\frac{1 + ETR(1)}{2}\right] \quad or \quad [1 + CTHERM(2)]\left[\frac{1 + ETR(2)}{2}\right] \quad . \; (A.19)$$

A.1.2 Analysis for Plastic Strains at Only One End of Joint

In this case, the adhesive stress-strain relation (A.3) is supplemented by the relations

$$\gamma = \frac{(\delta_i - \delta_o)}{\eta} \quad , \qquad \tau = \tau_p \qquad (A.20)$$

throughout a plastic region of assumed length c at the more critical end of the joint (the "soft" Et end in the absence of thermal mismatch), as illustrated in Figure 8 by setting $a = 0$ and $b = c$, and by shifting the x - origin to the middle of the elastic region of the joint. Therefore,

$$\gamma = A \sinh(\lambda x) + B \cosh(\lambda x) \qquad (A.21)$$

throughout the elastic region and

$$\gamma = \left(\frac{\lambda^2 \tau_p}{2G}\right)\xi^2 + C\xi + F \quad , \qquad \left[\xi = x - \frac{(\ell - c)}{2}\right] \qquad (A.22)$$

throughout the plastic region. The relevant boundary conditions obviously depend upon which end of the joint is critical. It is readily established that the appropriate procedure is to start by assuming arbitrarily that either end is critical and to compute the joint strength. One then interchanges ETR(2) for ETR(1) and CTHERM(2) for CTHERM(1) to see if the other end was less or more critical. The appropriate critical end and joint strength are identified by the lower of the two strengths.

It is assumed that the end $x = +\ell/2$ is critical for reference. In this event, the relevant boundary conditions are

$$\gamma = \gamma_e = \tau_p / G \text{ at } x = (\ell - c) / 2 \quad , \quad \xi = 0 \quad , \qquad (A.23)$$

$$\gamma = \gamma_e + \gamma_p \text{ at } \xi = 0 \quad , \qquad (A.24)$$

$$\frac{d\gamma}{dx} = \frac{d\gamma}{d\xi} \text{ at } x = \frac{(\ell - c)}{2} \quad , \quad \xi = 0 \quad , \qquad (A.25)$$

$$\frac{d\gamma}{dx} = -\frac{\tau_{av}\ell}{\eta E_o t_o} + \frac{(\alpha_i - \alpha_o)\Delta T}{\eta} \text{ at } x = -\frac{(\ell - c)}{2} \quad , \qquad (A.26)$$

and

$$\frac{d\gamma}{d\xi} = \frac{2\tau_{av}\ell}{nE_i t_i} + \frac{(\alpha_i - \alpha_o)\Delta T}{n} \quad \text{at} \quad \xi = c \ . \tag{A.27}$$

While the elastic analysis is just as conveniently performed in terms of either the adhesive shear stress τ or shear strain γ, the appropriate variable is the shear strain when adhesive plasticity is included. Thus, conditions (A.26) and (A.27) derive from

$$\frac{d\gamma}{dx} = A\lambda \cosh(\lambda x) + B\lambda \sinh(\lambda x) = \frac{1}{n}\left[\frac{T_i}{E_i t_i} - \frac{T_o}{E_o t_o} + (\alpha_i - \alpha_o)\Delta T\right] \ , \tag{A.28}$$

which is equivalent to equation (A.7). The solution of equations (A.23) through (A.28) for the integration constants yields

$$F = \gamma_e = \tau_p / G \ , \tag{A.29}$$

$$\gamma_e = \tau_p / G = A \sinh[\lambda(\frac{\ell - c}{2})] + B \cosh[\lambda(\frac{\ell - c}{2})] \ , \tag{A.30}$$

$$\gamma_p = \left(\frac{\lambda^2 \tau_p}{2G}\right)c^2 + Cc \ , \tag{A.31}$$

$$A\lambda \cosh[\lambda(\frac{\ell - c}{2})] + B\lambda \sinh[\lambda(\frac{\ell - c}{2})] = C \ , \tag{A.32}$$

$$A\lambda \cosh[\lambda(\frac{\ell - c}{2})] - B\lambda \sinh[\lambda(\frac{\ell - c}{2})] = -\frac{\tau_{av}\ell}{nE_o t_o} + \frac{(\alpha_i - \alpha_o)\Delta T}{n} \ , \tag{A.33}$$

and

$$\left(\frac{\lambda^2 \tau_p}{G}\right)c + C = \frac{2\tau_{av}\ell}{nE_i t_i} + \frac{(\alpha_i - \alpha_o)\Delta T}{n} \ . \tag{A.34}$$

After some algebraic manipulation it is found that

$$1 + (\frac{\lambda c}{2})\left[\tanh[\lambda(\frac{\ell - c}{2})] + \frac{1}{\tanh[\lambda(\frac{\ell - c}{2})]}\right]$$

$$= \tanh[\lambda(\frac{\ell - c}{2})]\left[\frac{\tau_{av}}{\tau_p}(\frac{\lambda \ell}{2})\left(\frac{1 - ETR(1)}{1 + ETR(1)}\right) - CTHERM(1)\right]$$

$$+ \frac{1}{\tanh[\lambda(\frac{\ell - c}{2})]}\left[\frac{\tau_{av}}{\tau_p}(\frac{\lambda \ell}{2})\right] \tag{A.35}$$

and

$$\lambda c = \left[\frac{\tau_{av}}{\tau_p}(\frac{\lambda \ell}{2})\left(\frac{2}{1 + \text{ETR}(1)}\right) - \text{CTHERM}(1)\right]$$

$$\pm \sqrt{\left[\frac{\tau_{av}}{\tau_p}(\frac{\lambda \ell}{2})\left(\frac{2}{1 + \text{ETR}(1)}\right) - \text{CTHERM}(1)\right]^2 - 2\frac{\gamma_p}{\gamma_e}} \quad . \tag{A.36}$$

These can be solved by iteration for the unknowns (c/ℓ) and (τ_{av}/τ_p). This solution is tedious but, for sufficiently long overlaps, $\tanh[\lambda(\ell - c)/2] \to 1$, and it is found that

$$\left(\frac{\tau_{av}}{\tau_p}\right)(\frac{\lambda \ell}{2}) \to \left[\sqrt{1 + 2\frac{\gamma_p}{\gamma_e}} + \text{CTHERM}(1)\right]\left[\frac{1 + \text{ETR}(1)}{2}\right] \quad . \tag{A.37}$$

Were the end $x = -\ell/2$ critical instead, the following quantity would be lower in value than equation (A.37)

$$\left(\frac{\tau_{av}}{\tau_p}\right)(\frac{\lambda \ell}{2}) \to \left[\sqrt{1 + 2\frac{\gamma_p}{\gamma_e}} + \text{CTHERM}(2)\right]\left[\frac{1 + \text{ETR}(2)}{2}\right] \quad . \tag{A.38}$$

A.1.3 Analysis for Plastic Strains at Both Ends of Joint

The governing equations are given in Sections (A.1.1) and (A.1.2) above and, with the co-ordinate system adopted in Figure 8, it is found that the boundary conditions are expressible in the form:

$$\gamma = \gamma_e = \tau_p / G \quad \text{at} \quad x = +d/2 \ , \quad \xi = 0 \ , \quad \text{and at} \quad x = -d/2 \ , \quad \zeta = 0 \ , \quad \text{(A.39)}$$

$$\gamma = \gamma_e + \gamma_p \quad \text{at} \quad \xi = b \ , \quad \text{(assuming adherend end i critical)} \quad \text{(A.40)}$$

$$\frac{d\gamma}{dx} = \frac{d\gamma}{d\xi} \quad \text{at} \quad x = +d/2 \ , \quad \xi = 0 \ , \quad \text{(A.41)}$$

$$\frac{d\gamma}{dx} = -\frac{d\gamma}{d\zeta} \quad x = -d/2 \ , \quad \zeta = 0 \ , \quad \text{(A.42)}$$

$$\frac{d\gamma}{d\zeta} = \frac{\tau_{av}\ell}{nE_o t_o} - \frac{(\alpha_i - \alpha_o)\Delta T}{n} \quad \text{at} \quad \zeta = a \ , \quad \text{(A.43)}$$

and

$$\frac{d\gamma}{d\xi} = \frac{2\tau_{av}\ell}{nE_i t_i} + \frac{(\alpha_i - \alpha_o)\Delta T}{n} \quad \text{at} \quad \xi = b \ . \quad \text{(A.44)}$$

The strains in the respective regions are

$$\gamma = A \sinh(\lambda x) + B \cosh(\lambda x) \ , \quad \text{(A.45)}$$

$$\gamma = \left(\frac{\lambda^2 \tau_p}{2G}\right)\xi^2 + C\xi + F \ , \quad \text{(A.46)}$$

and

$$\gamma = \left(\frac{\lambda^2 \tau_p}{2G}\right)\zeta^2 + H\zeta + J \ . \quad \text{(A.47)}$$

Hence

$$A = 0 \ , \quad \text{(A.48)}$$

$$F = J = \gamma_e = B \cosh\left(\frac{\lambda d}{2}\right) \ , \quad \text{(A.49)}$$

$$\gamma_p = \left(\frac{\lambda^2 \tau_p}{2G}\right)b^2 + Cb \ , \quad \text{(A.50)}$$

92

$$B\lambda \sinh(\frac{\lambda d}{2}) = C = H \quad , \tag{A.51}$$

$$\frac{\lambda^2 \tau_p}{G} b + C = \frac{2\tau_{av}\ell}{\eta E_i t_i} + \frac{(\alpha_i - \alpha_o)\Delta T}{\eta} \quad , \tag{A.52}$$

$$\frac{\lambda^2 \tau_p}{G} a + H = \frac{\tau_{av}\ell}{\eta E_o t_o} - \frac{(\alpha_i - \alpha_o)\Delta T}{\eta} \quad , \tag{A.53}$$

where

$$a + b + d = \ell \quad . \tag{A.58}$$

Straightforward algebraic manipulation yields

$$[\lambda b + \tanh(\frac{\lambda d}{2})]^2 = \tanh^2(\frac{\lambda d}{2}) + 2\frac{\gamma_p}{\gamma_e} \quad , \tag{A.55}$$

$$\frac{\tau_{av}}{\tau_p} = 1 - \frac{d}{\ell} + \frac{\tanh(\frac{\lambda d}{2})}{(\frac{\lambda \ell}{2})} \quad , \tag{A.56}$$

$$\lambda b + \tanh(\frac{\lambda d}{2}) = \frac{\tau_{av}}{\tau_p}(\frac{\lambda\ell}{2})\left(\frac{2}{1 + \frac{E_i t_i}{2E_o t_o}}\right) + \frac{(\alpha_i - \alpha_o)\Delta T}{\tau_p\left(\frac{1}{E_o t_o} + \frac{2}{E_i t_i}\right)} \quad , \tag{A.57}$$

and

$$\lambda a + \tanh(\frac{\lambda d}{2}) = \frac{\tau_{av}}{\tau_p}(\frac{\lambda\ell}{2})\left(\frac{2}{1 + \frac{2E_o t_o}{E_i t_i}}\right) + \frac{(\alpha_o - \alpha_i)\Delta T}{\tau_p\left(\frac{2}{E_i t_i} + \frac{1}{E_o t_o}\right)} \quad . \tag{A.58}$$

These equations may be re-arranged into the set

$$\frac{\tau_{av}}{\tau_p} = 1 - \frac{d}{\ell} + \frac{\tanh(\frac{\lambda d}{2})}{(\frac{\lambda \ell}{2})} \tag{A.59}$$

and

$$\frac{\tau_{av}}{\tau_p}(\frac{\lambda\ell}{2})\left(\frac{2}{1 + \text{ETR}(1)}\right) = \text{CTHERM}(1) + \sqrt{\tanh^2(\frac{\lambda d}{2}) + 2\frac{\gamma_p}{\gamma_e}} \quad , \tag{A.60}$$

which can be solved by iteration for the unknowns d/ℓ and τ_{av}/τ_p. Restricting attention to sufficiently long overlaps,

$$\frac{\tau_{av}}{\tau_p}(\frac{\lambda \ell}{2}) \rightarrow \left[\sqrt{1 + 2\frac{\gamma_p}{\gamma_e}} + \text{CTHERM(1)} \right] \left[\frac{1 + \text{ETR(1)}}{2} \right] . \qquad (A.61)$$

Equations (A.60) and (A.61) are evaluated for each of adherends (1) and (2) in turn to identify the lesser positive value of τ_{av}/τ_p, and thence, the critical end of the joint.

It is evident from equation (A.61) that the two adherend imbalances can either compound or alleviate each other. In the one case b is greater than a for adherend(s) (1) end of the joint critical while a is greater than b for adherend(s) (2) end critical. In the latter event, a replaces b in equation (A.55).

A comparison of equations (A.61), (A.37) and (A.19) confirms that the same asymptote is approached whether there be two, one, or no plastic zones in the adhesive.

A.1.4 Analysis for Fully-Plastic Adhesive-Bonded Joint

In the digital computer program A4EB analyzing adhesive-bonded double-lap joints, it is necessary to identify both the critical end and the transitional extent of the joint, beyond which the adhesive must contain some elastic region. The analysis for the fully-plastic joint is the simplest case, yet it is very powerful. For any practical ductile adhesive, it closely approximates the maximum joint strength between a given pair of adherends. Indeed, as a first approximation, the inclusion of the adhesive elastic behavior is an unwarranted complication for all but brittle adhesives.

The governing equations are as follows. For horizontal force equilibrium,

$$\frac{dT_o}{dx} + \tau_p = 0 \quad , \qquad \frac{dT_i}{dx} - 2\tau_p = 0 \quad , \tag{A.62}$$

where τ_p is the (uniform) adhesive stress. For displacement compatibility,

$$\frac{d\delta_o}{dx} = \frac{T_o}{E_o t_o} + \alpha_o \Delta T \quad , \qquad \frac{d\delta_i}{dx} = \frac{T_i}{E_i t_i} + \alpha_i \Delta T \quad , \tag{A.63}$$

and

$$\gamma = \frac{\delta_i - \delta_o}{\eta} \quad . \tag{A.64}$$

The solution follows from

$$\frac{d\gamma}{dx} = \frac{1}{\eta}\left(\frac{T_i}{E_i t_i} - \frac{T_o}{E_o t_o}\right) + \frac{(\alpha_i - \alpha_o)\Delta T}{\eta} \tag{A.65}$$

through

$$\frac{d^2\gamma}{dx^2} = \frac{\tau_p}{\eta}\left(\frac{2}{E_i t_i} + \frac{1}{E_o t_o}\right) = \frac{\lambda^2}{G}\tau_p \tag{A.66}$$

as

$$\gamma = \left(\frac{\lambda^2 \tau_p}{2G}\right)x^2 + Ax + B \quad . \tag{A.67}$$

The x - origin is chosen as that location at which $\gamma = \gamma_e$ and $d\gamma/dx = 0$. This origin may be outside the extent of the joint. For this origin,

$$B = \gamma_e \quad \text{and} \quad A = 0 \quad . \tag{A.68}$$

There are two possibilities, depending upon the relative magnitudes of the adherend imbalances. In the event that the adherend (i) end of the joint is critical,

$$\gamma_p = \frac{\lambda^2 \tau_p}{2G} b^2 \quad , \tag{A.69}$$

as is evident from Figure 8 in the absence of any elastic adhesive behavior, whence

$$\lambda b = \sqrt{2 \frac{\gamma_p}{\gamma_e}} \quad . \tag{A.70}$$

Were the other end [adherends (o)] of the joint to develop the maximum adhesive shear strain $(\gamma_e + \gamma_p)$, the equivalent relation would be

$$\lambda a = \sqrt{2 \frac{\gamma_p}{\gamma_e}} \quad . \tag{A.71}$$

Corresponding to equation (A.70),

$$\frac{\lambda^2 \tau_p}{G} b = \frac{T_i}{n E_i t_i} + \frac{(\alpha_i - \alpha_o)\Delta T}{n} = \frac{2\tau_p \ell}{n E_i t_i} + \frac{(\alpha_i - \alpha_o)\Delta T}{n} \quad , \tag{A.72}$$

whence

$$\frac{\lambda \ell}{2} \leq \lambda b = \left(\frac{1}{1 + \text{ETR}(1)} \right) (\lambda \ell) - \text{CTHERM}(1) \quad , \tag{A.73}$$

so that

$$\frac{\lambda \ell}{2} = \left[\sqrt{2 \frac{\gamma_p}{\gamma_e}} + \text{CTHERM}(1) \right] \left[\frac{1 + \text{ETR}(1)}{2} \right] \quad . \tag{A.74}$$

Corresponding to equation (A.71),

$$-\frac{\lambda^2 \tau_p}{G} a = -\frac{T_o}{n E_o t_o} + \frac{(\alpha_i - \alpha_o)\Delta T}{n} = -\frac{\tau_p \ell}{n E_o t_o} + \frac{(\alpha_i - \alpha_o)\Delta T}{n} \quad , \tag{A.75}$$

whence

$$\frac{\lambda \ell}{2} = \left[\sqrt{2 \, \frac{\gamma_p}{\gamma_e}} + \text{CTHERM(2)} \right] \left[\frac{1 + \text{ETR(2)}}{2} \right] \, . \qquad (A.76)$$

The procedure to identify the appropriate transitional overlap is to take the lesser positive value of (A.74) and (A.76). Regardless of the sign of CTHERM and its magnitude relative to γ_p/γ_e it is evident that at least one of (A.74) and (A.76) must yield a real solution. In the event that the other equation does not, it must be concluded that the thermally-induced residual stresses are beyond the capacity of the adhesive to resist them.

For very short overlaps it is not necessary that the adhesive shear strain γ vary from its maximum of $(\gamma_e + \gamma_p)$ at the critical location all the way down to γ_e elsewhere. For such short overlaps the critical end is identified by the sign of $d\gamma/dx$ at the critical end. With reference to Figure 8, then, if the adherend (i) end be critical,

$$0 < \left. \frac{d\gamma}{dx} \right|_b = \frac{T_i}{\eta E_i t_i} + \frac{(\alpha_i - \alpha_o) \Delta T}{\eta} \propto \frac{\lambda \ell}{1 + \text{ETR(1)}} - \text{CTHERM(1)} \quad , \quad (A.77)$$

while, were the adherends (o) end critical (with the same sense for the x - coordinate),

$$0 > \left. \frac{d\gamma}{dx} \right|_{-a} = -\frac{T_o}{\eta E_o t_o} + \frac{(\alpha_i - \alpha_o) \Delta T}{\eta} \propto -\frac{\lambda \ell}{1 + \text{ETR(2)}} + \text{CTHERM(2)} \, . \quad (A.78)$$

For positive values of CTHERM(1) it is evident that the critical end of the joint may be changed throughout the fully-plastic overlaps.

A.2 Computer Program A4EB for Shear Strength of Double-Lap Bonded Joints

A Fortran IV digital computer program has been prepared and checked out for solving the general equations of Appendix A.1 in non-dimensionalized form. The solution employs an iterative technique for the strength of bonded joints only slightly longer than the length for which the adhesive behaves plastically throughout. Arbitrary combinations of adherend stiffness and thermal imbalance are provided for. The complete listing follows and sample output pages are included. The format of the input data is identified below.

CARD 1:

> FORMAT (5I5)
>
> IMAX = Number of thermal mismatch coefficients. IMAX .LE. 20
>
> JMAX = Number of non-dimensionalized overlaps. JMAX .LE. 40
>> (Note that this is one more than the number of overlaps to read in.)
>
> KMAX = Number of adherend stiffness imbalances. KMAX .LE. 10
>
> LMAX = Number of plastic-to-elastic adhesive shear strain ratios.
>> LMAX .LE. 20
>
> NMAX = Number of iteration cycles. NMAX .GE. 10 .AND. .LE. 50
>> (Note NMAX = 20 is recommended.)

CARDS 2, 2A, 2B, etc:

> FORMAT (12F6.2)
>
> OL(J) = Overlaps.
>> (Note that OL(J) must be in ascending order and OL(2) must be less than 0.2. OL(1) is set at zero by the program and not read in.)

CARDS 3, 3A, 3B, etc:

> FORMAT (10F5.2)
>
> ETR(K) = Adherend stiffness imbalances.
>> (Note that ETR(K) must be greater than zero and less than or equal

to unity. The array should be read in in ascending or descending order.)

CARDS 4, 4A, 4B, etc:

    FORMAT (10F7.3)

    CTHERM(I) = Adherend thermal mismatches.
               (Note that equal and opposite values must be read in consecutively to account for the difference between tensile and compressive application of the shear load.)
               (Values of ± 5 are sufficient for the available range of adhesives. Greater values of CTHERM are associated with joints breaking apart under internal thermal stress without external load application.)

CARDS 5, 5A, 5B, etc:

    FORMAT (14F5.2)

    GPOVGE(L) = Adhesive plastic-to-elastic shear strain ratios.

Having demonstrated that this iteration cycle is convergent (while other possible arrangements were found not to be) the program can be readily extended by the user to dimensional form for his specific requirements. Likewise, rather than showing non-dimensionalized parametric trends as the program is now set up, it may be adapted to operate on single joint specifications.

The output of program A4EB is in pairs of tables, with the average-to-maximum adhesive shear stress ratio (τ_{av}/τ_p) and the non-dimensionalized joint strength $(\tau_{av}/\tau_p)(\lambda\ell)$ listed as functions of the adherend stiffness ratio ETR $\leq$ 1 horizontally and the non-dimensionalized overlap $\lambda\ell = \sqrt{\dfrac{G}{\eta}\left(\dfrac{2}{E_i t_i} + \dfrac{1}{E_o t_o}\right)\ell^2}$ vertically.

Each table is prepared for a single value of the thermal mismatch coefficient

$$CTHERM = \frac{(\alpha_o - \alpha_i)\Delta T\lambda}{\tau_p\left(\dfrac{2}{E_o t_o} + \dfrac{1}{E_i t_i}\right)}$$ and equal and opposite values are treated in turn to cover both tensile and compressive shear loadings.

```
CDECK A4EB
C  ELASTIC-PLASTIC ANALYSIS OF DOUBLE-LAP JOINTS                          A4EB0010
C  NON-DIMENSIONALIZED AVERAGE SHEAR STRESSES COMPUTED                    A4EB0020
C  NON-DIMENSIONALIZED STRENGTHS COMPUTED                                 A4EB0030
C  RANGE OF ADHESIVE DUCTILITIES INCLUDED                                 A4EB0040
C  RANGES OF ADHEREND STIFFNESS AND THERMAL IMBALANCES ACCOUNTED FOR      A4EB0050
C  DATA PRESENTATION FOR TENSILE SHEAR LOADING                            A4EB0060
C  CHANGE SIGN OF CTHERM FOR COMPRESSIVE SHEAR LOADS                      A4EB0070
C  SET CTHERM .EQ. 0. AND REPLACE ADHEREND ET'S WITH GT'S FOR IN-PLANE    A4EB0080
C     1  (EDGEWISE) SHEAR LOADING                                         A4EB0090
C                                                                         A4EB0100
C  DIMENSION OL(J), ETR(K), CTHERM(I), GPOVGE(L), TAUAVG(J,K),            A4EB0110
C     1  STRGTH(J,K), ICRTND(J,K), THERMC(NCRTND), VR(NCRTND),            A4EB0120
C     2  TLMSTR(NCRTND), CLMSTR(NCRTND), OLTRNT(NCRTND), OLTRNC(NCRTND)    A4EB0130
C     3  OLREF(NCRTND), TRATIO(NCRTND), TRANSL(K)                         A4EB0140
      DIMENSION OL(40), ETR(10), CTHERM(20), GPOVGE(20), TAUAVG(40,10),   A4EB0150
     1  STRGTH(40,10), ICRTND(40,10), THERMC(2), VR(2), TLMSTR(2),        A4EB0160
     2  CLMSTR(2), OLTRNT(2), OLTRNC(2), OLREF(2), TRATIO(2), TRANSL(10)  A4EB0170
C                                                                         A4EB0180
C  READ IN INPUT DATA                                                     A4EB0190
C  READ IN ARRAY SIZES                                                    A4EB0200
      READ (5,10) IMAX, JMAX, KMAX, LMAX, NMAX                            A4EB0210
   10 FORMAT (5I5)                                                        A4EB0220
C  IMAX .LE. 20, JMAX .LE. 40, KMAX .LE. 10, LMAX .LE. 20,                A4EB0230
C     1  NMAX .GE. 10 .AND. .LE. 50                                       A4EB0240
C  IF NOT, MODIFY DIMENSION STATEMENT                                     A4EB0250
C  READ IN NON-DIMENSIONALIZED OVERLAPS                                   A4EB0260
      OL(1) = 0.                                                          A4EB0270
C  OL(J) MUST BE IN ASCENDING ORDER                                       A4EB0280
C  OL(2) MUST BE .LT. 0.2 FOR IDENTIFICATION OF CRITICAL END OF JOINT     A4EB0290
C     1  OF ZERO OVERLAP (LIMITING CASE)                                  A4EB0300
C  OL(J) MUST BE .LT. 100. FOR COMPATIBILITY WITH FORMAT STATEMENT 480    A4EB0310
      READ (5,20) (OL(J), J = 2, JMAX)                                    A4EB0320
   20 FORMAT (12F6.2)                                                     A4EB0330
C  READ IN STIFFNESS IMBALANCES                                           A4EB0340
C  IDENTIFY ADHERENDS SUCH THAT ETR(K) = ET(1)/ET(2) .LE. 1.             A4EB0350
C  STIFFNESS RATIOS SHOULD BE IN ASCENDING OR DESCENDING ORDER            A4EB0360
C  ETR(K) SHOULD INCLUDE VALUE 1. BUT MUST EXCLUDE VALUE 0.               A4EB0370
      READ (5,30) (ETR(K), K = 1, KMAX)                                   A4EB0380
   30 FORMAT (10F5.2)                                                     A4EB0390
C  READ IN NON-DIMENSIONALIZED THERMAL MISMATCH COEFFICIENTS              A4EB0400
C  CTHERM .PROPNL. (ALPHA(2)-ALPHA(1))*(OPERATING TEMP. - CURE TEMP.)     A4EB0410
C  NEED CTHERM(I) ARRAY TO CONTAIN BOTH POSITIVE AND NEGATIVE VALUES      A4EB0420
C     1  TO COVER BOTH TENSILE AND COMPRESSIVE LOADS                      A4EB0430
      READ (5,40) (CTHERM(I), I = 1, IMAX)                                A4EB0440
   40 FORMAT (10F7.3)                                                     A4EB0450
C  READ IN PLASTIC-TO-ELASTIC STRAIN RATIOS                               A4EB0460
      READ (5,50) (GPOVGE(L), L = 1, LMAX)                                A4EB0470
   50 FORMAT(14F5.2)                                                      A4EB0480
C                                                                         A4EB0490
C  PRINT OUT INPUT DATA                                                   A4EB0500
      WRITE (6,60) IMAX, JMAX, KMAX, LMAX, NMAX                           A4EB0510
   60 FORMAT (1H1, 9H  IMAX = , I2, 9H  JMAX = , I2, 9H  KMAX = , I2,     A4EB0520
     1  9H  LMAX = , I2, 9H  NMAX = , I2)                                 A4EB0530
      WRITE (6,70)                                                        A4EB0540
   70 FORMAT(10H  OVERLAPS)                                               A4EB0550
      WRITE (6,80) (OL(J), J = 1, JMAX)                                   A4EB0560
   80 FORMAT (12F6.2)                                                     A4EB0570
      WRITE (6,90)                                                        A4EB0580
   90 FORMAT (22H  STIFFNESS IMBALANCES)                                  A4EB0590
      WRITE (6,100) (ETR(K), K = 1, KMAX)                                 A4EB0600
  100 FORMAT (14F5.2)                                                     A4EB0610
      WRITE (6,110)                                                       A4EB0620
  110 FORMAT (20H  THERMAL MISMATCHES)                                    A4EB0630
      WRITE (6,120) (CTHERM(I), I = 1, IMAX)                              A4EB0640
  120 FORMAT (10F7.3)                                                     A4EB0650
      WRITE (6,130)                                                       A4EB0660
  130 FORMAT (34H  PLASTIC-TO-ELASTIC STRAIN RATIOS)                      A4EB0670
      WRITE (6,140) (GPOVGE(L), L = 1, LMAX)                              A4EB0680
  140 FORMAT (14F5.1)                                                     A4EB0690
C                                                                         A4EB0700
C  START COMPUTATIONAL DO LOOPS                                           A4EB0710
      DO 650 L = 1, LMAX                                                  A4EB0720
      GAMMAR = GPOVGE(L)                                                  A4EB0730
      GR = 2. * GAMMAR                                                    A4EB0740
      ROOTGR = SQRT(GR)                                                   A4EB0750
      RADGMR = SQRT(1. + GR)                                              A4EB0760
      DO 650 I = 1, IMAX                                                  A4EB0770
      THERMC(1) = CTHERM(I)                                               A4EB0780
      THERMC(2) = - THERMC(1)                                             A4EB0790
      DO 370 K = 1, KMAX                                                  A4EB0800
      VR(1) = ETR(K)                                                      A4EB0810
      VR(2) = 1. / VR(1)                                                  A4EB0820
C                                                                         A4EB0830
      IF (GAMMAR .GT. 0.) GO TO 200                                       A4EB0840
C  IF NOT, USE SPECIAL SOLUTION FOR PURELY ELASTIC JOINTS                 A4EB0850
      DO 190 J = 2, JMAX                                                  A4EB0860
      OLAP = OL(J) / 2.                                                   A4EB0870
                                                                         A4EB0880
```

```
      V10 = OL(J)                                                       A4EB0890
      V2 = TANH(OLAP)                                                   A4EB0900
      V3=(1.+V2*THERMC(1))/(OLAP*((1./V2)+V2*(1.-VR(1))/(1.+VR(1))))    A4EB0910
      V4=(1.+V2*THERMC(2))/(OLAP*((1./V2)+V2*(1.-VR(2))/(1.+VR(2))))    A4EB0920
      IF ( (V3 .GT. 0.) .AND. (V3 .LT. V4) ) GO TO 150                  A4EB0930
      IF ( (V4 .GT. 0.) .AND. (V4 .LT. V3) ) GO TO 160                  A4EB0940
      IF ( (V3 .GT. 0.) .AND. (V4 .EQ. V3) ) GO TO 170                  A4EB0950
C IF NONE OF THESE, JOINT HAS BROKEN WITHOUT EXTERNALLY APPLIED LOAD    A4EB0960
C   1   BECAUSE OF EXCESSIVE THERMAL MISMATCH BETWEEN ADHERENDS         A4EB0970
      GO TO 180                                                         A4EB0980
C ADHEREND(S) (1) END OF JOINT CRITICAL                                 A4EB0990
  150 TAUAVG(J,K) = V3                                                  A4EB1000
      STRGTH(J,K) = V3 * V10                                            A4EB1010
      ICRTND(J,K) = 1                                                   A4EB1020
      GO TO 190                                                         A4EB1030
C ADHEREND(S) (2) END OF JOINT CRITICAL                                 A4EB1040
  160 TAUAVG(J,K) = V4                                                  A4EB1050
      STRGTH(J,K) = V4 * V10                                            A4EB1060
      ICRTND(J,K) = 2                                                   A4EB1070
      GO TO 190                                                         A4EB1080
C BOTH ENDS OF JOINT EQUALLY CRITICAL FROM NULLIFYING (OR ZERO)        A4EB1090
C   1   ADHEREND IMBALANCES                                             A4EB1100
  170 TAUAVG(J,K) = V3                                                  A4EB1110
      STRGTH(J,K) = V3 * V10                                            A4EB1120
      ICRTND(J,K) = 0                                                   A4EB1130
      GO TO 190                                                         A4EB1140
C EXCESSIVE THERMAL MISMATCH BREAKS JOINT WITHOUT EXTERNAL LOAD        A4EB1150
  180 TAUAVG(J,K) = 0.                                                  A4EB1160
      STRGTH(J,K) = 0.                                                  A4EB1170
      ICRTND(J,K) = 0                                                   A4EB1180
  190 CONTINUE                                                          A4EB1190
C SET ZERO TRANSITIONAL LENGTH FOR PURELY ELASTIC JOINTS               A4EB1200
      TRANSL(K) = 0.                                                    A4EB1210
      GO TO 370                                                         A4EB1220
C                                                                       A4EB1230
C COMPUTATIONS FOR ELASTIC-PLASTIC BEHAVIOUR                           A4EB1240
C                                                                       A4EB1250
C FOLLOWING STATEMENTS ESTABLISH LIMITING VALUES FOR LONG OVERLAPS     A4EB1260
C OBSERVE HOW IMBALANCES CAN REINFORCE OR COUNTERACT EACH OTHER        A4EB1270
C RELATIVE VALUES ESTABLISH CRITICAL END OF JOINT FOR GIVEN LOAD DIR'N A4EB1280
C FOLLOWING EQUATIONS ESTABLISH LIMITING STRENGTHS FOR TENSILE SHEAR   A4EB1290
  200 TLMSTR(1) = (RADGMR + THERMC(1)) * (1. + VR(1))                   A4EB1300
      TLMSTR(2) = (RADGMR + THERMC(2)) * (1. + VR(2))                   A4EB1310
C FOLLOWING EQUATIONS WOULD ESTABLISH LIMITING STRENGTHS FOR COMPRESSIONA4EB1320
C     CLMSTR(1) = (RADGMR - THERMC(1)) * (1. + VR(1))                   A4EB1330
C     CLMSTR(2) = (RADGMR - THERMC(2)) * (1. + VR(2))                   A4EB1340
C FOLLOWING EQUATIONS ESTABLISH TRANSITIONAL LENGTHS FOR TENSILE SHEAR  A4EB1350
      OLTRNT(1) = (ROOTGR + THERMC(1)) * (1. + VR(1))                   A4EB1360
      OLTRNT(2) = (ROOTGR + THERMC(2)) * (1. + VR(2))                   A4EB1370
C NEXT EQUATIONS WOULD ESTABLISH TRANSITIONAL LENGTHS FOR COMPRESSION   A4EB1380
C     OLTRNC(1) = (ROOTGR - THERMC(1)) * (1. + VR(1))                   A4EB1390
C     OLTRNC(2) = (ROOTGR - THERMC(2)) * (1. + VR(2))                   A4EB1400
C                                                                       A4EB1410
C SPECIAL ROUTINE FOR SHORT (FULLY-PLASTIC) OVERLAPS                    A4EB1420
      DO 250 J = 2, JMAX                                                A4EB1430
      JSAVE = J                                                         A4EB1440
      V4 = OL(J)                                                        A4EB1450
C COMPARE OVERLAP WITH TRANSITIONAL OVERLAP                            A4EB1460
C IF LESS, JOINT IS FULLY PLASTIC THROUGHOUT                           A4EB1470
C IF MORE, JOINT CONTAINS ELASTIC TROUGH IN SHEAR STRESS DISTRIBUTION   A4EB1480
      IF ( (V4 .GT. OLTRNT(1)) .OR. (V4 .GT. OLTRNT(2)) ) GO TO 260     A4EB1490
C IF NOT, SET FULLY-PLASTIC ADHESIVE BEHAVIOUR FOR SHORT OVERLAPS       A4EB1500
C IDENTIFY CRITICAL END OF JOINT FOR SHORT OVERLAPS                     A4EB1510
C NCRTND FOR SHORT OVERLAPS MAY DIFFER FROM NCRTND FOR LONG OVERLAPS    A4EB1520
C IDENTIFY CRITICAL END FROM SHEAR STRAIN GRADIENTS                     A4EB1530
      V2 = (1. / (1. + VR(1))) - (THERMC(1) / V4)                       A4EB1540
      V3 = (1. / (1. + VR(2))) - (THERMC(2) / V4)                       A4EB1550
      V5 = V2 - V3                                                      A4EB1560
      IF (V5)230,220,210                                                A4EB1570
  210 MCRTND = 1                                                        A4EB1580
      GO TO 240                                                         A4EB1590
  220 MCRTND = 0                                                        A4EB1600
      GO TO 240                                                         A4EB1610
  230 MCRTND = 2                                                        A4EB1620
  240 ICRTND(J,K) = MCRTND                                              A4EB1630
      TAUAVG(J,K) = 1.                                                  A4EB1640
      STRGTH(J,K) = V4                                                  A4EB1650
  250 CONTINUE                                                          A4EB1660
  260 CONTINUE                                                          A4EB1670
C STORE TRANSITIONAL OVERLAP                                            A4EB1680
      IF (MCRTND .EQ. 0) MCRTND = 1                                     A4EB1690
C THIS ARISES ONLY IN THE ABSENCE OF BOTH ADHEREND IMBALANCES          A4EB1700
      TRANSL(K) = OLTRNT(MCRTND)                                        A4EB1710
      IF (TRANSL(K) .LT. 0.) TRANSL(K) = 0.                            A4EB1720
      DO 360 J = JSAVE, JMAX                                            A4EB1730
      OLAP = OL(J) / 2.                                                 A4EB1740
      V4 = OL(J)                                                        A4EB1750
      DO 300 NCRTND = 1, 2                                              A4EB1760
```

```
C ITERATION ROUTINE TO ESTABLISH STRENGTH OF INTERMEDIATE OVERLAPS          A4EB1770
C ESTABLISH IF OVERLAP IS GREATER THAN ONE ONLY OF TRNT(NCRTND)             A4EB1780
C IF SO, SET TRATIO(NCRTND) .EQ. 1. FOR FULLY-PLASTIC JOINT POSSIBILITY     A4EB1790
      IF ( (V4 .LE. OLTRNT(1)) .AND. (NCRTND .EQ. 1) ) GO TO 280            A4EB1800
      IF ( (V4 .LE. OLTRNT(2)) .AND. (NCRTND .EQ. 2) ) GO TO 290            A4EB1810
C IF NEITHER OF THESE, (TRATIO(1) .AND. TRATIO(2) ) .LT. 1.                 A4EB1820
      V5 = OLTRNT(NCRTND) / 2.                                              A4EB1830
      DO 270 N = 1, NMAX                                                    A4EB1840
      V6 = TANH(V5)                                                         A4EB1850
      V7 = (THERMC(NCRTND) + SQRT(V6*V6 + GR)) * (1.+VR(NCRTND)) / V4       A4EB1860
      V8 = (1. - V7 + V6/OLAP) * OLAP                                       A4EB1870
C COMPARE V5 AND V8.  CONVERGENCE ESTABLISHED WHEN EQUAL                    A4EB1880
C ENSURE AT LEAST 10 ITERATION CYCLES BUT LIMIT TO LESS THAN NMAX           A4EB1890
      IF (N .LE. 10) GO TO 270                                              A4EB1900
      V9 = V8 / V5                                                          A4EB1910
      IF ( (1.00001 .GT. V9) .AND. (0.99999 .LT. V9) ) GO TO 300           A4EB1920
  270 V5 = V8                                                               A4EB1930
      GO TO 300                                                             A4EB1940
  280 V7 = 1.                                                               A4EB1950
      GO TO 300                                                             A4EB1960
  290 V7 = 1.                                                               A4EB1970
  300 TRATIO(NCRTND) = V7                                                   A4EB1980
C                                                                           A4EB1990
C IDENTIFY CRITICAL END OF JOINT                                           A4EB2000
      IF (TRATIO(1) .LT. TRATIO(2)) GO TO 310                              A4EB2010
      IF (TRATIO(2) .LT. TRATIO(1)) GO TO 320                              A4EB2020
      IF (TRATIO(2) .EQ. TRATIO(1)) GO TO 330                              A4EB2030
C ADHEREND(S) (1) END OF JOINT CRITICAL                                    A4EB2040
  310 TAUAVG(J,K) = TRATIO(1)                                              A4EB2050
      STRGTH(J,K) = TRATIO(1) * V4                                         A4EB2060
      ICRTND(J,K) = 1                                                      A4EB2070
      GO TO 340                                                            A4EB2080
C ADHEREND(S) (2) END OF JOINT CRITICAL                                    A4EB2090
  320 TAUAVG(J,K) = TRATIO(2)                                              A4EB2100
      STRGTH(J,K) = TRATIO(2) * V4                                         A4EB2110
      ICRTND(J,K) = 2                                                      A4EB2120
      GO TO 340                                                            A4EB2130
C BOTH ENDS OF JOINT EQUALLY CRITICAL FROM NULLIFYING (OR ZERO)            A4EB2140
C   1 ADHEREND IMBALANCES                                                  A4EB2150
  330 TAUAVG(J,K) = TRATIO(1)                                              A4EB2160
      STRGTH(J,K) = TRATIO(1) * V4                                         A4EB2170
      ICRTND(J,K) = 0                                                      A4EB2180
  340 IF (TAUAVG(J,K) .GE. 0.) GO TO 350                                   A4EB2190
C IF NOT, JOINT HAS BROKEN DUE TO THERMAL STRESSES WITHOUT EXTERNAL LOAD    A4EB2200
      TAUAVG(J,K) = 0.                                                     A4EB2210
      STRGTH(J,K) = 0.                                                     A4EB2220
      GO TO 360                                                            A4EB2230
C REFINE ITERATIVE COMPUTATIONS FOR LONG OVERLAPS BY COMPARISON WITH        A4EB2240
C   1 LIMITING STRENGTHS COMPUTED DIRECTLY                                  A4EB2250
  350 MCRTND = ICRTND(J,K)                                                 A4EB2260
C COVER POSSIBILITY OF LONG JOINT WITH ZERO ADHEREND IMBALANCES            A4EB2270
      IF (MCRTND .EQ. 0)  MCRTND = 1                                       A4EB2280
      IF (STRGTH(J,K) .GT. TLMSTR(MCRTND)) STRGTH(J,K) = TLMSTR(MCRTND)    A4EB2290
      IF (TAUAVG(J,K) .LE. 1.) GO TO 360                                   A4EB2300
C IF NOT, THERE HAS BEEN A COMPUTATIONAL ERROR                             A4EB2310
C PRINT ASTERISKS TO IDENTIFY FAILURE TO CONVERGE                          A4EB2320
C RERUN WITH GREATER VALUE OF NMAX                                         A4EB2330
      TAUAVG(J,K) = 100.                                                   A4EB2340
      STRGTH(J,K) = 1000.                                                  A4EB2350
  360 CONTINUE                                                             A4EB2360
  370 CONTINUE                                                             A4EB2370
C                                                                           A4EB2380
C SET UNIFORM STRESS FOR ZERO OVERLAP                                      A4EB2390
  380 DO 390 K = 1, KMAX                                                   A4EB2400
      TAUAVG(1,K) = 1.                                                     A4EB2410
      STRGTH(1,K) = 0.                                                     A4EB2420
  390 ICRTND(1,K) = ICRTND(2,K)                                            A4EB2430
C HENCE NEED FOR OL(2) TO BE SMALL ENOUGH TO BE LESS THAN THAT AT WHICH     A4EB2440
C   1 NCRTND CHANGES                                                       A4EB2450
C                                                                           A4EB2460
C END OF COMPUTATIONS.  START OF PRINTING OUT OF TABULATED RESULTS          A4EB2470
C                                                                           A4EB2480
C PRINT OUT AVERAGE STRESS HEADING                                         A4EB2490
      WRITE (6,400)                                                        A4EB2500
  400 FORMAT (1H1/, 5(1H0/), 25X,    61HADHESIVE-BONDED DOUBLE-LAP JOINTS   A4EB2510
     1 (ELASTIC-PLASTIC ANALYSIS)/,                                        A4EB2520
     2 39X, 31HNON-DIMENSIONALIZED FORMULATION)                            A4EB2530
      IF (GAMMAR .NE. 0.) GO TO 420                                        A4EB2540
      WRITE (6,410)                                                        A4EB2550
  410 FORMAT(1H0, 42X, 23HPURELY ELASTIC ADHESIVE)                         A4EB2560
      GO TO 440                                                            A4EB2570
  420 WRITE (6,430) GAMMAR                                                 A4EB2580
  430 FORMAT(1H0, 27X, 49HPLASTIC TO ELASTIC ADHESIVE SHEAR STRAIN RATIO    A4EB2590
     1 = , F5.2)                                                           A4EB2600
  440 IF (CTHERM(I) .NE. 0.) GO TO 460                                     A4EB2610
      WRITE (6,450)                                                        A4EB2620
  450 FORMAT (1H , 37X, 33HZERO THERMAL MISMATCH COEFFICIENT)              A4EB2630
      GO TO 480                                                            A4EB2640
```

103

```
  460 WRITE (6,470) THERMC(1), THERMC(2)                                   A4EB2650
  470 FORMAT (1H , 16X, 31HTHERMAL MISMATCH COEFFICIENT = , F6.3,          A4EB2660
     1  17H FOR TENSION,  = , F6.3, 16H FOR COMPRESSION)                   A4EB2670
  480 WRITE (6,490) (ETR(K), K = 1, KMAX)                                  A4EB2680
  490 FORMAT (   1H0,  67X, 30H0 = BOTH ENDS EQUALLY CRITICAL/, 20X,       A4EB2690
     1  72HAVERAGE SHEAR STRESS / MAXIMUM SHEAR STRESS   ,  1 = SOFT ET EA4EB2700
     2ND CRITICAL/, 68X, 25H2 = STIFF ET END CRITICAL/,                    A4EB2710
     3  8H0 SCALED, 31X, 39HEXTENSIONAL STIFFNESS (THICKNESS) RATIO/,      A4EB2720
     4  7H    L/T/, 7H  RATIO, F7.1, 9F10.1/, 1H0)                         A4EB2730
C                                                                          A4EB2740
C WRITE OUT TABULATIONS OF AVERAGE BOND STRESSES                           A4EB2750
      DO 510 J = 1, JMAX                                                   A4EB2760
      WRITE (6,500) OL(J), ((TAUAVG(J,K), ICRTND(J,K)), K = 1, KMAX)       A4EB2770
  500 FORMAT (1H , F6.2, 2X, 10(F7.5, 1X, I1, 1X))                         A4EB2780
  510 CONTINUE                                                             A4EB2790
C                                                                          A4EB2800
      WRITE (6,520)                                                        A4EB2810
C PRINT OUT JOINT STRENGTH HEADING                                         A4EB2820
  520 FORMAT (1H1/, 5(1H0/), 25X,   61HADHESIVE-BONDED DOUBLE-LAP JOINTSA4EB2830
     1  (ELASTIC-PLASTIC ANALYSIS)/,                                       A4EB2840
     2  39X, 31HNON-DIMENSIONALIZED FORMULATION)                          A4EB2850
      IF (GAMMAR .NE. 0.) GO TO 540                                        A4EB2860
      WRITE (6,530)                                                        A4EB2870
  530 FORMAT(1H0, 42X, 23HPURELY ELASTIC ADHESIVE)                        A4EB2880
      GO TO 560                                                            A4EB2890
  540 WRITE (6,550) GAMMAR                                                 A4EB2900
  550 FORMAT(1H0, 27X, 49HPLASTIC TO ELASTIC ADHESIVE SHEAR STRAIN RATIOA4EB2910
     1 = , F5.2)                                                          A4EB2920
  560 IF (CTHERM(1) .NE. 0.) GO TO 580                                     A4EB2930
      WRITE (6,570)                                                        A4EB2940
  570 FORMAT (1H , 37X, 33HZERO THERMAL MISMATCH COEFFICIENT)             A4EB2950
      GO TO 600                                                            A4EB2960
  580 WRITE (6,590) THERMC(1), THERMC(2)                                   A4EB2970
  590 FORMAT (1H , 16X, 31HTHERMAL MISMATCH COEFFICIENT = , F6.3,          A4EB2980
     1  17H FOR TENSION,  = , F6.3, 16H FOR COMPRESSION)                   A4EB2990
  600 WRITE (6,610) (ETR(K), K = 1, KMAX)                                  A4EB3000
  610 FORMAT (   1H0,  67X, 30H0 = BOTH ENDS EQUALLY CRITICAL/, 20X,       A4EB3010
     1  72HNON-DIMENSIONALIZED JOINT STRENGTH   ,        1 = SOFT ET EA4EB3020
     2ND CRITICAL/, 68X, 25H2 = STIFF ET END CRITICAL/,                    A4EB3030
     3  8H0 SCALED, 31X, 39HEXTENSIONAL STIFFNESS (THICKNESS) RATIO/,      A4EB3040
     4  7H    L/T/, 7H  RATIO, F7.1, 9F10.1/, 1H0)                         A4EB3050
C                                                                          A4EB3060
C WRITE OUT TABULATIONS OF JOINT STRENGTHS                                 A4EB3070
      DO 630 J = 1, JMAX                                                   A4EB3080
      WRITE (6,620) OL(J), ((STRGTH(J,K), ICRTND(J,K)), K = 1, KMAX)       A4EB3090
  620 FORMAT (1H , F6.2, 2X, 10(F7.4, 1X, I1, 1X))                         A4EB3100
  630 CONTINUE                                                             A4EB3110
C WRITE OUT TRANSITIONAL JOINT STRENGTHS                                   A4EB3120
      WRITE (6,640) (TRANSL(K), K = 1, KMAX)                               A4EB3130
  640 FORMAT (8H0 TRANSL, 1X, 10(F7.4, 3X))                               A4EB3140
  650 CONTINUE                                                             A4EB3150
      WRITE (6,660)                                                        A4EB3160
  660 FORMAT (1H1, 18H PROGRAM COMPLETED)                                 A4EB3170
      STOP                                                                 A4EB3180
      END                                                                  A4EB3190
```

104

ADHESIVE-BONDED DOUBLE-LAP JOINTS   (ELASTIC-PLASTIC ANALYSIS)
NON-DIMENSIONALIZED FORMULATION

PLASTIC TO ELASTIC ADHESIVE SHEAR STRAIN RATIO = 5.0
THERMAL MISMATCH COEFFICIENT = 1.000 FOR TENSION, = -1.000 FOR COMPRESSION

NON-DIMENSIONALIZED JOINT STRENGTH ,

```
0 = BOTH ENDS EQUALLY CRITICAL
1 = SOFT ET END CRITICAL
2 = STIFF ET END CRITICAL
```

EXTENSIONAL STIFFNESS (THICKNESS) RATIO

SCALED L/T RATIO	0.1	0.2	0.3	0.4	0.5	0.6	0.7	0.8	0.9	1.0
0.0	0.0 2	0.0 2	0.0 2	0.0 2	0.0 2	0.0 2	0.0 2	0.0 2	0.0 2	0.0 2
0.10	0.1000 2	0.1000 2	0.1000 2	0.1000 2	0.1000 2	0.1000 2	0.1000 2	0.1000 2	0.1000 2	0.1000 2
0.15	0.1500 2	0.1500 2	0.1500 2	0.1500 2	0.1500 2	0.1500 2	0.1500 2	0.1500 2	0.1500 2	0.1500 2
0.20	0.2000 2	0.2000 2	0.2000 2	0.2000 2	0.2000 2	0.2000 2	0.2000 2	0.2000 2	0.2000 2	0.2000 2
0.30	0.3000 2	0.3000 2	0.3000 2	0.3000 2	0.3000 2	0.3000 2	0.3000 2	0.3000 2	0.3000 2	0.3000 2
0.50	0.5000 2	0.5000 2	0.5000 2	0.5000 2	0.5000 2	0.5000 2	0.5000 2	0.5000 2	0.5000 2	0.5000 2
0.70	0.7000 2	0.7000 2	0.7000 2	0.7000 2	0.7000 2	0.7000 2	0.7000 2	0.7000 2	0.7000 2	0.7000 2
1.00	1.0000 2	1.0000 2	1.0000 2	1.0000 2	1.0000 2	1.0000 2	1.0000 2	1.0000 2	1.0000 2	1.0000 2
1.20	1.2000 2	1.2000 2	1.2000 2	1.2000 2	1.2000 2	1.2000 2	1.2000 2	1.2000 2	1.2000 2	1.2000 2
1.50	1.5000 2	1.5000 2	1.5000 2	1.5000 2	1.5000 2	1.5000 2	1.5000 2	1.5000 2	1.5000 2	1.5000 2
1.70	1.7000 2	1.7000 2	1.7000 2	1.7000 2	1.7000 2	1.7000 2	1.7000 2	1.7000 2	1.7000 2	1.7000 2
2.00	2.0000 2	2.0000 2	2.0000 2	2.0000 2	2.0000 2	2.0000 2	2.0000 2	2.0000 2	2.0000 2	2.0000 2
2.50	2.5000 1	2.5000 2	2.5000 2	2.5000 2	2.5000 2	2.5000 2	2.5000 2	2.5000 2	2.5000 2	2.5000 2
3.00	3.0000 1	3.0000 1	3.0000 2	3.0000 2	3.0000 2	3.0000 2	3.0000 2	3.0000 2	3.0000 2	3.0000 2
4.00	4.0000 1	4.0000 1	4.0000 1	4.0000 2	4.0000 2	4.0000 2	4.0000 2	4.0000 2	4.0000 2	4.0000 2
5.00	4.6630 1	5.0000 1	5.0000 1	5.0000 1	5.0000 2	5.0000 2	5.0000 2	4.9345 2	4.7142 2	4.5079 2
6.00	4.7210 1	5.1326 1	5.5280 1	5.9468 1	6.0000 1	5.8922 2	5.4795 2	5.1245 2	4.8315 2	4.5903 2
7.00	4.7386 1	5.1636 1	5.5339 1	5.9961 1	6.3938 1	6.0738 2	5.5748 2	5.1911 2	4.8695 2	4.6178 2
8.00	4.7448 1	5.1740 1	5.6017 1	6.0267 1	6.4473 1	6.1421 1	5.6075 2	5.2010 2	4.8829 2	4.6276 2
9.00	4.7470 1	5.1778 1	5.6080 1	6.0373 1	6.4650 1	6.1647 2	5.6193 2	5.2082 2	4.8878 2	4.6312 2
10.00	4.7478 1	5.1792 1	5.6103 1	6.0411 1	6.4713 1	6.1729 2	5.6236 2	5.2109 2	4.8896 2	4.6325 2
12.00	4.7482 1	5.1798 1	5.6114 1	6.0430 1	6.4744 1	6.1770 2	5.6257 2	5.2122 2	4.8905 2	4.6331 2
15.00	4.7483 1	5.1799 1	5.6115 1	6.0433 1	6.4749 1	6.1776 2	5.6261 2	5.2124 2	4.8906 2	4.6332 2
20.00	4.7483 1	5.1799 1	5.6116 1	6.0433 1	6.4749 1	6.1777 2	5.6261 2	5.2124 2	4.8906 2	4.6332 2
25.00	4.7483 1	5.1799 1	5.6116 1	6.0433 1	6.4749 1	6.1777 2	5.6261 2	5.2124 2	4.8906 2	4.6332 2
TRANSL	4.5785	4.9947	5.4110	5.8272	6.2434	5.7661	5.2512	4.8651	4.5649	4.3246

ADHESIVE-BONDED DOUBLE-LAP JOINTS   (ELASTIC-PLASTIC ANALYSIS)
NON-DIMENSIONALIZED FORMULATION

PLASTIC TO ELASTIC ADHESIVE SHEAR STRAIN RATIO = 5.0
THERMAL MISMATCH COEFFICIENT = 1.000 FOR TENSION, = -1.000 FOR COMPRESSION

AVERAGE SHEAR STRESS / MAXIMUM SHEAR STRESS ,

```
0 = BOTH ENDS EQUALLY CRITICAL
1 = SOFT ET END CRITICAL
2 = STIFF ET END CRITICAL
```

EXTENSIONAL STIFFNESS (THICKNESS) RATIO

SCALED L/T RATIO	0.1	0.2	0.3	0.4	0.5	0.6	0.7	0.8	0.9	1.0
0.0	1.00000 2	1.00000 2	1.00000 2	1.00000 2	1.00000 2	1.00000 2	1.00000 2	1.00000 2	1.00000 2	1.00000 2
0.10	1.00000 2	1.00000 2	1.00000 2	1.00000 2	1.00000 2	1.00000 2	1.00000 2	1.00000 2	1.00000 2	1.00000 2
0.15	1.00000 2	1.00000 2	1.00000 2	1.00000 2	1.00000 2	1.00000 2	1.00000 2	1.00000 2	1.00000 2	1.00000 2
0.20	1.00000 2	1.00000 2	1.00000 2	1.00000 2	1.00000 2	1.00000 2	1.00000 2	1.00000 2	1.00000 2	1.00000 2
0.30	1.00000 2	1.00000 2	1.00000 2	1.00000 2	1.00000 2	1.00000 2	1.00000 2	1.00000 2	1.00000 2	1.00000 2
0.50	1.00000 2	1.00000 2	1.00000 2	1.00000 2	1.00000 2	1.00000 2	1.00000 2	1.00000 2	1.00000 2	1.00000 2
0.70	1.00000 2	1.00000 2	1.00000 2	1.00000 2	1.00000 2	1.00000 2	1.00000 2	1.00000 2	1.00000 2	1.00000 2
1.00	1.00000 2	1.00000 2	1.00000 2	1.00000 2	1.00000 2	1.00000 2	1.00000 2	1.00000 2	1.00000 2	1.00000 2
1.20	1.00000 2	1.00000 2	1.00000 2	1.00000 2	1.00000 2	1.00000 2	1.00000 2	1.00000 2	1.00000 2	1.00000 2
1.50	1.00000 2	1.00000 2	1.00000 2	1.00000 2	1.00000 2	1.00000 2	1.00000 2	1.00000 2	1.00000 2	1.00000 2
1.70	1.00000 2	1.00000 2	1.00000 2	1.00000 2	1.00000 2	1.00000 2	1.00000 2	1.00000 2	1.00000 2	1.00000 2
2.00	1.00000 2	1.00000 2	1.00000 2	1.00000 2	1.00000 2	1.00000 2	1.00000 2	1.00000 2	1.00000 2	1.00000 2
2.50	1.00000 1	1.00000 2	1.00000 2	1.00000 2	1.00000 2	1.00000 2	1.00000 2	1.00000 2	1.00000 2	1.00000 2
3.00	1.00000 1	1.00000 1	1.00000 2	1.00000 2	1.00000 2	1.00000 2	1.00000 2	1.00000 2	1.00000 2	1.00000 2
4.00	1.00000 1	1.00000 1	1.00000 1	1.00000 2	1.00000 2	1.00000 2	1.00000 2	1.00000 2	1.00000 2	1.00000 2
5.00	0.93260 1	1.00000 1	1.00000 1	1.00000 1	1.00000 2	1.00000 2	1.00000 2	0.98689 2	0.94283 2	0.90159 2
6.00	0.78684 1	0.85543 1	0.92133 1	0.98114 1	1.00000 1	0.98038 2	0.91325 2	0.85408 2	0.80525 2	0.76504 2
7.00	0.67695 1	0.73765 1	0.79760 1	0.85658 1	0.91340 1	0.86940 2	0.79539 2	0.74016 2	0.69564 2	0.65968 2
8.00	0.59310 1	0.64576 1	0.70021 1	0.75334 1	0.80591 1	0.76776 2	0.70094 2	0.65013 2	0.61037 2	0.57845 2
9.00	0.52744 1	0.57531 1	0.62311 1	0.67081 1	0.71833 1	0.68496 2	0.62436 2	0.57869 2	0.54309 2	0.51457 2
10.00	0.47478 1	0.51792 1	0.56103 1	0.60411 1	0.64713 1	0.61729 2	0.56236 2	0.52109 2	0.48896 2	0.46325 2
12.00	0.39569 1	0.43165 1	0.46762 1	0.50358 1	0.53954 1	0.51475 2	0.46841 2	0.43435 2	0.40754 2	0.39610 2
15.00	0.31555 1	0.34533 1	0.37411 1	0.40288 1	0.43166 1	0.41194 2	0.37537 2	0.34749 2	0.32604 2	0.30888 2
20.00	0.23741 1	0.25900 1	0.28058 1	0.30216 1	0.32375 1	0.30888 2	0.28130 2	0.26062 2	0.24453 2	0.23166 2
25.00	0.18993 1	0.20720 1	0.22446 1	0.24173 1	0.25900 1	0.24711 2	0.22504 2	0.20850 2	0.19563 2	0.18533 2

ADHESIVE-BONDED DOUBLE-LAP JOINTS (ELASTIC-PLASTIC ANALYSIS)
NON-DIMENSIONALIZED FORMULATION

PLASTIC TO ELASTIC ADHESIVE SHEAR STRAIN RATIO = 5.0
THERMAL MISMATCH COEFFICIENT = -1.000 FOR TENSION, = 1.000 FOR COMPRESSION

NON-DIMENSIONALIZED JOINT STRENGTH ,

0 = BOTH ENDS EQUALLY CRITICAL
1 = SOFT ET END CRITICAL
2 = STIFF ET END CRITICAL

(Each tabulated value is followed in the original by the critical-end indicator "1".)

SCALED L/T RATIO	EXTENSIONAL STIFFNESS (THICKNESS) RATIO									
	0.1	0.2	0.3	0.4	0.5	0.6	0.7	0.8	0.9	1.0
0.0	0.0	0.0	0.0	0.0	0.0	0.0	0.0	0.0	0.0	0.0
0.10	0.1000	0.1000	0.1000	0.1000	0.1000	0.1000	0.1000	0.1000	0.1000	0.1000
0.15	0.1500	0.1500	0.1500	0.1500	0.1500	0.1500	0.1500	0.1500	0.1500	0.1500
0.20	0.2000	0.2000	0.2000	0.2000	0.2000	0.2000	0.2000	0.2000	0.2000	0.2000
0.30	0.3000	0.3000	0.3000	0.3000	0.3000	0.3000	0.3000	0.3000	0.3000	0.3000
0.50	0.5000	0.5000	0.5000	0.5000	0.5000	0.5000	0.5000	0.5000	0.5000	0.5000
0.70	0.7000	0.7000	0.7000	0.7000	0.7000	0.7000	0.7000	0.7000	0.7000	0.7000
1.00	1.0000	1.0000	1.0000	1.0000	1.0000	1.0000	1.0000	1.0000	1.0000	1.0000
1.20	1.2000	1.2000	1.2000	1.2000	1.2000	1.2000	1.2000	1.2000	1.2000	1.2000
1.50	1.5000	1.5000	1.5000	1.5000	1.5000	1.5000	1.5000	1.5000	1.5000	1.5000
1.70	1.7000	1.7000	1.7000	1.7000	1.7000	1.7000	1.7000	1.7000	1.7000	1.7000
2.00	2.0000	2.0000	2.0000	2.0000	2.0000	2.0000	2.0000	2.0000	2.0000	2.0000
2.50	2.4175	2.5000	2.5000	2.5000	2.5000	2.5000	2.5000	2.5000	2.5000	2.5000
3.00	2.4817	2.6840	2.8777	3.0000	3.0000	3.0000	3.0000	3.0000	3.0000	3.0000
4.00	2.5262	2.7493	2.9691	3.1845	3.3938	3.5940	3.7906	3.9431	4.0000	4.0079
5.00	2.5404	2.7691	2.9967	3.2229	3.4473	3.6691	3.8876	4.1014	4.3090	4.5079
6.00	2.5454	2.7760	3.0062	3.2359	3.4650	3.6932	3.9203	4.1458	4.3694	4.5903
7.00	2.5472	2.7785	3.0096	3.2406	3.4713	3.7017	3.9317	4.1612	4.3899	4.6178
8.00	2.5479	2.7794	3.0109	3.2423	3.4736	3.7048	3.9359	4.1667	4.3973	4.6276
9.00	2.5481	2.7798	3.0113	3.2429	3.4744	3.7059	3.9374	4.1687	4.4000	4.6312
10.00	2.5482	2.7799	3.0115	3.2431	3.4749	3.7064	3.9379	4.1695	4.4010	4.6325
12.00	2.5483	2.7799	3.0116	3.2433	3.4749	3.7066	3.9383	4.1699	4.4015	4.6331
15.00	2.5483	2.7799	3.0116	3.2433	3.4749	3.7066	3.9383	4.1699	4.4016	4.6332
20.00	2.5483	2.7799	3.0116	3.2433	3.4749	3.7066	3.9383	4.1699	4.4016	4.6332
25.00	2.5483	2.7799	3.0116	3.2433	3.4749	3.7066	3.9383	4.1699	4.4016	4.6332
TRANSL	2.3785	2.5947	2.8110	3.0272	3.2434	3.4596	3.6759	3.8921	4.1083	4.3246

ADHESIVE-BONDED DOUBLE-LAP JOINTS (ELASTIC-PLASTIC ANALYSIS)
NON-DIMENSIONALIZED FORMULATION

PLASTIC TO ELASTIC ADHESIVE SHEAR STRAIN RATIO = 5.0
THERMAL MISMATCH COEFFICIENT = -1.000 FOR TENSION, = 1.000 FOR COMPRESSION

AVERAGE SHEAR STRESS / MAXIMUM SHEAR STRESS ,

0 = BOTH ENDS EQUALLY CRITICAL
1 = SOFT ET END CRITICAL
2 = STIFF ET END CRITICAL

(Each tabulated value is followed in the original by the critical-end indicator "1".)

SCALED L/T RATIO	EXTENSIONAL STIFFNESS (THICKNESS) RATIO									
	0.1	0.2	0.3	0.4	0.5	0.6	0.7	0.8	0.9	1.0
0.0	1.00000	1.00000	1.00000	1.00000	1.00000	1.00000	1.00000	1.00000	1.00000	1.00000
0.10	1.00000	1.00000	1.00000	1.00000	1.00000	1.00000	1.00000	1.00000	1.00000	1.00000
0.15	1.00000	1.00000	1.00000	1.00000	1.00000	1.00000	1.00000	1.00000	1.00000	1.00000
0.20	1.00000	1.00000	1.00000	1.00000	1.00000	1.00000	1.00000	1.00000	1.00000	1.00000
0.30	1.00000	1.00000	1.00000	1.00000	1.00000	1.00000	1.00000	1.00000	1.00000	1.00000
0.50	1.00000	1.00000	1.00000	1.00000	1.00000	1.00000	1.00000	1.00000	1.00000	1.00000
0.70	1.00000	1.00000	1.00000	1.00000	1.00000	1.00000	1.00000	1.00000	1.00000	1.00000
1.00	1.00000	1.00000	1.00000	1.00000	1.00000	1.00000	1.00000	1.00000	1.00000	1.00000
1.20	1.00000	1.00000	1.00000	1.00000	1.00000	1.00000	1.00000	1.00000	1.00000	1.00000
1.50	1.00000	1.00000	1.00000	1.00000	1.00000	1.00000	1.00000	1.00000	1.00000	1.00000
1.70	1.00000	1.00000	1.00000	1.00000	1.00000	1.00000	1.00000	1.00000	1.00000	1.00000
2.00	1.00000	1.00000	1.00000	1.00000	1.00000	1.00000	1.00000	1.00000	1.00000	1.00000
2.50	0.96698	1.00000	1.00000	1.00000	1.00000	1.00000	1.00000	1.00000	1.00000	1.00000
3.00	0.82723	0.89468	0.95691	1.00000	1.00000	1.00000	1.00000	1.00000	1.00000	1.00000
4.00	0.63156	0.68732	0.74228	0.79614	0.84844	0.89851	0.94516	0.98578	1.00000	1.00000
5.00	0.50808	0.55382	0.59934	0.64459	0.68946	0.73383	0.77751	0.82029	0.86181	0.90159
6.00	0.42424	0.46267	0.50104	0.53932	0.57750	0.61553	0.65338	0.69097	0.72823	0.76504
7.00	0.36389	0.39593	0.42905	0.46294	0.49590	0.52882	0.56167	0.59445	0.62713	0.65968
8.00	0.31849	0.34743	0.37636	0.40529	0.43420	0.46310	0.49198	0.52084	0.54967	0.57845
9.00	0.28313	0.30886	0.33459	0.36032	0.38605	0.41177	0.43749	0.46319	0.48889	0.51457
10.00	0.25482	0.27799	0.30115	0.32431	0.34749	0.37064	0.39379	0.41695	0.44010	0.46325
12.00	0.21236	0.23166	0.25077	0.27027	0.28958	0.30888	0.32818	0.34749	0.36679	0.38610
15.00	0.16989	0.18533	0.20077	0.21622	0.23166	0.24711	0.26255	0.27799	0.29344	0.30888
20.00	0.12741	0.13900	0.15058	0.16216	0.17375	0.18533	0.19691	0.20850	0.22009	0.23166
25.00	0.10193	0.11120	0.12046	0.12973	0.13900	0.14826	0.15753	0.16680	0.17606	0.18533

106